Gut Microbiota Modulation of Host Feeding Behavior

Thesis by

James Anthony Ousey

In Partial Fulfillment of the Requirements for

the Degree of

Doctor of Philosophy

CALIFORNIA INSTITUTE OF TECHNOLOGY

Pasadena, California

2023

(Defended November 10th, 2022)

James Anthony Ousey
ORCID: 0000-0003-4886-0053

ACKNOWLEDGEMENTS

I am grateful for the support of my advisor, Sarkis Mazmanian. I thank my lab members, my graduate committee, the Caltech Office of Laboratory Animal Resources, and the Caltech Institutional Animal Care and Use Committee for their assistance and feedback during this research endeavor. Finally, I am supported by the love of my close friends and family.

ABSTRACT

The rich, diverse community of microorganisms in the gastrointestinal tract of animals, or gut microbiota, regulates aspects of host metabolism, immunity, and neural function, with resulting effects on the expression of complex behaviors, including feeding.

In this thesis, we sought to characterize gut microbiota influences on the behavioral response to palatable foods in mice. We discover that binge-like consumption of palatable foods, including high-sucrose pellets and a high-fat diet, is exacerbated in mice in the absence of a gut microbiota. Furthermore, using automated feeding dispensers and video analysis, we find that microbiota depletion with oral antibiotics results in elongated feeding bouts and conserved changes in the dynamics of palatable food intake. We show the hyperphagic phenotype of antibiotic-treated mice is reversible upon microbiota reconstitution via fecal microbiota transplant. Operant conditioning tests reveal that the motivation to pursue high-sucrose rewards is augmented in microbiota-depleted mice. The mesolimbic brain region activity induced upon high-sucrose pellet consumption is elevated in antibiotic-treated mice. Gut bacteria from the family S24-7 and genus *Lactobacillus* were identified by differential antibiotic treatment and fecal microbiota transplants as correlating with reduction of high-sucrose pellet consumption. Indeed, colonization of vancomycin-treated mice with a mixture of S24-7 and *Lactobacillus johnsonii* reduces overconsumption of high-sucrose pellets in a limited-access binge-eating model. The work in this thesis comprehensively demonstrates that the gut microbiota regulates feeding induced in response to palatable foods in mice.

PUBLISHED CONTENT AND CONTRIBUTIONS

CHAPTER III

James Ousey, Joseph C. Boktor, Sarkis K. Mazmanian. "Gut microbiota suppress feeding induced by palatable foods." **(A version of this chapter has been accepted for publication in *Current Biology*)**

DOI: https://doi.org/10.1016/j.cub.2022.10.066.

J.O.: Conceptualization, investigation, formal analysis, and writing.

TABLE OF CONTENTS

LIST OF ILLUSTRATIONS AND TABLES

Number *Page*

ABBREVIATIONS

A	Ampicillin
A. muc	*Akkermansia muciniphila*
ABX	Antibiotics
AgRP	Agouti-related peptide
ARC	Arcuate nucleus of the hypothalamus
ASV	Amplicon sequence variant
BDNF	Brain-derived neurotrophic factor
BHIS	Supplemented brain heart infusion
BLA	Basolateral amygdala
DA	Dopamine
DIO	Diet-induced obesity
DRD1/DRD2	Dopamine receptor 1/2
eCB	Endocannabinoid
EPM	Elevated plus maze
FED	Feeding Experimentation Device
FMT	Fecal microbiota transplant
FR	Fixed ratio
GF	Germ-free
GFP	Green fluorescent protein
GI	Gastrointestinal
HFD	High-fat diet
HFHS	High-fat High-sugar
i.g.	Intragastric
L. johnsonii	*Lactobacillus johnsonii*
LH	Lateral hypothalamus
M	Metronidazole
N	Neomycin
NAc	Nucleus accumbens
NPY	Neuropeptide Y
OFT	Open field test
PCoA	Principle coordinate analysis
PCR	Polymerase chain reaction
POMC	Proopiomelanocortin
PR	Progressive ratio
qPCR	Quantitative PCR
rRNA	Ribosomal RNA
s.c.	Subcutaneous
SCFA	Short-chain fatty acid
SPF	Specific pathogen-free
SRA	Sequence Read Archive
TH	Tyrosine hydroxylase
V	Vancomycin
VEH	Vehicle
VTA	Ventral tegmental area

Chapter 1

MUS MUSCULUS AS A MODEL FOR HOST-MICROBE INTERACTIONS

1.1 INTRODUCTION

The totality of observable characteristics of an organism, or "phenotype," is a complex output of inherited genetic attributes and environmental influences. A major route of environmental input in some organisms is the gastrointestinal (GI) tract, constituting a semi-permeable membrane allowing for nutrient sensing and energy harvest. In humans, the GI tract harbors a multitudinous community of microorganisms, including bacteria, viruses, and archaea, termed the gut microbiota, that have evolved to resiliently colonize and persist in a commensal relationship with the host.[1] Human studies have revealed that many disease states, including obesity, cancer, and neurodegenerative disorders, present with consistent changes in the structure and predicted functional potential of the gut microbiome, suggesting potential gut microbial roles in maintenance of host health.[2–5] Curiously, research in a variety of animal models reveals that gut microbiota influences extend to regulation of behavioral phenotypes, including feeding, learning, fear and sensory responses, sociability, and anxiety.[6–14]

The house mouse, *Mus musculus*, is an ideal model organism to interrogate gut microbiome contributions to emergent behavioral phenotypes. *Mus musculus* exhibits an extensive range of complex behaviors not observed in lower animal models with commensal microbiotas, like *Drosophila melanogaster* and *Caenorhabditis elegans*, and the long history of behavioral and microbiota-centric studies in mice provides a rich foundation of accessible protocols and experimental strategies. Strains of laboratory mice are genetically tractable, facilitating targeted observation of specific cell populations, and

their ease of handling and social housing conditions enable moderate throughput of behavioral experiments.

1.2 GUT MICROBIOTA OF *MUS MUSCULUS*

The human gut is among the most densely populated naturally occurring microbial communities on Earth. Similar to humans, the large intestine of *Mus musculus* harbors ~10^{11}-10^{12} live microbes per gram of feces, which metabolize diverse nutrients consumed by the host along with secreted intestinal glycans. The wide range of available nutrients produces a tremendous amount of phylogenetic diversity within the gut microbiota, spanning multiple phyla, and is predominantly comprised of Bacteroides and Firmicutes. In mice, immediately after birth, maternal and environmental bacteria colonize the originally germ-free GI tract and compete for their respective niches, eventually forming a resilient and stable community in which over 100 distinct microbial species exist in equilibrium.[1]

The intestinal tract is inhomogeneous and factors like oxygen concentration, pH, nutrient profile, and proximity to the epithelial wall drive local differences in community composition. pH levels increase and oxygen levels decrease from the proximal to distal ends of the GI tract, resulting in aero- and acid-tolerant *Enterobacter* and *Lactobacillus* thriving in the small intestine, while obligate anaerobes dominate the cecum and colon of the mouse.[1] Given the diversity in metabolic capabilities and genetic profiles of commensal gut microbes, host actions, including changes in dietary habits and ingestion of antibiotics or probiotics, can have staggering effects on the makeup of the gut

microbiota.[15–17] Indeed, the use of diet and antibiotics to perturb gut microbiota homeostasis serves as a reliable experimental method to investigate gut microbiota effects on the host.[18,19]

Reflecting humans, mouse models of disease frequently present with shifts in gut community composition.[20,21] However, untangling whether changes in the microbiota contribute to disease etiology or are a result of the disease state itself is a formidable challenge and an avenue for further discovery.

1.3 HOST-GUT MICROBIOTA RELATIONSHIPS IN *MUS MUSCULUS*

During development and in adulthood, the gut microbiota has profound effects across multiple aspects of host biology. The substantial impact of the gut microbiota is illustrated in germ-free (GF) mice, which are raised under sterile conditions, and as such never develop a gut microbiota. GF mice, compared to conventionally colonized specific-pathogen free (SPF) controls, have reduced fat mass, changes in circulating metabolic hormones, abnormal immune responses, deficits in sociability, alterations in feeding behavior, and suppressed circadian cycles, amongst other differences.[11,22,23] While the comparisons between animals colonized with a full microbiota to animals devoid of microorganisms may provide high-level insight, differences among animals colonized with different microbiotas can reveal how host phenotype relates to gut community composition, or even by the presence or absence of individual species. Indeed, specific commensal gut microbes have been reported to affect social behavior, development of regulatory T-cells, and the susceptibility to develop cancer.[4,11,24,25] The assortment of

microbiota-dependent influences, which encompass multiple organ systems, requires a comparable variety of communication routes between the gut microbiota and host pathways.

Gut microbes are capable of metabolizing otherwise indigestible dietary polysaccharides and converting them into molecules capable of affecting the host. Among these secreted molecules are short-chain fatty acids (SCFAs), reported to reduce food intake through central signaling pathways,[26,27] regulate the activation state of microglia,[28] and act through fatty-acid receptors to control host adiposity.[29] Other small organic molecules exclusively produced by gut microbes, including 4-ethylphenol and indole sulfate, exacerbate anxiety-like behaviors in rodents.[30,31] Some pathogenic microbes, like *Clostridium dificile* and *Escherichia coli*, can secrete small-molecule toxins that damage the intestinal lining.[32] Multiple species of *Enterobacter* produce amyloid aggregates, which reportedly stimulate the aggregation of native amyloidogenic host proteins, leading to worsening of neurodegenerative disease symptoms.[33]

In addition to the production of active molecules, antigens produced by microbiota constantly induce host immune responses through innate and adaptive pathways. For instance, polysaccharide A, a complex glycan produced by *Bacteroides fragilis*, stimulates anti-inflammatory immune responses in the intestine.[34] Specific consortia of bacteria as well as individual microbes are being investigated for their ability to selectively induce immune cell differentiation, which can shape outcomes in mouse models of autoimmunity and cancer.[25] Bacterial products may also act as molecular

"mimics" and stimulate adaptive immune responses leading to autoimmunity against host proteins, as demonstrated in a mouse model of cardiomyopathy and with the anorexigenic *E. coli*–derived ClpB protein.[35,36]

Finally, the vagus nerve represents a direct line of communication between the gut microbiota and activity in the central nervous system. Strains of *Lactobacillus* have been reported to affect expression of complex behaviors through vagal-mediated pathways,[37] and the neural activity in vagal-connected ganglia is increased upon microbiota depletion, either via germ-free status or through treatment with oral antibiotics.[38]

1.4 EXPERIMENTAL METHODS TO STUDY THE GUT MICROBIOTA

Research into the complex relationships between the gut microbiota and host necessitates specialized experimental methods and tools. GF animals, born and reared in a microbe-free environment, are an essential tool in establishing host phenotypes modulated in the absence of gut microbial colonization. GF animals can also serve as a blank slate for colonization with microbiotas or individual microbes of interest. Transplantation of the gut microbiota from one animal to another, usually through oral gavage of fecal bacterial slurries, termed fecal microbiota transplant (FMT), is a standard approach applied when testing if a phenotype may be conferred by transfer of the gut microbiota. The reproduction of donor phenotypes in FMT recipient mice provides suggestive evidence that the gut microbiota contributes to the expression of the phenotype in the donor. The experimental strategy of differentially colonizing GF mice with human microbiotas sources from diseased or healthy controls has been applied to investigate gut microbiota

contributions in neurodegenerative and behavioral disorders.[39,40] Colonization of GF mice with individual microbes, or "mono-colonization," can elucidate specific microbe-host relationships, and mono-colonization with genetically engineered mutant bacterial strains is a clean route to demonstrate how host phenotype depends on specific genetic traits of the gut microbiome.[30]

The practical application of GF mice for research is limited due to the logistical challenges of breeding and raising mice in a sterile environment. Furthermore, the neural and behavioral development of mice in the absence of microbial exposure is permanently stunted, which confounds observations made in GF mice colonized as adults. To address these drawbacks of the GF system, the use of oral antibiotics (ABX) to deplete the intestinal microbiota has gained prominence as a research tool. Broad-spectrum oral antibiotics significantly reduce gut microbial loads and produce systemic changes that broadly reflect the GF state.[18] Similar to GF mice, ABX depletion can be followed by FMT to establish sufficiency of the gut microbiota to transfer donor phenotypes. Antibiotics have distinct ranges of antimicrobial activity, and differential antibiotic treatment of mice to target different swaths of gut microorganisms is a reliable strategy to identify microorganisms in the gut milieu that correlate with the host phenotype of interest.[41]

Advancements in high-throughput sequencing and taxonomic classification technology have advanced the study of the gut microbiome. 16S rRNA profiling, a technique to classify amplicons of the 16S variable regions from a microbial community generated

from universal bacterial primers against publicly available databases of species and amplicon pairs, is a method to quickly determine the relative composition of a microbiome.[42] The similarity of microbiomes across experimental treatment conditions or over time can be measured through ecology metrics like Bray-Curtis dissimilarity and phylogenetically-informed UniFrac distances. Unique amplicon sequences, known as amplicon sequence variants (ASVs), can undergo differential abundance analysis to identify particular sequences that correlate most strongly with specific treatments or host phenotype.[43]

REFERENCES

1. Donaldson, G.P., Lee, S.M., and Mazmanian, S.K. (2016). Gut biogeography of the bacterial microbiota. Nat Rev Microbiol *14*, 20–32. 10.1038/nrmicro3552.

2. Tremaroli, V., and Bäckhed, F. (2012). Functional interactions between the gut microbiota and host metabolism. Nature *489*, 242–249. 10.1038/nature11552.

3. Ley, R.E., Turnbaugh, P.J., Klein, S., and Gordon, J.I. (2006). Human gut microbes associated with obesity. Nature *444*, 1022–1023. 10.1038/4441022a.

4. Sepich-Poore, G.D., Zitvogel, L., Straussman, R., Hasty, J., Wargo, J.A., and Knight, R. (2021). The microbiome and human cancer. Science *371*, eabc4552. 10.1126/science.abc4552.

5. Fang, P., Kazmi, S.A., Jameson, K.G., and Hsiao, E.Y. (2020). The Microbiome as a Modifier of Neurodegenerative Disease Risk. Cell Host & Microbe *28*, 201–222. 10.1016/j.chom.2020.06.008.

6. Trevelline, B.K., and Kohl, K.D. (2022). The gut microbiome influences host diet selection behavior. Proceedings of the National Academy of Sciences *119*, e2117537119. 10.1073/pnas.2117537119.

7. Leitão-Gonçalves, R., Carvalho-Santos, Z., Francisco, A.P., Fioreze, G.T., Anjos, M., Baltazar, C., Elias, A.P., Itskov, P.M., Piper, M.D.W., and Ribeiro, C. (2017). Commensal bacteria and essential amino acids control food choice behavior and reproduction. PLOS Biology *15*, e2000862. 10.1371/journal.pbio.2000862.

8. Chu, C., Murdock, M.H., Jing, D., Won, T.H., Chung, H., Kressel, A.M., Tsaava, T., Addorisio, M.E., Putzel, G.G., Zhou, L., et al. (2019). The microbiota regulate neuronal function and fear extinction learning. Nature *574*, 543–548. 10.1038/s41586-019-1644-y.

9. O'Donnell, M.P., Fox, B.W., Chao, P.-H., Schroeder, F.C., and Sengupta, P. (2020). A neurotransmitter produced by gut bacteria modulates host sensory behaviour. Nature *583*, 415–420. 10.1038/s41586-020-2395-5.

10. Lee, K., Vuong, H.E., Nusbaum, D.J., Hsiao, E.Y., Evans, C.J., and Taylor, A.M.W. (2018). The gut microbiota mediates reward and sensory responses associated with regimen-selective morphine dependence. Neuropsychopharmacol *43*, 2606–2614. 10.1038/s41386-018-0211-9.

11. Wu, W.-L., Adame, M.D., Liou, C.-W., Barlow, J.T., Lai, T.-T., Sharon, G., Schretter, C.E., Needham, B.D., Wang, M.I., Tang, W., et al. (2021). Microbiota regulate social behaviour via stress response neurons in the brain. Nature *595*, 409–414. 10.1038/s41586-021-03669-y.

12. Sherwin, E., Bordenstein, S.R., Quinn, J.L., Dinan, T.G., and Cryan, J.F. (2019). Microbiota and the social brain. Science *366*, eaar2016. 10.1126/science.aar2016.

13. Nishino, R., Mikami, K., Takahashi, H., Tomonaga, S., Furuse, M., Hiramoto, T., Aiba, Y., Koga, Y., and Sudo, N. (2013). Commensal microbiota modulate murine behaviors in a

strictly contamination-free environment confirmed by culture-based methods. Neurogastroenterology & Motility *25*, 521-e371. 10.1111/nmo.12110.

14. Crumeyrolle-Arias, M., Jaglin, M., Bruneau, A., Vancassel, S., Cardona, A., Daugé, V., Naudon, L., and Rabot, S. (2014). Absence of the gut microbiota enhances anxiety-like behavior and neuroendocrine response to acute stress in rats. Psychoneuroendocrinology *42*, 207–217. 10.1016/j.psyneuen.2014.01.014.

15. Rothschild, D., Weissbrod, O., Barkan, E., Kurilshikov, A., Korem, T., Zeevi, D., Costea, P.I., Godneva, A., Kalka, I.N., Bar, N., et al. (2018). Environment dominates over host genetics in shaping human gut microbiota. Nature *555*, 210–215. 10.1038/nature25973.

16. Carmody, R.N., Gerber, G.K., Luevano, J.M., Gatti, D.M., Somes, L., Svenson, K.L., and Turnbaugh, P.J. (2015). Diet Dominates Host Genotype in Shaping the Murine Gut Microbiota. Cell Host & Microbe *17*, 72–84. 10.1016/j.chom.2014.11.010.

17. Suez, J., Zmora, N., Zilberman-Schapira, G., Mor, U., Dori-Bachash, M., Bashiardes, S., Zur, M., Regev-Lehavi, D., Ben-Zeev Brik, R., Federici, S., et al. (2018). Post-Antibiotic Gut Mucosal Microbiome Reconstitution Is Impaired by Probiotics and Improved by Autologous FMT. Cell *174*, 1406-1423.e16. 10.1016/j.cell.2018.08.047.

18. Zarrinpar, A., Chaix, A., Xu, Z.Z., Chang, M.W., Marotz, C.A., Saghatelian, A., Knight, R., and Panda, S. (2018). Antibiotic-induced microbiome depletion alters metabolic homeostasis by affecting gut signaling and colonic metabolism. Nat Commun *9*, 2872. 10.1038/s41467-018-05336-9.

19. Olson, C.A., Vuong, H.E., Yano, J.M., Liang, Q.Y., Nusbaum, D.J., and Hsiao, E.Y. (2018). The Gut Microbiota Mediates the Anti-Seizure Effects of the Ketogenic Diet. Cell *173*, 1728-1741.e13. 10.1016/j.cell.2018.04.027.

20. Bisanz, J.E., Upadhyay, V., Turnbaugh, J.A., Ly, K., and Turnbaugh, P.J. (2019). Meta-Analysis Reveals Reproducible Gut Microbiome Alterations in Response to a High-Fat Diet. Cell Host & Microbe *26*, 265-272.e4. 10.1016/j.chom.2019.06.013.

21. Buffington, S.A., Dooling, S.W., Sgritta, M., Noecker, C., Murillo, O.D., Felice, D.F., Turnbaugh, P.J., and Costa-Mattioli, M. (2021). Dissecting the contribution of host genetics and the microbiome in complex behaviors. Cell *184*, 1740-1756.e16. 10.1016/j.cell.2021.02.009.

22. Backhed, F., Ding, H., Wang, T., Hooper, L.V., Koh, G.Y., Nagy, A., Semenkovich, C.F., and Gordon, J.I. (2004). The gut microbiota as an environmental factor that regulates fat storage. Proceedings of the National Academy of Sciences *101*, 15718–15723. 10.1073/pnas.0407076101.

23. Marcinkevicius, E.V., and Shirasu-Hiza, M.M. (2015). Message in a Biota: Gut Microbes Signal to the Circadian Clock. Cell Host & Microbe *17*, 541–543. 10.1016/j.chom.2015.04.013.

24. Sgritta, M., Dooling, S.W., Buffington, S.A., Momin, E.N., Francis, M.B., Britton, R.A., and Costa-Mattioli, M. (2019). Mechanisms Underlying Microbial-Mediated Changes in

Social Behavior in Mouse Models of Autism Spectrum Disorder. Neuron *101*, 246-259.e6. 10.1016/j.neuron.2018.11.018.

25. Tanoue, T., Morita, S., Plichta, D.R., Skelly, A.N., Suda, W., Sugiura, Y., Narushima, S., Vlamakis, H., Motoo, I., Sugita, K., et al. (2019). A defined commensal consortium elicits CD8 T cells and anti-cancer immunity. Nature *565*, 600–605. 10.1038/s41586-019-0878-z.

26. Frost, G., Sleeth, M.L., Sahuri-Arisoylu, M., Lizarbe, B., Cerdan, S., Brody, L., Anastasovska, J., Ghourab, S., Hankir, M., Zhang, S., et al. (2014). The short-chain fatty acid acetate reduces appetite via a central homeostatic mechanism. Nat Commun *5*, 3611. 10.1038/ncomms4611.

27. Li, Z., Yi, C.-X., Katiraei, S., Kooijman, S., Zhou, E., Chung, C.K., Gao, Y., van den Heuvel, J.K., Meijer, O.C., Berbée, J.F.P., et al. (2018). Butyrate reduces appetite and activates brown adipose tissue via the gut-brain neural circuit. Gut *67*, 1269–1279. 10.1136/gutjnl-2017-314050.

28. Erny, D., Hrabě de Angelis, A.L., Jaitin, D., Wieghofer, P., Staszewski, O., David, E., Keren-Shaul, H., Mahlakoiv, T., Jakobshagen, K., Buch, T., et al. (2015). Host microbiota constantly control maturation and function of microglia in the CNS. Nat Neurosci *18*, 965–977. 10.1038/nn.4030.

29. Samuel, B.S., Shaito, A., Motoike, T., Rey, F.E., Backhed, F., Manchester, J.K., Hammer, R.E., Williams, S.C., Crowley, J., Yanagisawa, M., et al. (2008). Effects of the gut microbiota on host adiposity are modulated by the short-chain fatty-acid binding G protein-coupled receptor, Gpr41. Proceedings of the National Academy of Sciences *105*, 16767–16772. 10.1073/pnas.0808567105.

30. Needham, B.D., Funabashi, M., Adame, M.D., Wang, Z., Boktor, J.C., Haney, J., Wu, W.-L., Rabut, C., Ladinsky, M.S., Hwang, S.-J., et al. (2022). A gut-derived metabolite alters brain activity and anxiety behaviour in mice. Nature *602*, 647–653. 10.1038/s41586-022-04396-8.

31. Jaglin, M., Rhimi, M., Philippe, C., Pons, N., Bruneau, A., Goustard, B., Daugé, V., Maguin, E., Naudon, L., and Rabot, S. (2018). Indole, a Signaling Molecule Produced by the Gut Microbiota, Negatively Impacts Emotional Behaviors in Rats. Frontiers in Neuroscience *12*.

32. Wilson, M.R., Jiang, Y., Villalta, P.W., Stornetta, A., Boudreau, P.D., Carrá, A., Brennan, C.A., Chun, E., Ngo, L., Samson, L.D., et al. (2019). The human gut bacterial genotoxin colibactin alkylates DNA. Science *363*, eaar7785. 10.1126/science.aar7785.

33. Sampson, T.R., Challis, C., Jain, N., Moiseyenko, A., Ladinsky, M.S., Shastri, G.G., Thron, T., Needham, B.D., Horvath, I., Debelius, J.W., et al. (2020). A gut bacterial amyloid promotes α-synuclein aggregation and motor impairment in mice. eLife *9*, e53111. 10.7554/eLife.53111.

34. Mazmanian, S.K., Round, J.L., and Kasper, D.L. (2008). A microbial symbiosis factor prevents intestinal inflammatory disease. Nature *453*, 620–625. 10.1038/nature07008.

35. Gil-Cruz, C., Perez-Shibayama, C., De Martin, A., Ronchi, F., van der Borght, K., Niederer, R., Onder, L., Lütge, M., Novkovic, M., Nindl, V., et al. (2019). Microbiota-derived peptide mimics drive lethal inflammatory cardiomyopathy. Science *366*, 881–886. 10.1126/science.aav3487.

36. Fetissov, S.O. (2017). Role of the gut microbiota in host appetite control: bacterial growth to animal feeding behaviour. Nat Rev Endocrinol *13*, 11–25. 10.1038/nrendo.2016.150.

37. Bravo, J.A., Forsythe, P., Chew, M.V., Escaravage, E., Savignac, H.M., Dinan, T.G., Bienenstock, J., and Cryan, J.F. (2011). Ingestion of Lactobacillus strain regulates emotional behavior and central GABA receptor expression in a mouse via the vagus nerve. PNAS *108*, 16050–16055. 10.1073/pnas.1102999108.

38. Muller, P.A., Schneeberger, M., Matheis, F., Wang, P., Kerner, Z., Ilanges, A., Pellegrino, K., del Mármol, J., Castro, T.B.R., Furuichi, M., et al. (2020). Microbiota modulate sympathetic neurons via a gut–brain circuit. Nature *583*, 441–446. 10.1038/s41586-020-2474-7.

39. Sampson, T.R., Debelius, J.W., Thron, T., Janssen, S., Shastri, G.G., Ilhan, Z.E., Challis, C., Schretter, C.E., Rocha, S., Gradinaru, V., et al. (2016). Gut Microbiota Regulate Motor Deficits and Neuroinflammation in a Model of Parkinson's Disease. Cell *167*, 1469-1480.e12. 10.1016/j.cell.2016.11.018.

40. Sharon, G., Cruz, N.J., Kang, D.-W., Gandal, M.J., Wang, B., Kim, Y.-M., Zink, E.M., Casey, C.P., Taylor, B.C., Lane, C.J., et al. (2019). Human Gut Microbiota from Autism Spectrum Disorder Promote Behavioral Symptoms in Mice. Cell *177*, 1600-1618.e17. 10.1016/j.cell.2019.05.004.

41. Bostick, J.W., Wang, Y., Shen, Z., Ge, Y., Brown, J., Chen, Z.E., Mohamadzadeh, M., Fox, J.G., and Zhou, L. (2019). Dichotomous regulation of group 3 innate lymphoid cells by nongastric Helicobacter species. Proceedings of the National Academy of Sciences *116*, 24760–24769. 10.1073/pnas.1908128116.

42. Bolyen, E., Rideout, J.R., Dillon, M.R., Bokulich, N.A., Abnet, C.C., Al-Ghalith, G.A., Alexander, H., Alm, E.J., Arumugam, M., Asnicar, F., et al. (2019). Reproducible, interactive, scalable and extensible microbiome data science using QIIME 2. Nat Biotechnol *37*, 852–857. 10.1038/s41587-019-0209-9.

43. Mallick, H., Rahnavard, A., McIver, L.J., Ma, S., Zhang, Y., Nguyen, L.H., Tickle, T.L., Weingart, G., Ren, B., Schwager, E.H., et al. (2021). Multivariable association discovery in population-scale meta-omics studies. PLOS Computational Biology *17*, e1009442. 10.1371/journal.pcbi.1009442.

Chapter 2

REGULATION OF FEEDING AND FOOD REWARD IN *MUS MUSCULUS*

2.1 INTRISIC AND EXTRINSIC INFLUENCES ON FEEDING BEHAVIOR

All life requires energy. Animals have developed strategies to seek and consume food sources to maintain energy stores and ensure survival in times of need. These feeding behaviors are tightly regulated by internal mechanisms operating on multiple timescales and are subject to external influences, including the quality of food and risk associated with retrieving it. Feeding behaviors in animals are frequently divided in two categories: homeostatic feeding, which is feeding performed for energy, and hedonic feeding, done for pleasure.[1]

Multiple organ systems are involved in the self-regulation of homeostatic feeding. In mice and humans, adipose tissue secretes the anorexigenic hormone leptin into the bloodstream after meals, temporarily suppressing food intake through actions on hypothalamic neurons. Adipose tissue also releases ghrelin, an orexigenic hormone that stimulates food intake. Other peripheral mechanisms regulating short-term intake include mechanosensitive neurons in the GI tract and intestinally produced cholecystokinin (CCK) and glucagon-like peptide 1 (GLP-1), all of which are reported to act through vagal pathways to reduce food intake. Feeding in mice is also affected by the circadian cycle, and mice consume greater amounts of food during their active phase than during their rest phase.[1]

While many signals suppress food intake, specific properties of foods can encourage further intake, either through positive oral sensations or learned associations from post-ingestive reinforcement. Sweetness and fat, both detected via specialized receptors

located on the tongue, provide positive signals that can induce further food intake.[2,3] Once consumed, the value of glucose-containing foods is reinforced through glucose absorption in the small intestine, and analogous post-ingestive reinforcement is reported to occur with fat-containing foods.[4–6]

Environmental cues beyond dietary properties can also regulate feeding behavior. Animals will hesitate to initially consume a completely novel food source, termed "hyponeophagia."[7] In mice, generalized anxiety, stress, and fear may suppress food intake, and positive and negative associations with food can be entrained in mice through reward and fear conditioning.[8]

2.2 HEDONIC FEEDING AND CONSUMPTION INDUCED BY PALATABLE FOOD

Foods which provide pleasure upon consumption will be readily eaten by mice in the absence of immediate energetic need. These foods are often described in the scientific literature as "palatable" and the act of consuming them is termed "hedonic feeding."[9] While the palatability of a food is often encoded by its resulting gustatory sensation, dependent on sweetness or fat content, palatability can extend to foods that provide comfort when eaten or are associated with positive reward through learned cues or prior experiences.[9]

In mice, short-term access to a palatable food, including high-sucrose or high-fat diets, results in spontaneous food intake.[10–13] The consumption behavior observed when given brief or intermittent access to a palatable food is frequently referred to as "binge-like"

and is characterized by a sharp burst of intake in the moments after dietary presentation.[10] Prior work in which sucrose solutions of increasing concentration were administered to rats has found that the intake rate after palatable food exposure can be modeled using a function that exponentially decays and that the rate of intake is proportional to the perceived palatability of the food.[14] Other reports corroborate this argument, finding that the lick rate after solution presentation correlates with the sweetness of the solution.[15] Separate aspects of feeding structure are found to be modified by food palatability. Mice feed in "bouts," which are abrupt bursts of food intake. The duration of feeding bouts and the amount of food consumed within each bout increases with food palatability.[16]

The binge-like intake behavior is subject to biological regulation. Endocannabinoids (eCBs) are host-produced fatty-acid molecules that act both centrally and peripherally to augment binge-like behavior, and inhibition of eCB receptors significantly dampens intake in response to a palatable food.[17] Furthermore, many of the same mechanisms that universally restrict meal size, like gastric stretching and hormonal vagal communication may also reduce the amount of palatable food consumed during a binge.[18] Upon palatable food consumption, increased transmission of dopamine from the ventral tegmental area to the striatal brain regions, including the nucleus accumbens, is observed.[13,19,20] Additionally, central infusion of opioid receptor inhibitors diminishes palatable food intake,[21,22] and the neural circuits underlying opioidergic modulation of palatable food intake are being investigated.[23] Curiously, the neural underpinnings of homeostatic food intake, understood to be encoded in proopiomelanocortin-expressing and agouti-related

peptide-expressing neurons in the arcuate nucleus of the hypothalamus, are separate and dispensable for binge-like responses toward palatable foods in mice.[24]

2.3 EXPERIMENTAL METHODS TO STUDY FEEDING AND FOOD-MOTIVATED BEHAVIOR

There is an extensive variety of experimental methods to interrogate feeding in mice. Homeostatic food intake over days can be measured by weighing the food available to a single-housed mouse at multiple timepoints and interpreting the difference as food consumed. However, for binge-like feeding behaviors, which consist of abrupt feeding bouts and occur on scales of minutes to hours, more precise and frequent measurements are necessary. For this purpose, investigators frequently turn to automated machines that track food intake, either pellet dispensers that record pellets consumed, or computer-connected scales that monitor changes in the weight of a food hopper.[25] For liquid diets, systems include “lickometers,” which use changes in electrical signals detected upon contact with the mouse tongue, or video recordings of liquid levels changing over time in graduated dispensers.[26] The widespread adoption of 3D-printing technology has led to the development of inexpensive open-source pellet dispensers that can be assembled and placed into the mouse home cage for moderate-throughput behavioral testing.[25,27]

For some research questions, it is necessary to induce a strong food intake response in the absence of a palatable stimulus. In these cases, fasting-refeeding assays are employed. Mice can safely be housed in the absence of food for up to two days.[28] After fasting, the mice will rapidly consume large amounts of food to restore their energy balance. This

fasting-refeeding response is encoded in the hypothalamus, affected by leptin, and the meal size is restricted through GLP-1 signaling and vagal feedback.[1]

Finally, some experimental setups aim to measure the motivation to retrieve a food reward, a separate readout from differences in general consumption. The classical approach to measure motivation is to train the mouse to associate an action involving effort with the delivery of a small food reward.[29] In many protocols, the animal is trained for multiple days to either press a lever or poke their nose in a port to receive a reward pellet. The delivery of the pellet is accompanied with visual and aural accompaniment to accelerate the training process. After the mouse has successfully been trained according to a criterion of accuracy and engagement, the ratio of effort to reward is increased according to an exponential relationship. At a certain poke or lever press requirement for pellet retrieval, the mouse will lose interest or give up pursuing the food reward, and the final ratio completed, or "breakpoint," is used as a metric for motivated behavior.[27,30]

2.5 GUT MICROBIOTA EFFECTS ON FEEDING BEHAVIOR

The potent effects of the gut microbiota on host metabolism, immunity, and neural activity have led to investigation of microbial effects on feeding behaviors in multiple model organisms. One landmark study compared the metabolic profiles of GF and conventionally colonized mice and measured homeostatic food intake of a standard chow diet, finding that GF mice consumed slightly more chow than controls, which was ascribed to compensation for reduced liberation of dietary sugars in the absence of gut

microbial carbohydrate degradation.[31] Observed differences in homeostatic food intake between SPF mice and microbiota-depleted mice, either GF or ABX-treated, vary by study, by age, and by the diet that the mice are maintained on.[32,33] Intriguingly, one of the major byproducts of gut microbial fermentation, SCFAs, are consistently reported to reduce food intake when administered by oral gavage or through central routes.[34,35]

Two papers target the intersection of gut microbiota depletion and the feeding response to specific nutrients in mice. GF mice given two-day access to solutions of sucrose of increasing concentration exhibit concentration-dependent differences in intake behavior compared to SPF mice. The GF mice overconsumed an 8-16% (w/v) sucrose solution but not 0.5-4% (w/v) solution, suggesting a concentration or palatability-dependent microbiota effect on feeding of sugar solutions in mice. The authors also performed a similar experiment with varying levels of saccharin, an artificial sweetener, with no microbiota-dependent differences observed.[36] In a separate study, the feeding response to solutions with escalating concentrations of fat (0.15-1.25% (w/v)) was measured over a two-day period in GF and SPF mice. Germ-free status was associated with a significant increase in consumption of the fat solutions.[37]

Specific microbes and microbial communities have been demonstrated to affect feeding behaviors in multiple settings. GF mice colonized with microbiotas sourced from different species of foraging rodents exhibit changes in macronutrient preference, measured by the choice of consuming a high-protein or low-protein diet.[38] Treatment of mice with *Bacteroides uniformis* has been reported to reduce the binge-like consumption

response after a fast and reduce the intake of sucrose solutions.[39] A strain of *Lactobacillus johnsonii* discovered in a mouse model of constitutively active mTORC1 in myeloid cell populations was found to reduce homeostatic food intake when administered orally.[40] Two bacterial products, ClpB and muropeptides derived from bacterial cell wall components, have been shown to affect feeding behavior in mice.[41,42] ClpB from *E. coli* is a molecular mimic of the anorexigenic host alpha-melanocyte-stimulating hormone (α-MSH), and development of cross-reactive antibodies against ClpB can result in α-MSH depletion, leading to increased food intake.[42] Muropeptide signaling in Nod2-positive neurons in the hypothalamus is reported to reduce food intake in older female mice.[41] Microbiota-dependent alterations in host feeding and sensory behavior have also been reported in *Drosophila melanogaster* and *Caenorhabditis elegans*.[43,44]

Some models of metabolic disease exhibit changes in feeding behavior that may be ascribed to the microbiota. For instance, diet-induced obese (DIO) mice show a reduction in preference of a high-fat high-sugar (HFHS) diet compared to lean mice. Microbiota sourced from DIO donor mice and transplanted via FMT to lean mice resulted in reduced binge-like intake of a HFHS diet compared to mice receiving transplants from lean donor mice, suggesting that alterations in the gut microbiota may underlie changes in feeding behavior in metabolic disease states.[45] In humans, many eating disorders, including binge-eating disorder and anorexia nervosa co-present with alterations in the gut microbiota.[46–48]

Given the potent regulation of host metabolism by the gut microbiota, preliminary reports of microbiota modulation of feeding behaviors, and the shifts in microbial community composition in humans with eating disorders, a research investigation into gut microbiota effects on feeding behaviors in binge-like settings is warranted. This thesis comprehensively examines the changes in mouse feeding behavior and neural activity in response to palatable foods in the absence of the gut microbiota, explores gut microbe-dependent changes in motivational state, and identifies particular microbial species that mediate the effects of gut microbiota depletion on the consumption of palatable foods.

REFERENCES

1. Watts, A.G., Kanoski, S.E., Sanchez-Watts, G., and Langhans, W. (2021). The Physiological Control of Eating: Signals, Neurons, and Networks. Physiological Reviews.

2. Saper, C.B., Chou, T.C., and Elmquist, J.K. (2002). The Need to Feed: Homeostatic and Hedonic Control of Eating. Neuron *36*, 199–211. 10.1016/S0896-6273(02)00969-8.

3. Rossi, M.A., and Stuber, G.D. (2018). Overlapping Brain Circuits for Homeostatic and Hedonic Feeding. Cell Metabolism *27*, 42–56. 10.1016/j.cmet.2017.09.021.

4. Sclafani, A., Zukerman, S., and Ackroff, K. (2015). Postoral Glucose Sensing, Not Caloric Content, Determines Sugar Reward in C57BL/6J Mice. Chem Senses *40*, 245–258. 10.1093/chemse/bjv002.

5. Tan, H.-E., Sisti, A.C., Jin, H., Vignovich, M., Villavicencio, M., Tsang, K.S., Goffer, Y., and Zuker, C.S. (2020). The gut–brain axis mediates sugar preference. Nature *580*, 511–516. 10.1038/s41586-020-2199-7.

6. Li, M., Tan, H.-E., Lu, Z., Tsang, K.S., Chung, A.J., and Zuker, C.S. (2022). Gut-Brain Circuits for Fat Preference. Nature, 1–2. 10.1038/s41586-022-05266-z.

7. Deacon, R.M.J. (2011). Hyponeophagia: A Measure of Anxiety in the Mouse. J Vis Exp, 2613. 10.3791/2613.

8. Johnson, A.W. (2013). Eating beyond metabolic need: how environmental cues influence feeding behavior. Trends in Neurosciences *36*, 101–109. 10.1016/j.tins.2013.01.002.

9. Berridge, K.C. (1996). Food reward: Brain substrates of wanting and liking. Neuroscience & Biobehavioral Reviews *20*, 1–25. 10.1016/0149-7634(95)00033-B.

10. Corwin, R.L.W., and Babbs, R.K. (2012). Rodent Models of Binge Eating: Are They Models of Addiction? ILAR Journal *53*, 23–34. 10.1093/ilar.53.1.23.

11. Babbs, R.K., Kelliher, J.C., Scotellaro, J.L., Luttik, K.P., Mulligan, M.K., and Bryant, C.D. (2018). Genetic differences in the behavioral organization of binge eating, conditioned food reward, and compulsive-like eating in C57BL/6J and DBA/2J strains. Physiology & Behavior *197*, 51–66. 10.1016/j.physbeh.2018.09.013.

12. Kirkpatrick, S.L., Goldberg, L.R., Yazdani, N., Babbs, R.K., Wu, J., Reed, E.R., Jenkins, D.F., Bolgioni, A.F., Landaverde, K.I., Luttik, K.P., et al. (2017). Cytoplasmic FMR1-Interacting Protein 2 Is a Major Genetic Factor Underlying Binge Eating. Biological Psychiatry *81*, 757–769. 10.1016/j.biopsych.2016.10.021.

13. Jones, S.R., and Fordahl, S.C. (2021). Bingeing on High-Fat Food Enhances Evoked Dopamine Release and Reduces Dopamine Uptake in the Nucleus Accumbens. Obesity *29*, 721–730. 10.1002/oby.23122.

14. Davis, J.D. (1989). The Microstructure of Ingestive Behavior. Annals of the New York Academy of Sciences *575*, 106–121. 10.1111/j.1749-6632.1989.tb53236.x.

15. Davis, J.D., and Smith, G.P. (1988). Analysis of lick rate measure the positive and negative feedback effects of carbohydrates on eating. Appetite *11*, 229–238. 10.1016/S0195-6663(88)80005-9.

16. Taha, S.A., and Fields, H.L. (2005). Encoding of Palatability and Appetitive Behaviors by Distinct Neuronal Populations in the Nucleus Accumbens. J. Neurosci. *25*, 1193–1202. 10.1523/JNEUROSCI.3975-04.2005.

17. Parsons, L.H., and Hurd, Y.L. (2015). Endocannabinoid signalling in reward and addiction. Nat Rev Neurosci *16*, 579–594. 10.1038/nrn4004.

18. Campos, C.A., Bowen, A.J., Schwartz, M.W., and Palmiter, R.D. (2016). Parabrachial CGRP Neurons Control Meal Termination. Cell Metabolism *23*, 811–820. 10.1016/j.cmet.2016.04.006.

19. Tellez, L.A., Han, W., Zhang, X., Ferreira, T.L., Perez, I.O., Shammah-Lagnado, S.J., van den Pol, A.N., and de Araujo, I.E. (2016). Separate circuitries encode the hedonic and nutritional values of sugar. Nat Neurosci *19*, 465–470. 10.1038/nn.4224.

20. Di Chiara, G., and Bassareo, V. (2007). Reward system and addiction: what dopamine does and doesn't do. Current Opinion in Pharmacology *7*, 69–76. 10.1016/j.coph.2006.11.003.

21. Kelley, A.E., Bless, E.P., and Swanson, C.J. (1996). Investigation of the effects of opiate antagonists infused into the nucleus accumbens on feeding and sucrose drinking in rats. J Pharmacol Exp Ther *278*, 1499–1507.

22. Bodnar, R.J. (2019). Endogenous opioid modulation of food intake and body weight: Implications for opioid influences upon motivation and addiction. Peptides *116*, 42–62. 10.1016/j.peptides.2019.04.008.

23. Castro, D.C., Oswell, C.S., Zhang, E.T., Pedersen, C.E., Piantadosi, S.C., Rossi, M.A., Hunker, A.C., Guglin, A., Morón, J.A., Zweifel, L.S., et al. (2021). An endogenous opioid circuit determines state-dependent reward consumption. Nature *598*, 646–651.

24. Denis, R.G.P., Joly-Amado, A., Webber, E., Langlet, F., Schaeffer, M., Padilla, S., Cansell, C., Dehouck, B., Castel, J., Delbés, A.-S., et al. (2015). Palatability can drive feeding independent of AgRP neurons. Cell Metab *22*, 646–657. 10.1016/j.cmet.2015.07.011.

25. Nguyen, K.P., O'Neal, T.J., Bolonduro, O.A., White, E., and Kravitz, A.V. (2016). Feeding Experimentation Device (FED): A flexible open-source device for measuring feeding behavior. Journal of Neuroscience Methods *267*, 108–114. 10.1016/j.jneumeth.2016.04.003.

26. Thiele, T.E., Crabbe, J.C., and Boehm, S.L. (2014). "Drinking in the Dark" (DID): A Simple Mouse Model of Binge-Like Alcohol Intake. Curr Protoc Neurosci *68*, 9.49.1-9.49.12. 10.1002/0471142301.ns0949s68.

27. Matikainen-Ankney, B.A., Earnest, T., Ali, M., Casey, E., Wang, J.G., Sutton, A.K., Legaria, A.A., Barclay, K.M., Murdaugh, L.B., Norris, M.R., et al. (2021). An open-source device for measuring food intake and operant behavior in rodent home-cages. eLife *10*, e66173. 10.7554/eLife.66173.

28. Burnett, C.J., Funderburk, S.C., Navarrete, J., Sabol, A., Liang-Guallpa, J., Desrochers, T.M., and Krashes, M.J. (2019). Need-based prioritization of behavior. eLife *8*, e44527. 10.7554/eLife.44527.

29. Skinner, B.F. (2019). The Behavior of Organisms: An Experimental Analysis (B. F. Skinner Foundation).

30. Devarakonda, K., Nguyen, K.P., and Kravitz, A.V. (2016). ROBucket: A low cost operant chamber based on the Arduino microcontroller. Behav Res *48*, 503–509. 10.3758/s13428-015-0603-2.

31. Backhed, F., Ding, H., Wang, T., Hooper, L.V., Koh, G.Y., Nagy, A., Semenkovich, C.F., and Gordon, J.I. (2004). The gut microbiota as an environmental factor that regulates fat storage. Proceedings of the National Academy of Sciences *101*, 15718–15723. 10.1073/pnas.0407076101.

32. Zarrinpar, A., Chaix, A., Xu, Z.Z., Chang, M.W., Marotz, C.A., Saghatelian, A., Knight, R., and Panda, S. (2018). Antibiotic-induced microbiome depletion alters metabolic homeostasis by affecting gut signaling and colonic metabolism. Nat Commun *9*, 2872. 10.1038/s41467-018-05336-9.

33. Niimi, K., and Takahashi, E. (2019). New system to examine the activity and water and food intake of germ-free mice in a sealed positive-pressure cage. Heliyon *5*, e02176. 10.1016/j.heliyon.2019.e02176.

34. Frost, G., Sleeth, M.L., Sahuri-Arisoylu, M., Lizarbe, B., Cerdan, S., Brody, L., Anastasovska, J., Ghourab, S., Hankir, M., Zhang, S., et al. (2014). The short-chain fatty acid acetate reduces appetite via a central homeostatic mechanism. Nat Commun *5*, 3611. 10.1038/ncomms4611.

35. Li, Z., Yi, C.-X., Katiraei, S., Kooijman, S., Zhou, E., Chung, C.K., Gao, Y., van den Heuvel, J.K., Meijer, O.C., Berbée, J.F.P., et al. (2018). Butyrate reduces appetite and activates brown adipose tissue via the gut-brain neural circuit. Gut *67*, 1269–1279. 10.1136/gutjnl-2017-314050.

36. Swartz, T.D., Duca, F.A., Wouters, T. de, Sakar, Y., and Covasa, M. (2012). Up-regulation of intestinal type 1 taste receptor 3 and sodium glucose luminal transporter-1 expression and increased sucrose intake in mice lacking gut microbiota. British Journal of Nutrition *107*, 621–630. 10.1017/S0007114511003412.

37. Duca, F.A., Swartz, T.D., Sakar, Y., and Covasa, M. (2012). Increased Oral Detection, but Decreased Intestinal Signaling for Fats in Mice Lacking Gut Microbiota. PLoS One *7*, e39748. 10.1371/journal.pone.0039748.

38. Trevelline, B.K., and Kohl, K.D. (2022). The gut microbiome influences host diet selection behavior. Proceedings of the National Academy of Sciences *119*, e2117537119. 10.1073/pnas.2117537119.

39. Agustí, A., Campillo, I., Balzano, T., Benítez-Páez, A., López-Almela, I., Romaní-Pérez, M., Forteza, J., Felipo, V., Avena, N.M., and Sanz, Y. (2021). Bacteroides uniformis CECT

7771 Modulates the Brain Reward Response to Reduce Binge Eating and Anxiety-Like Behavior in Rat. Mol Neurobiol *58*, 4959–4979. 10.1007/s12035-021-02462-2.

40. Chagwedera, D.N., Ang, Q.Y., Bisanz, J.E., Leong, Y.A., Ganeshan, K., Cai, J., Patterson, A.D., Turnbaugh, P.J., and Chawla, A. (2019). Nutrient Sensing in CD11c Cells Alters the Gut Microbiota to Regulate Food Intake and Body Mass. Cell Metabolism *30*, 364-373.e7. 10.1016/j.cmet.2019.05.002.

41. Gabanyi, I., Lepousez, G., Wheeler, R., Vieites-Prado, A., Nissant, A., Wagner, S., Moigneu, C., Dulauroy, S., Hicham, S., Polomack, B., et al. (2022). Bacterial sensing via neuronal Nod2 regulates appetite and body temperature. Science *376*, eabj3986. 10.1126/science.abj3986.

42. Fetissov, S.O. (2017). Role of the gut microbiota in host appetite control: bacterial growth to animal feeding behaviour. Nat Rev Endocrinol *13*, 11–25. 10.1038/nrendo.2016.150.

43. O'Donnell, M.P., Fox, B.W., Chao, P.-H., Schroeder, F.C., and Sengupta, P. (2020). A neurotransmitter produced by gut bacteria modulates host sensory behaviour. Nature *583*, 415–420. 10.1038/s41586-020-2395-5.

44. Leitão-Gonçalves, R., Carvalho-Santos, Z., Francisco, A.P., Fioreze, G.T., Anjos, M., Baltazar, C., Elias, A.P., Itskov, P.M., Piper, M.D.W., and Ribeiro, C. (2017). Commensal bacteria and essential amino acids control food choice behavior and reproduction. PLOS Biology *15*, e2000862. 10.1371/journal.pbio.2000862.

45. de Wouters d'Oplinter, A., Rastelli, M., Van Hul, M., Delzenne, N.M., Cani, P.D., and Everard, A. (2021). Gut microbes participate in food preference alterations during obesity. Gut Microbes *13*, 1959242. 10.1080/19490976.2021.1959242.

46. Morita, C., Tsuji, H., Hata, T., Gondo, M., Takakura, S., Kawai, K., Yoshihara, K., Ogata, K., Nomoto, K., Miyazaki, K., et al. (2015). Gut Dysbiosis in Patients with Anorexia Nervosa. PLOS ONE *10*, e0145274. 10.1371/journal.pone.0145274.

47. Prochazkova, P., Roubalova, R., Dvorak, J., Kreisinger, J., Hill, M., Tlaskalova-Hogenova, H., Tomasova, P., Pelantova, H., Cermakova, M., Kuzma, M., et al. (2021). The intestinal microbiota and metabolites in patients with anorexia nervosa. Gut Microbes *13*, 1902771. 10.1080/19490976.2021.1902771.

48. Leyrolle, Q., Cserjesi, R., Mulders, M.D.G.H., Zamariola, G., Hiel, S., Gianfrancesco, M.A., Rodriguez, J., Portheault, D., Amadieu, C., Leclercq, S., et al. (2021). Specific gut microbial, biological, and psychiatric profiling related to binge eating disorders: A cross-sectional study in obese patients. Clinical Nutrition *40*, 2035–2044. 10.1016/j.clnu.2020.09.025.

Chapter 3

GUT MICROBIOTA SUPPRESS FEEDING INDUCED BY PALATABLE FOODS

Gut microbiota suppress feeding induced by palatable foods

James Ousey,[1] Joseph C. Boktor,[1] and Sarkis K. Mazmanian[1,2]

[1]Division of Biology and Biological Engineering, California Institute of Technology, 1200 E California Blvd, Pasadena, CA, 91125, USA

[2]Lead contact

*Correspondence: jousey@caltech.edu (J.O.), sarkis@caltech.edu (S.K.M.)

SUMMARY

Feeding behaviors depend on intrinsic and extrinsic factors including genetics, food palatability, and the environment.[1–5] The gut microbiota is a major environmental contributor to host physiology and impacts feeding behavior.[6–12] Here, we explored the hypothesis that gut bacteria influence behavioral responses to palatable foods, and reveal that antibiotic depletion (ABX) of the gut microbiota in mice results in overconsumption of several palatable foods with conserved effects on feeding dynamics. Gut microbiota restoration via fecal transplant into ABX mice is sufficient to rescue overconsumption of high-sucrose pellets. Operant conditioning tests found that ABX mice exhibit intensified motivation to pursue high-sucrose rewards. Accordingly, neuronal activity in mesolimbic brain regions, which have been linked with motivation and reward-seeking behavior,[3] was elevated in ABX mice after consumption of high-sucrose pellets. Differential antibiotic treatment and functional microbiota transplants identified specific gut bacterial taxa from the family S24-7 and the genus *Lactobacillus* whose abundances associate with suppression of high-sucrose pellet consumption. Indeed, colonization of mice with S24-7 and *Lactobacillus johnsonii* was sufficient to reduce overconsumption of high-sucrose pellets in an antibiotic-induced model of binge eating. These results demonstrate that extrinsic influences from the gut microbiota can suppress the behavioral response toward palatable foods in mice.

RESULTS

Regulation of feeding behaviors is critical for health.[13] Circulating metabolic signals,[1–3] gastrointestinal (GI) feedback,[4,5] and food palatability[14] are integrated to coordinate food pursuit and consumption. In mammals, feeding behavior is subdivided into homeostatic feeding, necessary to maintain energy balance, and hedonic feeding, driven by pleasure.[2,3,14–16]

Hedonic feeding is influenced by food palatability, an ascribed valuation of food reward influenced by taste and past food-associated experiences.[16,17] Under conditions of limited access, palatable food exposure will promptly induce feeding in rodents, even when unfasted.[18,19] This “binge-like” consumption behavior is frequently observed upon access to high-sugar or high-fat foods.[20] Behavioral analyses have uncovered that temporal characteristics of intake, such as feeding bout duration and consumption rate, associate with the sensory pleasure of the diet.[21–25] Operant conditioning assays measure the incentive salience of a palatable food by tracking the effort exerted to obtain a food reward.[26–28] The neural circuitry underlying hedonic feeding, primarily residing within the mesolimbic system, appears distinct from the hypothalamic circuitry regulating homeostatic feeding.[3,29]

The gut microbiota affects host metabolism and expression of feeding behaviors.[6–12] Germ-free (GF) mice and mice whose gut bacterial communities have been depleted with antibiotics show changes in glycemia and levels of circulating feeding hormones.[7,8] Administration of short-chain fatty acids (SCFAs), byproducts of gut microbial

fermentation, has anorectic effects in mice.[30,31] Studies have suggested microbiome-mediated effects on homeostatic feeding, but these observations vary depending on diet and age of mice.[7,8,32–34] Recent findings have uncovered gut microbiota influences on host diet selection and that hypothalamic sensing of microbial peptides regulates appetite in mice.[11,12] Regarding hedonic feeding, GF mice consume greater amounts of a sucrose solution over a 2-day period than conventional controls at high (8–16%), but not low (0.5–4%), sucrose concentrations, thus demonstrating a palatability-dependent gut microbiota effect on intake behavior.[35] Additionally, fecal microbiota transplantation (FMT) from diet-induced obese (DIO) mice transfers DIO-associated reductions in binge-like consumption to recipient animals.[9] A thorough characterization of gut microbiota effects on palatability-induced food intake behaviors has yet to be reported. Here, we explore how gut microbiota depletion may regulate the intake dynamics and incentive salience of palatable foods and investigate if specific gut bacterial species mediate microbiota-dependent changes in host feeding behavior.

Gut microbiota suppress high-sucrose pellet consumption in mice

To uncover microbiota-dependent differences in response to a palatable food, we treated C57BL/6J specific-pathogen free (SPF) mice with an oral antibiotic mixture that resulted in near-complete depletion of the intestinal commensal microbiota[36–38] without durable weight loss[8,38–40] or changes in homeostatic food intake[8,41] (Figure S1A–D). Unfasted antibiotic (ABX) and vehicle-treated (VEH) mice were then given free access to high-sucrose pellets via dispensers which record the times at which pellets are retrieved from the delivery port.[42] We validated that pellet retrieval events reflect consumption behavior

via manual scoring of video recordings (Figure S1E–F). ABX mice promptly retrieved greater numbers of high-sucrose pellets than VEH mice, with differences in cumulative pellet retrieval persisting for at least 2 hours (Figure 1A). After 3 hours of high-sucrose pellet availability, 100% (17/17) of the ABX cohort had obtained at least 50 pellets (1 gram) compared to 13% (2/16) of the VEH mice (Figure 1B). Differences in the pellet retrieval rate between ABX and VEH mice were greatest immediately after diet presentation and normalized after 1 hour (Figure 1C), a feature not ascribable to differences in latency to retrieve the first pellet (Figure S1G).

Feeding behavior in rodents is characterized by discrete bursts, or "bouts," of intake.[21,43,44] Upon high-sucrose pellet access, feeding bouts of ABX mice were significantly longer than those of VEH mice, with more pellets retrieved per bout (Figure 1D–E). ABX mice also demonstrated a strong trend toward an increased number of feeding bouts (Figure S1H). ABX mice exclusively fed the same high-sucrose diet ad libitum consumed less than VEH controls (Figure S1I). We controlled for vehicle and possible off-target antibiotic effects by administering ABX via intragastric[8] or subcutaneous routes (Figure S1J–K). Additionally, GF mice overconsumed high-sucrose pellets compared to SPF controls, although significant between-group differences manifested only after more than 1 hour had passed (Figure S1L–M).

ABX mice consumed significantly more high-sucrose pellets than VEH mice in a hole-board arena despite exhibiting similar levels of exploratory behavior, suggesting novelty-induced hypophagia associated with the food dispenser did not drive differences in pellet

consumption[45,46] (Figures 1F, S1N). Further, VEH and ABX mice did not display differences in generalized anxiety, a potential contributor to hyponeophagia,[47] as measured by the elevated plus maze and open field assays[48–51] (Figure S1O–P). Our data demonstrate that the absence of a gut microbiota in mice results in high-sucrose pellet overconsumption.

Gut microbiota reduce intake of various palatable foods

To evaluate if ABX mice universally overconsume in states of excessive intake, perhaps due to reduced post-ingestive negative feedback,[52,53] we induced hyperphagia by fasting mice and refeeding with standard chow or high-sucrose pellets. There was no effect of microbiota depletion in mice refed with chow (Figure S1Q). By contrast, ABX mice refed with high-sucrose pellets consumed approximately 60% more than VEH mice within 2 hours (Figure S1R), suggesting that microbiota effects on hyperphagic behavior depend on dietary composition. Next, VEH and ABX mice were given access to high-sucrose pellets or a mimic containing taste-inert cellulose.[54] Only the sucrose-containing pellets induced differential consumption between groups (Figure S1S). Remarkably, ABX mice also overconsumed pellets containing the non-metabolizable sweetener sucralose compared to VEH controls, suggesting the energy provided by dietary sucrose was unnecessary for microbiota-dependent intake differences (Figure S1T).

We tested if microbiota intake suppression extended to other palatable foods reported to prompt binge-like consumption in mice.[55,56] Gut microbiota depletion significantly augmented consumption of a high-fat diet (HFD) (Figure S2A) and Ensure® (Figure

S2B–C). In agreement with our high-sucrose pellet observations, the differences in Ensure® intake rate were greatest at the beginning of food access (Figure S2D). However, significant effects on the number and duration of Ensure® drinking bouts were not observed (Figure S2E–F). Thus, microbiota depletion increases spontaneous feeding of various palatable foods.

Microbiota restoration reverses high-sucrose pellet overconsumption of ABX mice

The gut microbiota of ABX animals can be restored through FMT.[57] We treated ABX mice with fecal transplants from SPF donors (ABX+FMT) or saline (ABX+SHAM), and confirmed that after 2 weeks, ABX+FMT mice had greater fecal microbial load, increased gut microbiome diversity, and harbored gut communities phylogenetically more similar to their pre-ABX state than ABX+SHAM mice (Figure S2G–K). ABX+FMT mice retrieved fewer high-sucrose pellets than ABX+SHAM mice, with cumulative intake not significantly differing from VEH mice (Figure 1F–G). The pellet retrieval dynamics of ABX+FMT mice recapitulated those of VEH mice, notably with a blunted response in the first hour after high-sucrose pellet presentation compared to ABX+SHAM treatment (Figure 1H and S2L). Furthermore, gut microbiota restoration was sufficient to rescue the increase in average bout length (Figure S2M). These findings are unlikely to depend on microbially-produced SCFAs, as SCFA supplementation of ABX mice had no effect on high-sucrose pellet retrieval (Figure S2N). Collectively, a complex gut microbiota is sufficient to suppress feeding induced by a high-sucrose diet in mice.

Gut microbiota alter the incentive salience of a palatable reward

To test if gut microbiota regulate the incentive salience of a high-sucrose reward, we trained VEH and ABX mice in a nose-poke operant conditioning paradigm[58] (Figure 2A). During 1-hour fixed-ratio 1 (FR1) training sessions, ABX mice retrieved approximately 50% more high-sucrose pellets each day than VEH mice (Figure 2B), with no between-treatment differences in learning (Figure S2O–P). Successfully trained animals underwent progressive ratio (PR) breakpoint testing, in which ABX mice completed greater ratio requirements than VEH mice to receive a high-sucrose pellet (Figure 2C), suggesting the microbiota suppresses motivation to pursue a food reward.

Activity in reward-related brain regions is affected by the gut microbiota

The perceived incentive salience of a reward is associated with activity in the mesolimbic dopaminergic neural system.[2,3,59–61] In mice given 1 hour of access to high-sucrose pellets, ABX treatment significantly augmented the level of brain activity observed in the ventral tegmental area (VTA), nucleus accumbens (NAc) core, and NAc shell compared to VEH controls, as a likely consequence of consuming a greater number of high-sucrose rewards (Figure 2D–E). VEH and ABX mice that did not receive high-sucrose pellets did not exhibit differences in neural activity in the same regions (Figure S3A–B). In contrast to the VTA and NAc, there was no significant effect of microbiota status on high-sucrose pellet-induced brain activity in the dorsal striatum, lateral hypothalamus (LH), or basolateral amygdala (BLA) (Figure S3C–D). Further, there were no differences in baseline neuronal activity of homeostatic hunger-encoding Neuropeptide Y-expressing (*NPY*+) neurons in the arcuate nucleus of the hypothalamus[62,63] (Figure S3E–F), or in

expression of hypothalamic neuropeptides that vary with homeostatic need[64–66] (Figure S3G), suggesting changes in energy balance are unlikely to mediate gut microbial regulation of palatable food intake. These results demonstrate that the microbiota influences neural activity in reward-related brain regions in mice administered high-sucrose pellets, but whether these effects are required for overconsumption of palatable foods remains unknown.

Specific microbial taxa associate with suppression of high-sucrose pellet intake

The gut microbiota contains various bacterial taxa with specialized functions.[67] We sought to identify if hedonic feeding suppression is a general property of the gut microbiota or specific to certain bacterial species. Mice were administered individual antibiotics from the ABX mixture, each having a different spectrum of antimicrobial activity, and assayed for high-sucrose pellet consumption. Ampicillin (A) and vancomycin-treated (V) mice exhibited elevated consumption of high-sucrose pellets compared to vehicle (VEH) controls, while mice administered neomycin (N) or metronidazole (M) demonstrated no significant differences in intake compared to VEH mice (Figure 3A–B).

To verify functional changes to the gut microbiota, we performed fecal transplants from differentially treated antibiotic donor mice into ABX-treated recipients. Remarkably, microbiota transplants from A- or V-treated mice were insufficient to rescue increased pellet consumption behaviors compared to FMT from VEH donor mice (Figure 3C–D), demonstrating that specific antibiotics robustly and durably remodeled the gut microbiota

to adopt an altered profile incapable of reducing host feeding behavior. The loss of function suggests microbial taxa sensitive to A and V suppress high-sucrose pellet consumption in mice.

16S ribosomal RNA gene sequencing confirmed that antibiotic treatment modified microbiome community composition, and V-, N-, and M-treated mice showed no significant change in fecal microbial load compared to VEH mice (Figures 3E–F, S4A–D). Differential abundance analysis revealed four amplicon sequence variants (ASVs) depleted in the microbiome of V-treated mice compared to VEH, N-, and M-treated microbiomes (Figure 3G–H). Three of the four vancomycin-depleted ASVs aligned to members of family S24-7, a largely uncultured taxon within the order Bacteroidales,[68] and the fourth corresponded to *Lactobacillus johnsonii* and *Lactobacillus gasseri*. We isolated a strain of *Lactobacillus* from our SPF mouse colony with perfect 16S rRNA sequence identity to the differentially abundant ASV and confirmed its identity as *L. johnsonii* (Figure S4E). *Akkermansia muciniphila* was more abundant in V-treated mice compared to the intake-suppressing VEH, N, and M microbiomes, suggesting *A. muciniphila* is unlikely to suppress high-sucrose pellet intake (Figure 3H).

As the microbial features associated with reduced food intake were identified in reference to the V condition, and we aimed to capture potential microbe-microbe interactions absent in ABX mice, we used vancomycin treatment as a model to explore the effect of specific microbes on feeding behavior. Employing a limited-access binge intake assay,[19,69,70] we found microbial transplants from SPF donor mice into vancomycin-

treated mice (V+SPF) suppressed high-sucrose pellet consumption while autologous FMT (V+Auto) or saline gavage (V+Sal) did not (Figure 4A–B). Compared to V+Auto and V+Sal mice, both vancomycin-naïve (VEH) and V+SPF mice displayed distinct changes in microbiome diversity and greater relative abundances of family S24-7 and an ASV corresponding to *L. johnsonii* (Figures 4C and S4F–G). To test if S24-7 and *L. johnsonii* contributed to the binge-suppressing outcome, vancomycin-treated animals were administered a fecal microbiota suspension from an SPF mouse (V+SPF), a mixture of commercially available S24-7 isolates and the previously isolated strain of *L. johnsonii* (V+4-mix), or *A. muciniphila* as a control (V+*A. muc*) (Figure 4D). 4-mix treatment was sufficient to suppress high-sucrose pellet consumption compared to *A. muciniphila* treatment (Figure 4E). We confirmed greater abundances of S24-7 and an ASV corresponding to *L. johnsonii* in the V+4-mix treatment group compared to V+*A. muc* mice (Figure 4F), with significant effects on microbial diversity (Figure S4H–I). We conclude that specific members of the commensal gut microbiota can suppress feeding behavior in mice induced by a palatable food.

DISCUSSION

Herein, we reveal that the gut microbiota reduces feeding induced in response to various palatable foods in mice. We find the gut microbiota diminishes the incentive salience of high-sucrose pellets and regulates activity in reward-related brain regions. Gut community profiling exposed microbial taxa associated with feeding suppression, and S24-7 family members and *L. johnsonii* were sufficient to reduce binge intake in an antibiotic-treatment model of overconsumption.

We found that microbiota-depleted mice overconsumed high-sucrose pellets, a HFD, and Ensure®, suggesting our observations may generalize to other rewarding foods. Indeed, a recent report has demonstrated an antibiotic-induced increase in binge-like consumption of a high-fat high-sugar diet in mice.[9] While these sweet and fat stimuli model the processed diets contributing to disease in current Western populations,[71] their composite nature limits our ability to draw conclusions about specific dietary properties required for microbiota-dependent changes in feeding. Targeted experiments involving foods with controlled levels of sweetness and fat, coupled with sensory pathway intervention, are needed to define these relationships. Pertinently, two-bottle tests reveal GF mice overconsume sucrose solutions and fat emulsions, and differentially express lingual fat-detection proteins compared to SPF controls.[35,72]

We observed microbiota-dependent changes in neural activity in the VTA and NAc, regions associated with hedonic feeding,[2,3,15] in line with reports that microbiota perturbations may affect brain activity.[73–75] Central regulators of palatable food intake, including dopamine, brain-derived neurotrophic factor, and endocannabinoids, differ in GF mice compared to mice with intact microbiotas,[76–78] and may regulate reward pathways that influence microbiota-mediated effects on palatable food consumption. Future research will explore specific molecular pathways linking the gut microbiota to mesolimbic brain activity.

Microbes from the S24-7 family and *L. johnsonii* are sufficient to suppress high-sucrose pellet intake in our model system, compared to treatment with *A. muciniphila*. Intriguingly, a strain of *Bacteroides uniformis*, of the same phylogenetic order as S24-7, can suppress binge eating in mice, and multiple species of *Lactobacillus* are reported to affect metabolism and feeding.[10,79–81] A next stage of this research will define the mechanisms required for gut microbes to suppress palatable food consumption.

Altered gut microbiome profiles have been associated with human eating disorders, including anorexia nervosa and binge-eating disorder,[82–86] as well as in rodent studies of palatable food intake, dietary preference, and eating disorder models.[9–11,87–89] Our findings contribute new insights to growing evidence for functional gut microbiota modulation of host feeding behavior and identify candidate species for further study.[10,12,13]

Figures and Legends

Figure 1. Gut bacteria suppress consumption of high-sucrose pellets in mice.
(A) Cumulative retrieval of high-sucrose pellets between VEH (n=16) and ABX (n=17) mice. Shown is the mean (± SEM) plotted every 5 minutes. Significance calculated via two-way repeated measures ANOVA using 30-minute timepoints followed by Šidák's multiple comparisons test.
(B) Empirical cumulative distribution plot of mice in VEH and ABX cohorts that have retrieved 50 high-sucrose pellets (1 gram). Significance calculated via Mann-Whitney U test.
(C) Modeled rates of high-sucrose pellet retrieval events for VEH and ABX mice. Shown is the mean (± SEM). Significance calculated via two-way repeated measures ANOVA using 30-minute timepoints followed by Šidák's multiple comparisons test.

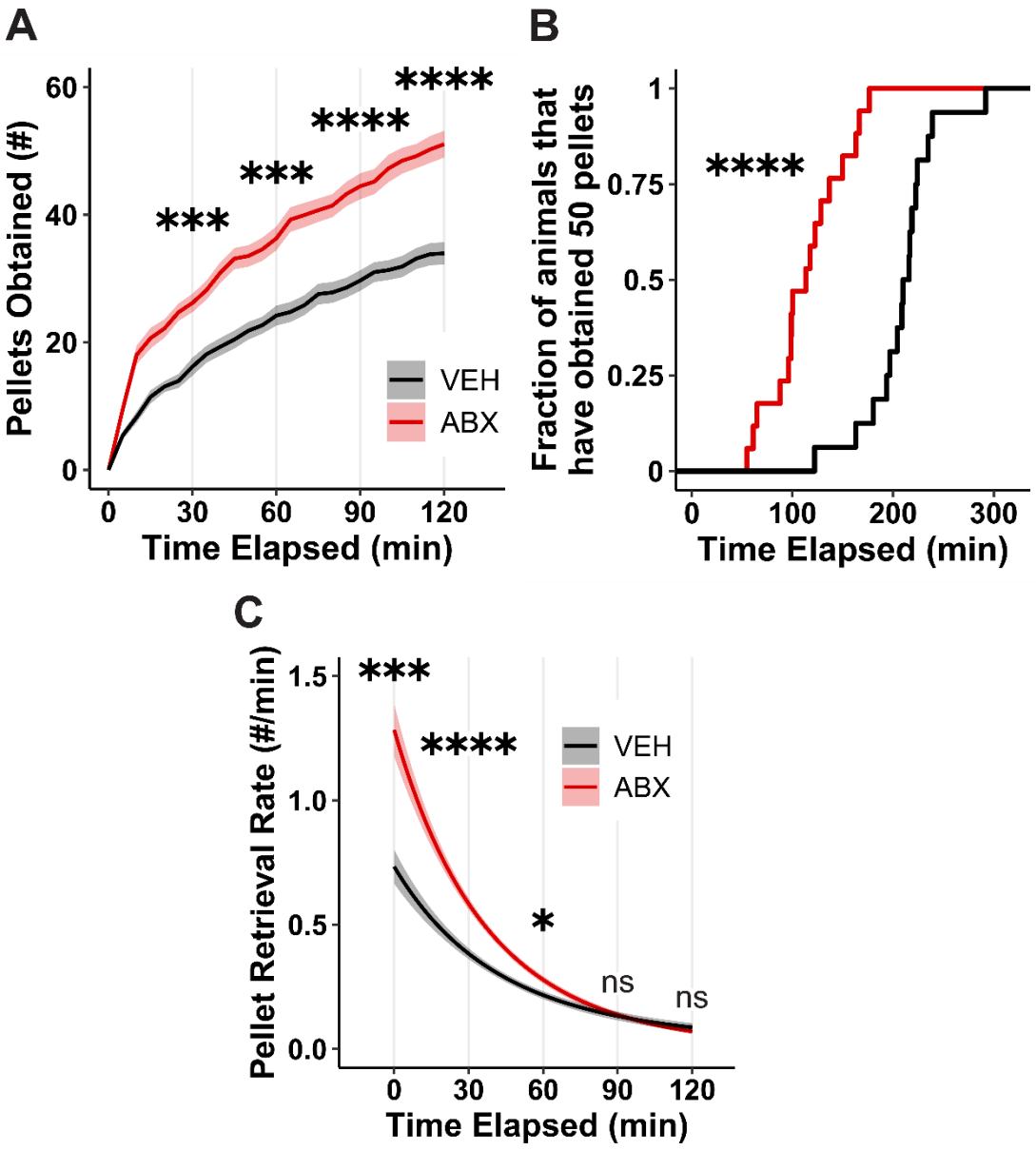

Figure 1. Gut bacteria suppress consumption of high-sucrose pellets in mice.
(D) Raster plot of pellet retrieval events.
(E) Bout structure analyses of high-sucrose pellet retrieval events over 2 hours of access. Shown is the mean (± SEM). Significance calculated via two-tailed Student's t-test.
(F) High-sucrose pellets eaten by VEH (n=9) and ABX (n=12) mice in a 10-minute stimulus-baited hole-board assay. Shown is the mean (± SEM). Significance calculated via two-tailed Student's t-test.

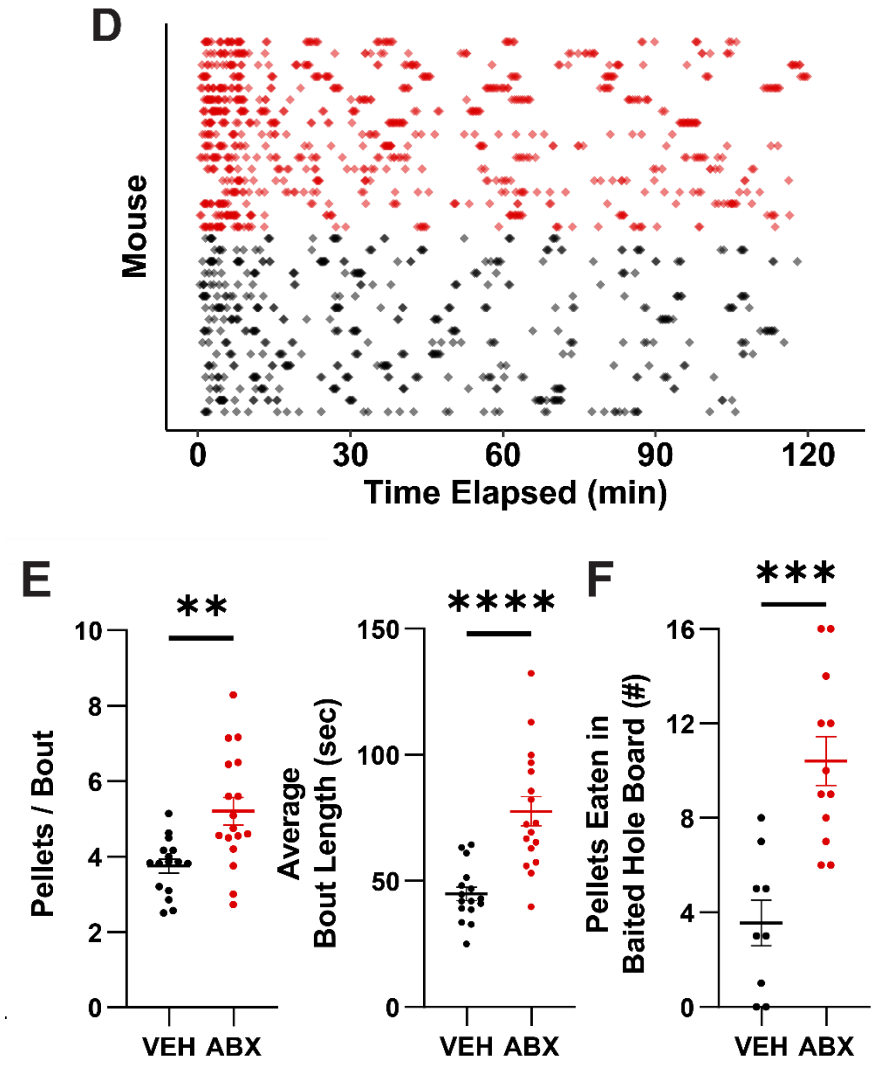

Figure 1. Gut bacteria suppress consumption of high-sucrose pellets in mice.
(G) Cumulative retrieval of high-sucrose pellets between VEH (n=10), ABX+SHAM (n=9), and ABX+FMT (n=10) mice. Shown is the mean (± SEM) plotted every 5 minutes. Significance calculated via two-way repeated measures ANOVA using 30-minute timepoints followed by Tukey's multiple comparisons test (within timepoints). Black and blue asterisks denote ABX+SHAM vs. VEH and ABX+SHAM vs. ABX+FMT comparison significance, respectively. See also Figure S1.
(H) Empirical cumulative distribution plot of mice in VEH, ABX+SHAM, and ABX+FMT cohorts that have retrieved 1 gram of high-sucrose pellets. Significance calculated via one-way ANOVA Kruskal-Wallis followed by Dunn's multiple comparisons test.
(I) Modeled rates of pellet retrieval events for VEH, ABX+SHAM, and ABX+FMT mice. Shown is the mean (± SEM). Significance calculated via two-way repeated measures ANOVA using 30-minute timepoints followed by Tukey's multiple comparisons test (within timepoints). Black and blue asterisks denote ABX+SHAM vs. VEH and ABX+SHAM vs. ABX+FMT comparison significance, respectively.

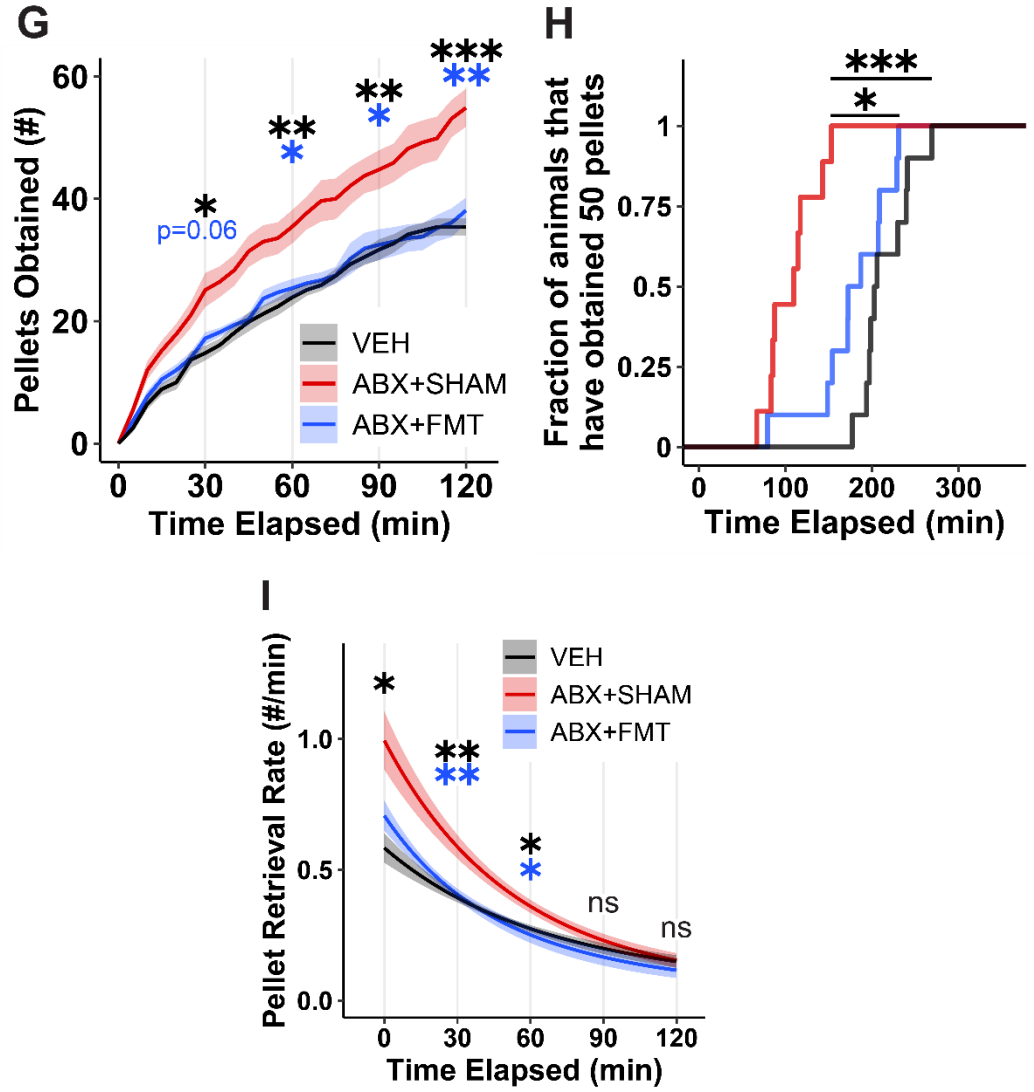

Figure S1. Physiological and behavioral measurements of microbiota-depleted mice reveal effects on food intake are robust and depend on dietary composition, Related to Figure 1.
(A) Quantification of aerobic and anaerobic microbial growth via colony-forming-unit analysis from fecal samples of VEH and ABX mice (n=5/group) on non-selective media after 4 weeks of treatment. n.d.: not detected. Shown is the mean (± SEM). Significance calculated via two-tailed Student's t-tests.
(B) Microbial load in fecal samples relative to VEH mice as measured by qPCR with universal bacterial primers. Shown is the mean (± SEM). Significance calculated via two-tailed Student's t-test (n=8/group).

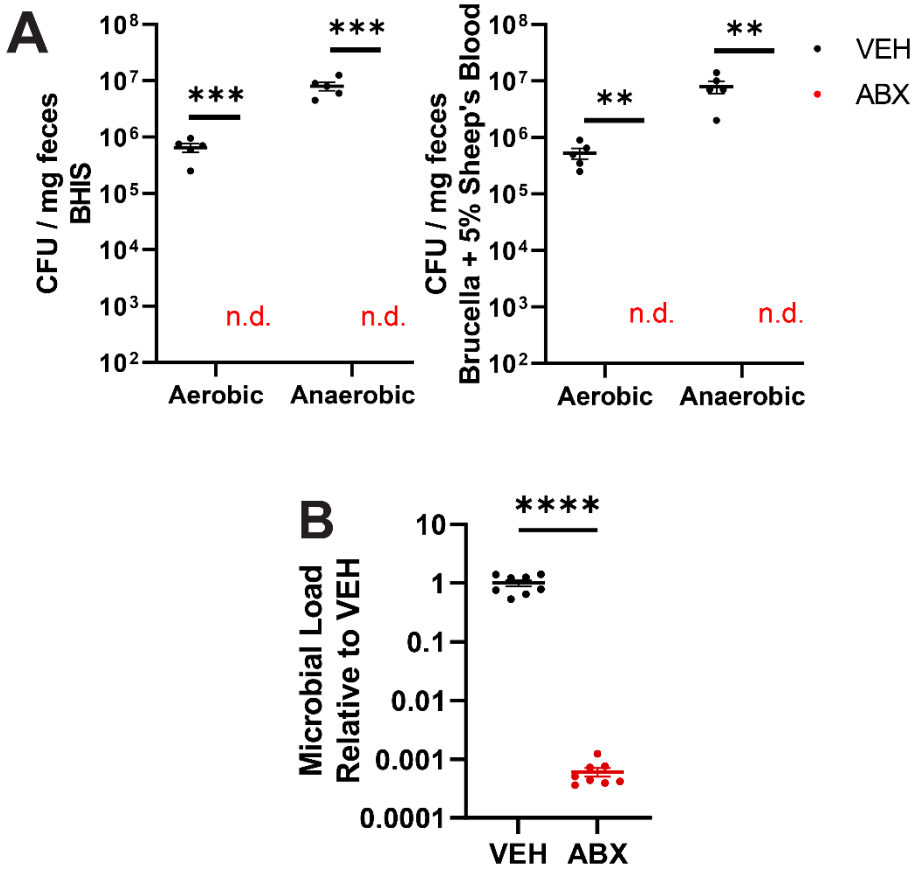

Figure S1. Physiological and behavioral measurements of microbiota-depleted mice reveal effects on food intake are robust and depend on dietary composition, Related to Figure 1.
(C) Body weight of VEH and ABX-treated animals (n=12/group) immediately prior to and after 4 weeks of treatment. Shown is the mean (± SEM). Treatment effect and Time × Treatment interaction effect significance calculated via two-way repeated measures ANOVA.
(D) Chow intake of single-housed VEH and ABX (n=10/group) mice over 4 weeks of treatment. Shown is the mean (± SEM). Significance calculated via two-tailed Student's t-test.
(E) Quantification of FED reflection of consumption behavior in VEH and ABX mice (n=5/group) determined via comparison of FED-recorded high-sucrose pellet retrieval events to manual video analysis of pellets consumed during 2 hours of free access. Shown is the mean (± SEM) for both treatment groups.
(F) K-S statistics and p-values of within-subject comparisons of cumulative distribution functions of FED-recorded pellet retrieval events and manually recorded pellet consumption events in VEH and ABX mice (n=5/group).

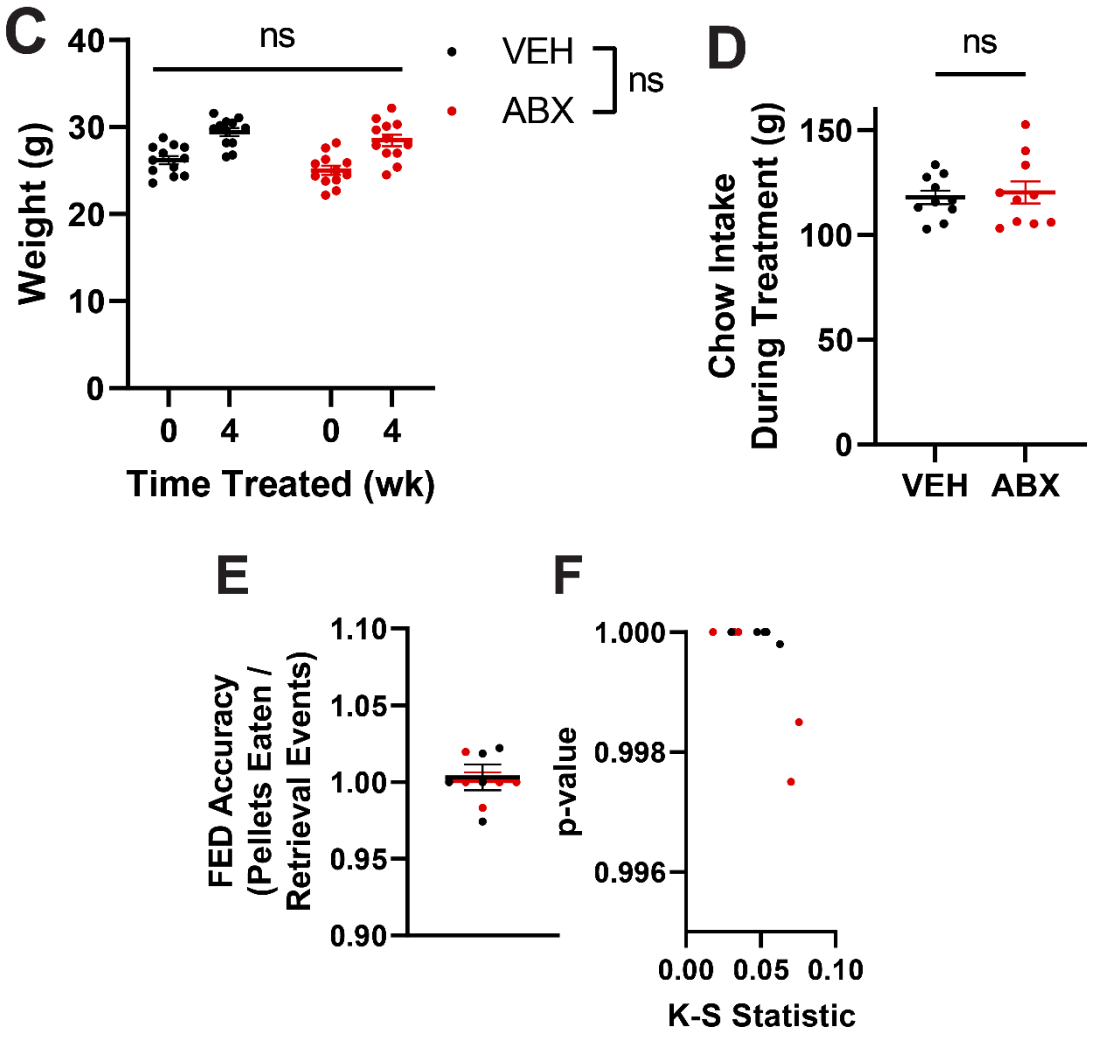

Figure S1. Physiological and behavioral measurements of microbiota-depleted mice reveal effects on food intake are robust and depend on dietary composition, Related to Figure 1.
(G) Latency to retrieve the first pellet in VEH (n=16) and ABX (n=17) mice. Shown is the mean (± SEM). Significance calculated via two-tailed Student's t-test.
(H) Cumulative feeding bouts over the first 2 hours of high-sucrose pellet exposure in VEH (n=16) and ABX (n=17) mice. Shown is the mean (± SEM). Significance calculated via two-tailed Student's t-test.
(I) Home cage intake of high-sucrose AIN-76A tablets in single-housed VEH and ABX (n=5/group) mice over 1 week. Shown is the mean (± SEM). Significance calculated via two-tailed Student's t-test.

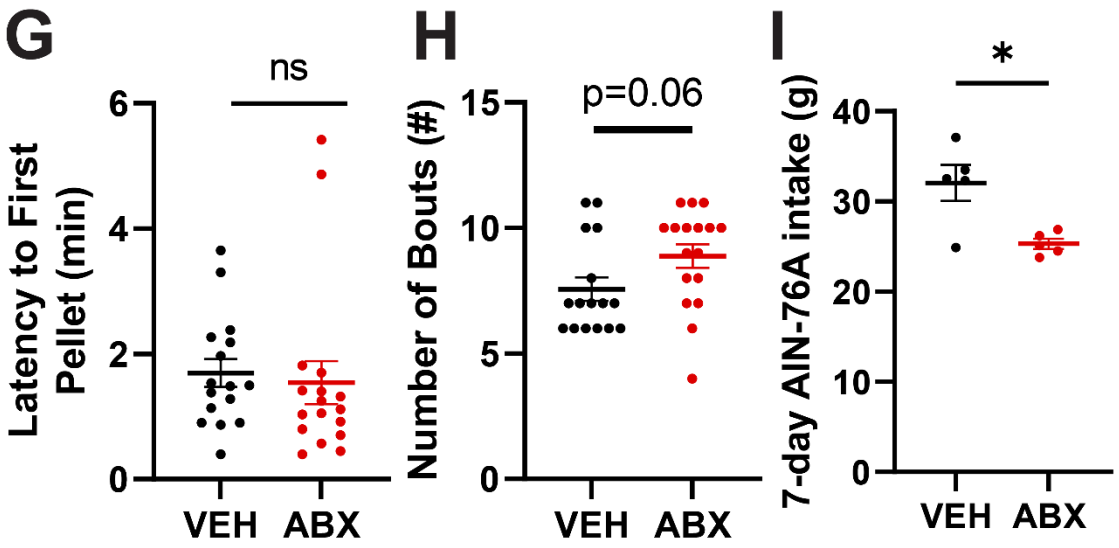

Figure S1. Physiological and behavioral measurements of microbiota-depleted mice reveal effects on food intake are robust and depend on dietary composition, Related to Figure 1.
(J) Cumulative retrieval of high-sucrose pellets between VEH-gavage (VEH – i.g., n=10) and ABX-gavage (ABX – i.g., n=8) mice. Shown is the mean (± SEM) plotted every 5 minutes. Significance calculated via two-way repeated measures ANOVA using 30-minute timepoints followed by Šidák's multiple comparisons test.
(K) Cumulative retrieval of high-sucrose pellets between VEH-subcutaneous (VEH – s.c.) and ABX-subcutaneous (ABX – s.c.) mice (n=8/group). Shown is the mean (± SEM) plotted every 5 minutes. Time × Treatment interaction effect significance calculated via two-way repeated measures ANOVA using 30-minute timepoints.
(L) Cumulative retrieval of high-sucrose pellets between SPF and germ-free (GF) mice (n=10/group). Shown is the mean (± SEM) plotted every 5 minutes. Timepoint and Time × Treatment interaction effect significance calculated via two-way repeated measures ANOVA using 30-minute timepoints followed by Šidák's multiple comparisons test.
(M) Empirical cumulative distribution plot of mice in SPF and GF cohorts that have retrieved 50 high-sucrose pellets (1 gram). Significance calculated via Mann-Whitney U test.

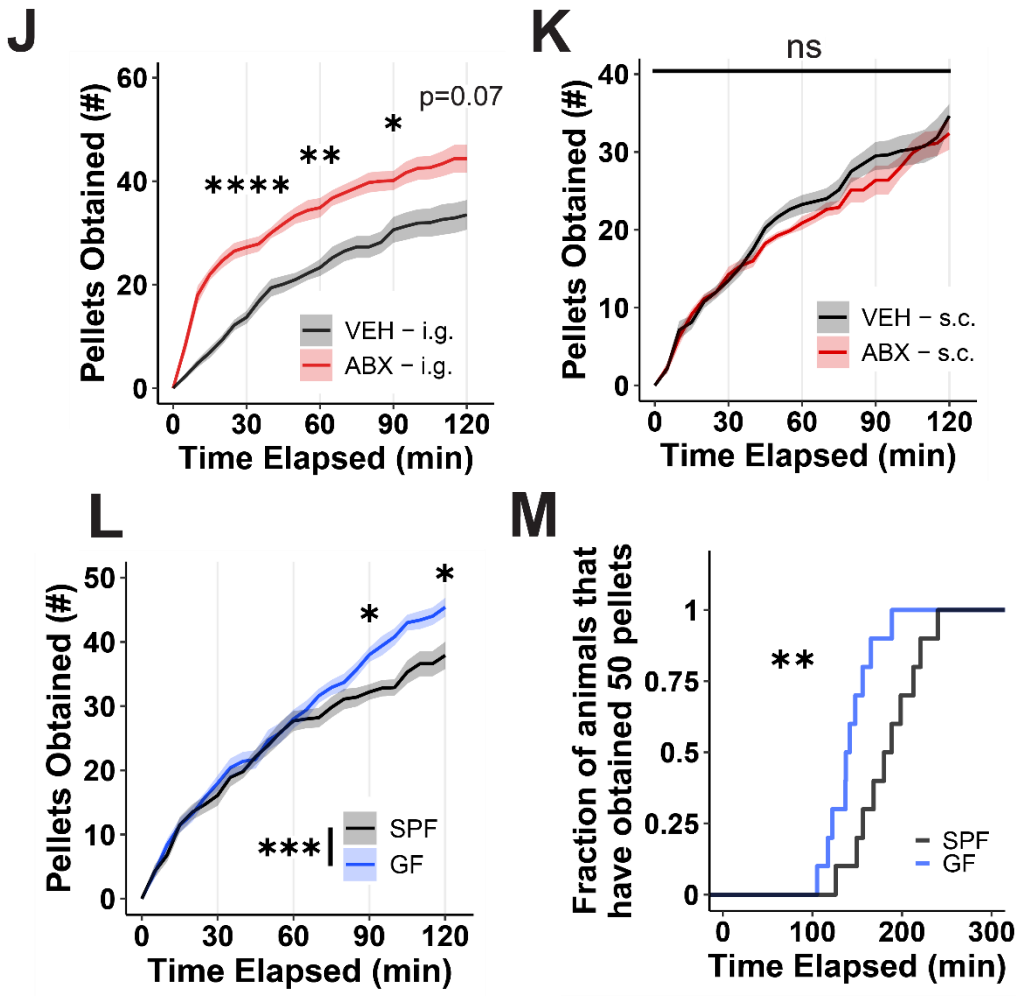

Figure S1. Physiological and behavioral measurements of microbiota-depleted mice reveal effects on food intake are robust and depend on dietary composition, Related to Figure 1.
(N) Spontaneous exploratory head dips from VEH (n=9) and ABX (n=11) mice in a 10-minute empty hole-board assay. Shown is the mean (± SEM). Significance calculated via two-tailed Student's t-test.
(O) Open-arm time measurements for VEH (n=8) and ABX (n=12) in an elevated plus maze assay for anxiety. Shown is the mean (± SEM). Significance calculated via two-tailed Student's t-test.
(P) Exposed center time measurements for VEH and ABX (n=10/group) in an open field assay for anxiety. Shown is the mean (± SEM). Significance calculated via two-tailed Student's t-test.

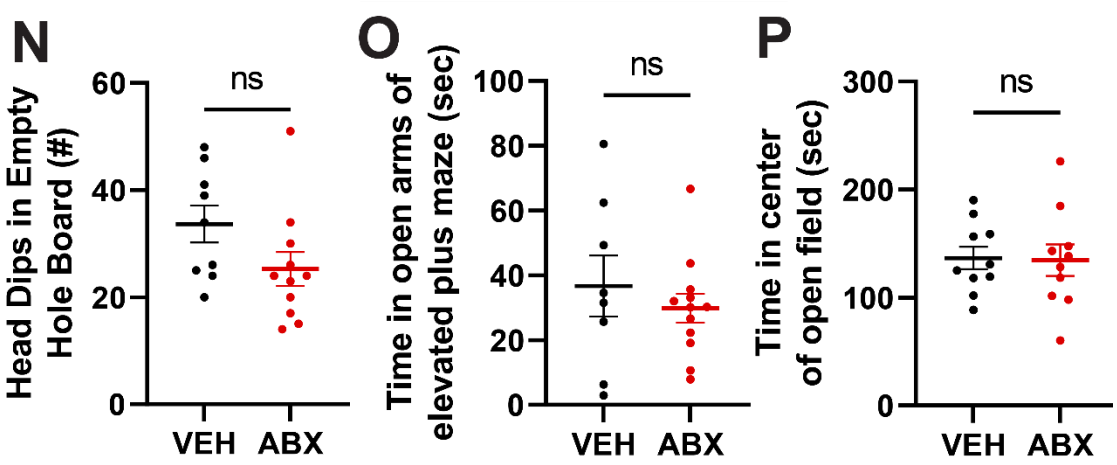

Figure S1. Physiological and behavioral measurements of microbiota-depleted mice reveal effects on food intake are robust and depend on dietary composition, Related to Figure 1.
(Q) Fasting-refeeding measurements of fasted VEH (n=8) and ABX (n=7) mice when refed with standard chow. Shown is the mean (± SEM). Time × Treatment interaction effect significance calculated via two-way repeated measures ANOVA.
(R) Fasting-refeeding pellet retrieval measurements of fasted VEH (n=6) and ABX (n=7) mice when refed with high-sucrose pellets. Shown is the mean (± SEM) plotted every 5 minutes. Significance calculated via two-way repeated measures ANOVA using 30-minute timepoints followed by Šidák's multiple comparisons test.
(S) Intake during 10-minute brief-access assays of different edible stimuli presented to VEH and ABX treated mice (n=12/group). Shown is the mean (± SEM). Significance calculated via two-way repeated measures ANOVA followed by Šidák's multiple comparisons test.
(T) Cumulative retrieval of 2% (w/w) sucralose pellets in VEH (n=8) and ABX (n=6) mice. Shown is the mean (± SEM) plotted every 5 minutes. Significance calculated via two-way repeated measures ANOVA using 30-minute timepoints followed by Šidák's multiple comparisons test.

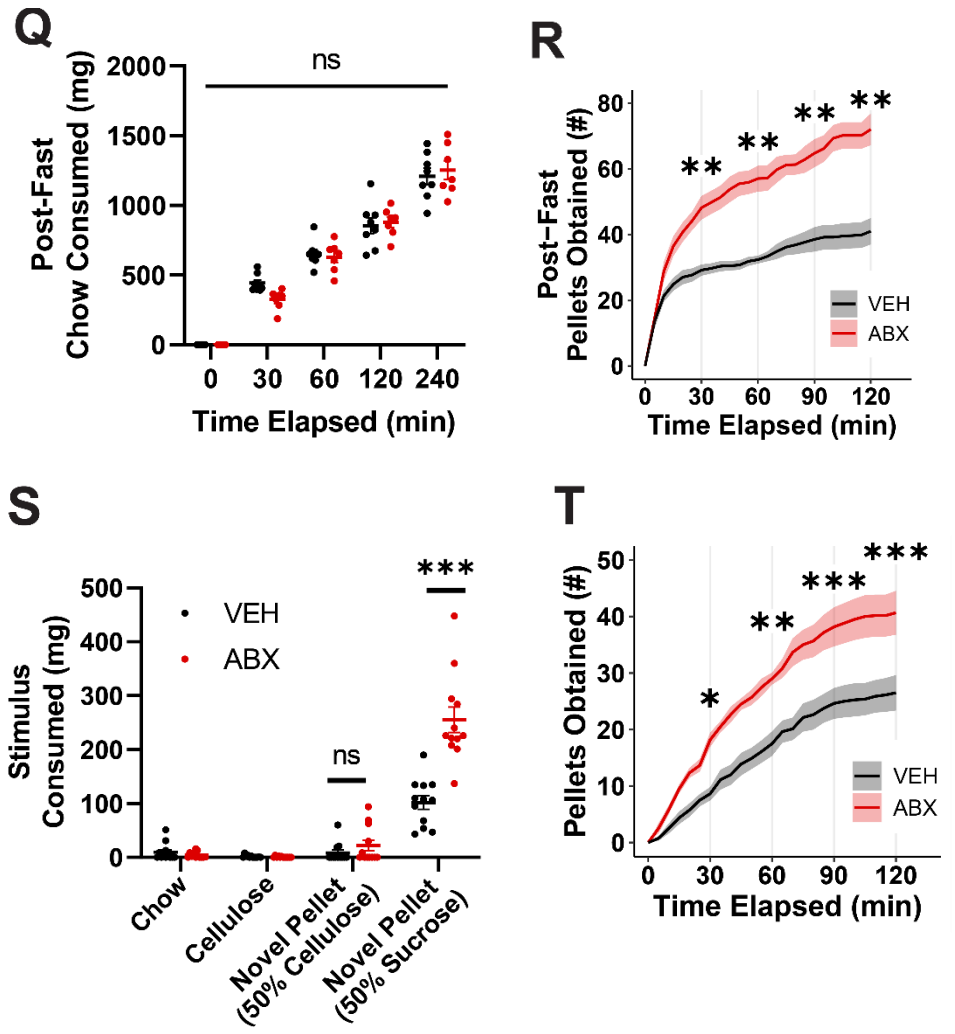

Figure 2. Gut microbiota reduce the incentive salience of a high-sucrose reward and decrease activity in mesolimbic brain regions linked to reward behaviors.
(A) Schematic illustrating timeline of fixed-ratio 1 (FR1) training and progressive-ratio (PR) breakpoint testing.
(B) High-sucrose pellets obtained during daily FR1 training sessions of VEH (n=12) and ABX (n=12) mice. Shown is the mean (± SEM). Significance calculated via two-way repeated measures ANOVA followed by Šidák's multiple comparisons test. See also Figure S2.
(C) Breakpoints of VEH (n=10) and ABX (n=12) mice from the progressive ratio requirement assay. Shown is the mean (± SEM). Significance calculated via two-tailed Student's t-test. See also Figure S2.

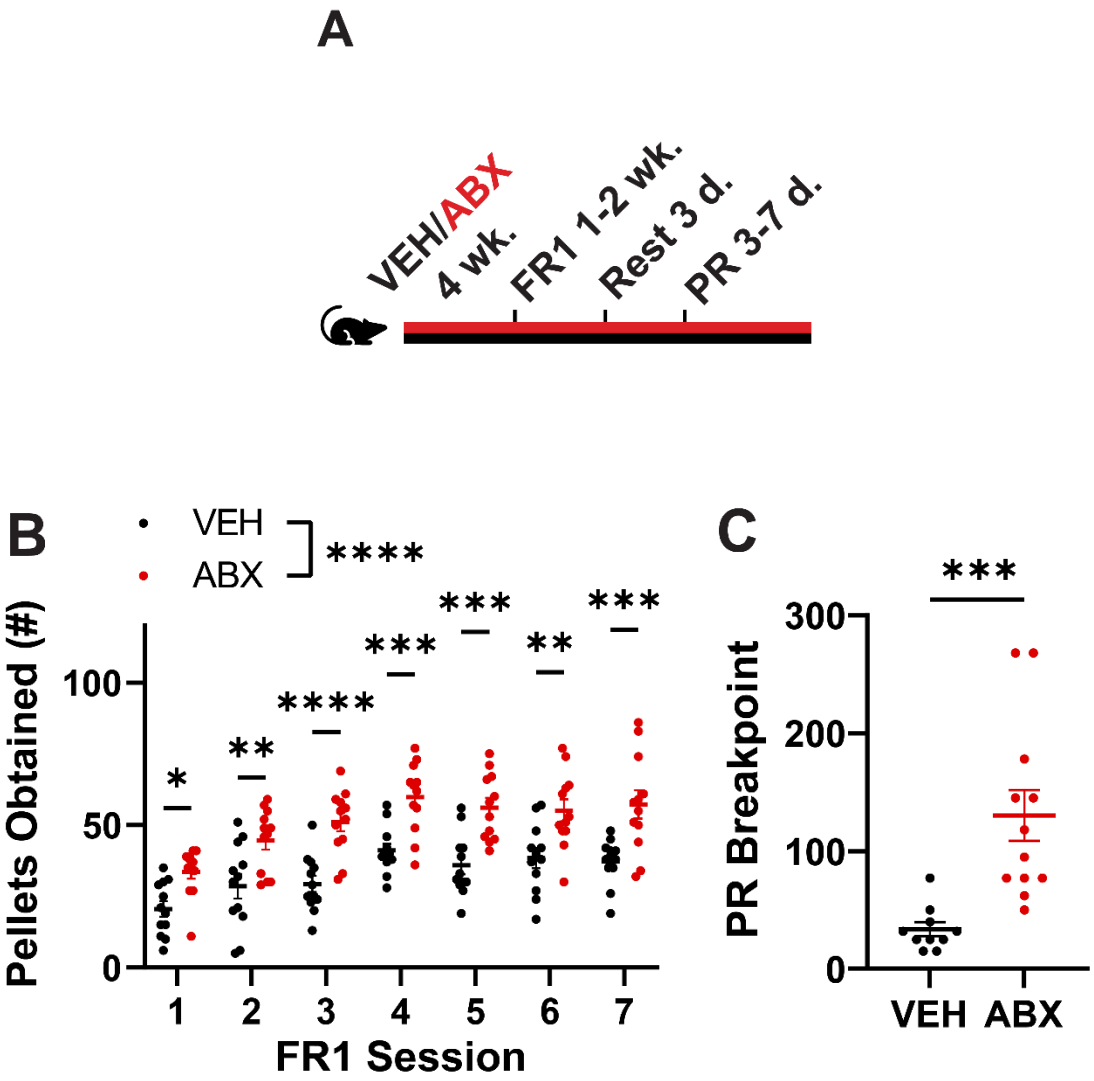

Figure 2. Gut microbiota reduce the incentive salience of a high-sucrose reward and decrease activity in mesolimbic brain regions linked to reward behaviors.
(D) Representative images of the nucleus accumbens (NAc) and ventral tegmental area (VTA) in VEH and ABX mice given 1 hour of free access to high-sucrose pellets, with c-Fos intensity represented in green. Scale bars are 100 microns. Images are cropped to emphasize the region of interest.
(E) Density of c-Fos+ neurons in the NAc shell, NAc core, and VTA (n=8/group) after 1 hour of access to high-sucrose pellets. Shown is the mean (± SEM). Significance calculated via two-way ANOVA with microbiota status and access to high-sucrose pellets as factors, followed by Bonferroni's multiple comparisons test (within brain regions). Data for mice not given access to high-sucrose pellets is shown in Figures S3A–B.

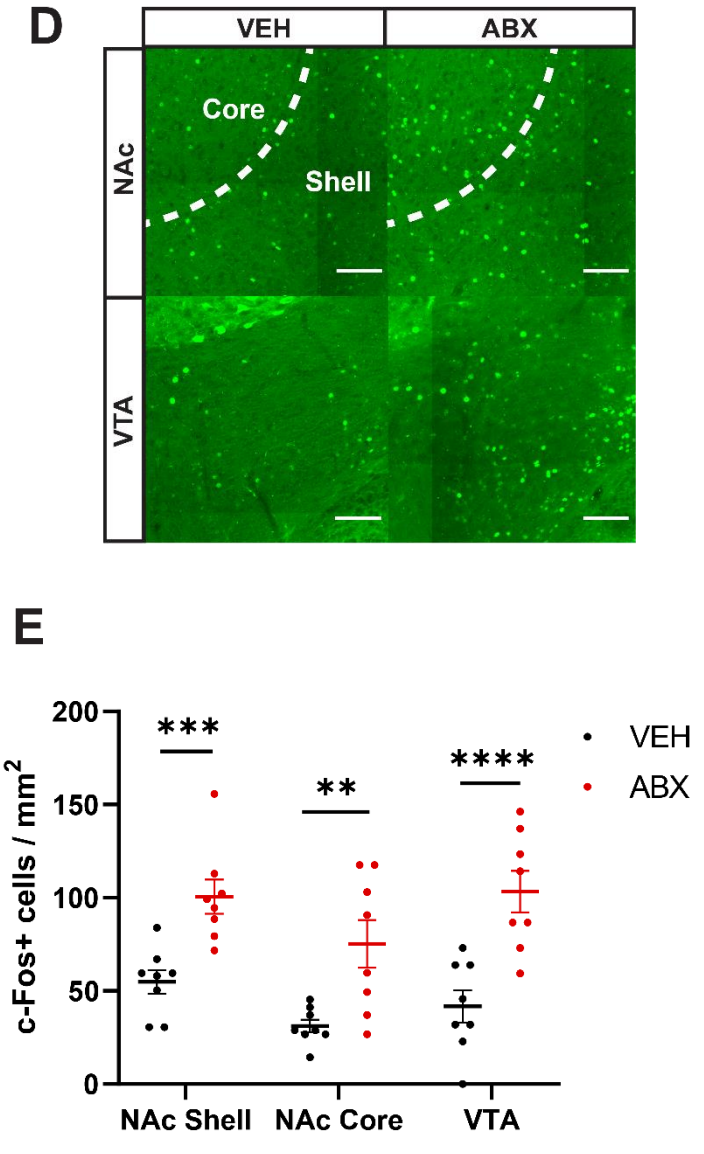

Figure S2. Additional behavioral parameters from free-feeding and operant conditioning assays and microbiome diversity measurements of FMT recipient mice, Related to Figures 1 and 2.

(A) Cumulative consumption of a high-fat diet in VEH and ABX mice (n=10/group). Shown is the mean (± SEM). Treatment effect significance calculated via two-way repeated measures ANOVA at 30-minute timepoints followed by Šidák's multiple comparisons test.

(B) Cumulative consumption of Ensure® in VEH and ABX mice (n=10/group). Shown is the mean (± SEM). Significance calculated via two-way repeated measures ANOVA at 30-minute timepoints followed by Šidák's multiple comparisons test.

(C) Cumulative time drinking Ensure® in VEH and ABX mice (n=10/group). Shown is the mean (± SEM). Significance calculated via two-way repeated measures ANOVA at 30-minute timepoints followed by Šidák's multiple comparisons test.

(D) Consumption of Ensure® in VEH and ABX mice (n=10/group) across 30-minute intervals. Shown is the mean (± SEM). Significance calculated via two-way repeated measures ANOVA followed by Šidák's multiple comparisons test.

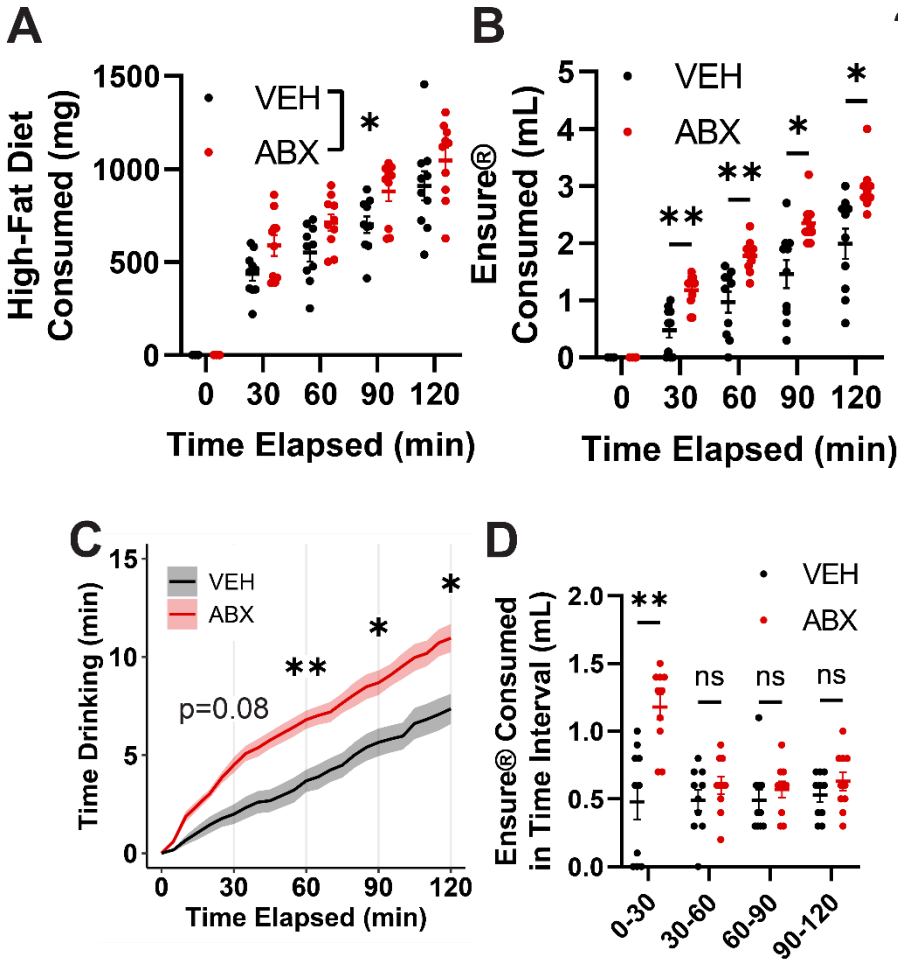

Figure S2. Additional behavioral parameters from free-feeding and operant conditioning assays and microbiome diversity measurements of FMT recipient mice, Related to Figures 1 and 2.

(E) Raster plot of Ensure® drinking bouts in VEH and ABX mice.

(F) Bout structure analyses of Ensure ® drinking bouts over 2 hours of access. Shown is the mean (± SEM). Significance calculated via two-tailed Student's t-test.

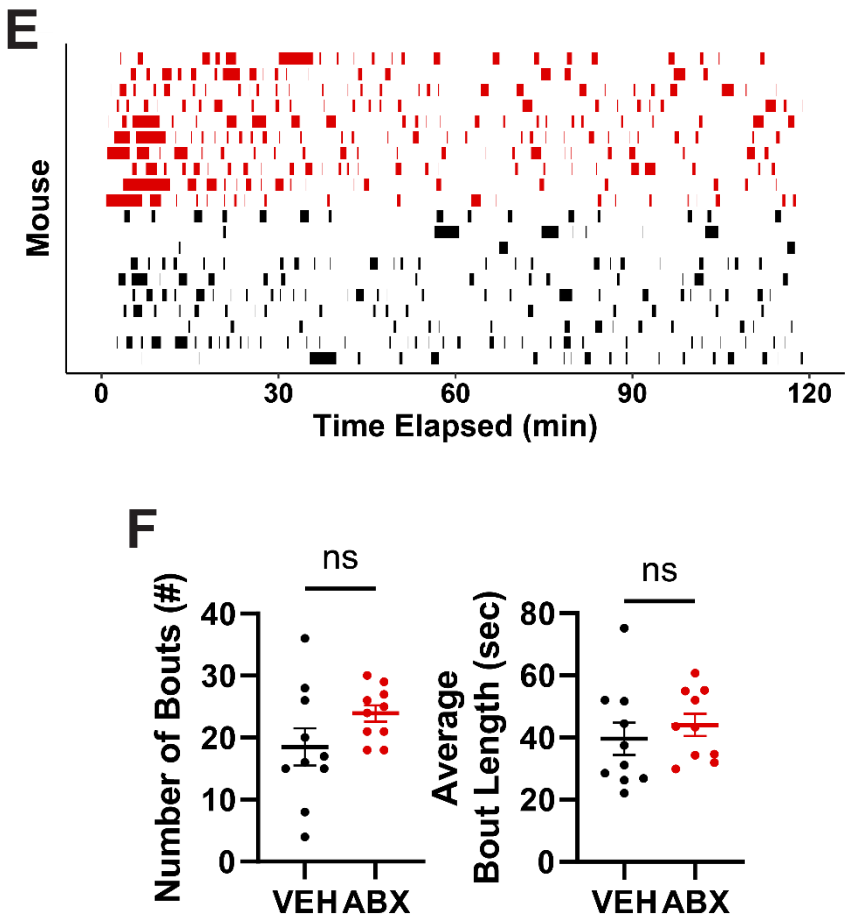

Figure S2. Additional behavioral parameters from free-feeding and operant conditioning assays and microbiome diversity measurements of FMT recipient mice, Related to Figures 1 and 2.

(G) Quantification of aerobic and anaerobic microbial growth via colony-forming-unit analysis from fecal samples of VEH, ABX+SHAM, and ABX+FMT mice ((Week 6, ABX+SHAM n=5), n=8/group all others) on non-selective media over the course of treatment. Shown is the mean (± SEM). Significance calculated via mixed-effects modeling followed by Tukey's multiple comparisons test (within timepoints). Black and blue asterisks denote ABX+SHAM vs. VEH and ABX+SHAM vs. ABX+FMT comparison significance, respectively.

(H) Microbial load in fecal samples of ABX+SHAM (n=5) and ABX+FMT (n=8) mice relative to VEH (n=8) mice at 6 weeks of treatment (2 weeks post-FMT) as measured by qPCR with universal bacterial primers. Shown is the mean (± SEM). Significance calculated via one-way ANOVA followed by Tukey's multiple comparisons test.

(I) Faith's Phylogenetic Diversity in VEH (n=8), ABX+SHAM (Week 0 n=8, Week 6 n=5), and ABX+FMT (n=8) mice at baseline and 6 weeks of treatment. Shown is the mean (± SEM). Significance calculated via mixed-effects modeling followed by Tukey's multiple comparisons test (within timepoints).

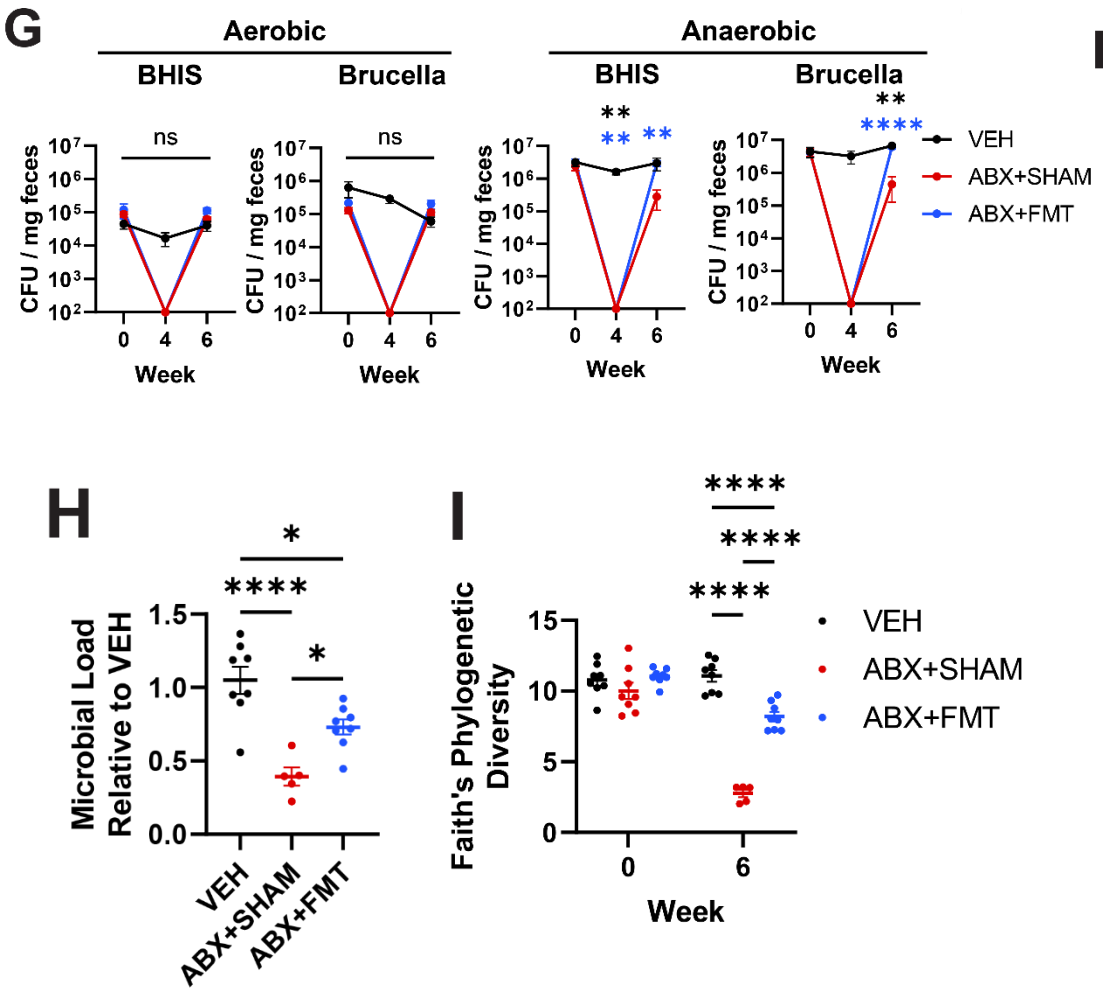

Figure S2. Additional behavioral parameters from free-feeding and operant conditioning assays and microbiome diversity measurements of FMT recipient mice, Related to Figures 1 and 2.

(J) PCoA of weighted UniFrac distances in VEH (n=8), ABX+SHAM (Week 0 n=8, Week 6 n=5), and ABX+FMT (n=8) mice at baseline and at 6 weeks of treatment.

(K) Within-subject weighted UniFrac distances in VEH (n=8), ABX+SHAM (n=5), and ABX+FMT (n=8) mice at 6 weeks of treatment compared to baseline. Shown is the mean (± SEM). Significance calculated via one-way ANOVA Kruskal-Wallis of within-subject distance comparisons to baseline followed by Mann-Whitney U tests subject to FDR correction as implemented in QIIME2. See also Table S1.

(L) Raster plot of pellet retrieval events of mice in VEH, ABX+SHAM, and ABX+FMT cohorts.

(M) Microstructure analyses of pellet retrieval events of mice in VEH, ABX+SHAM, and ABX+FMT cohorts over the first 2 hours of high-sucrose pellet exposure. Shown is the mean (± SEM). Significance calculated via one-way ANOVA followed by Tukey's multiple comparisons test.

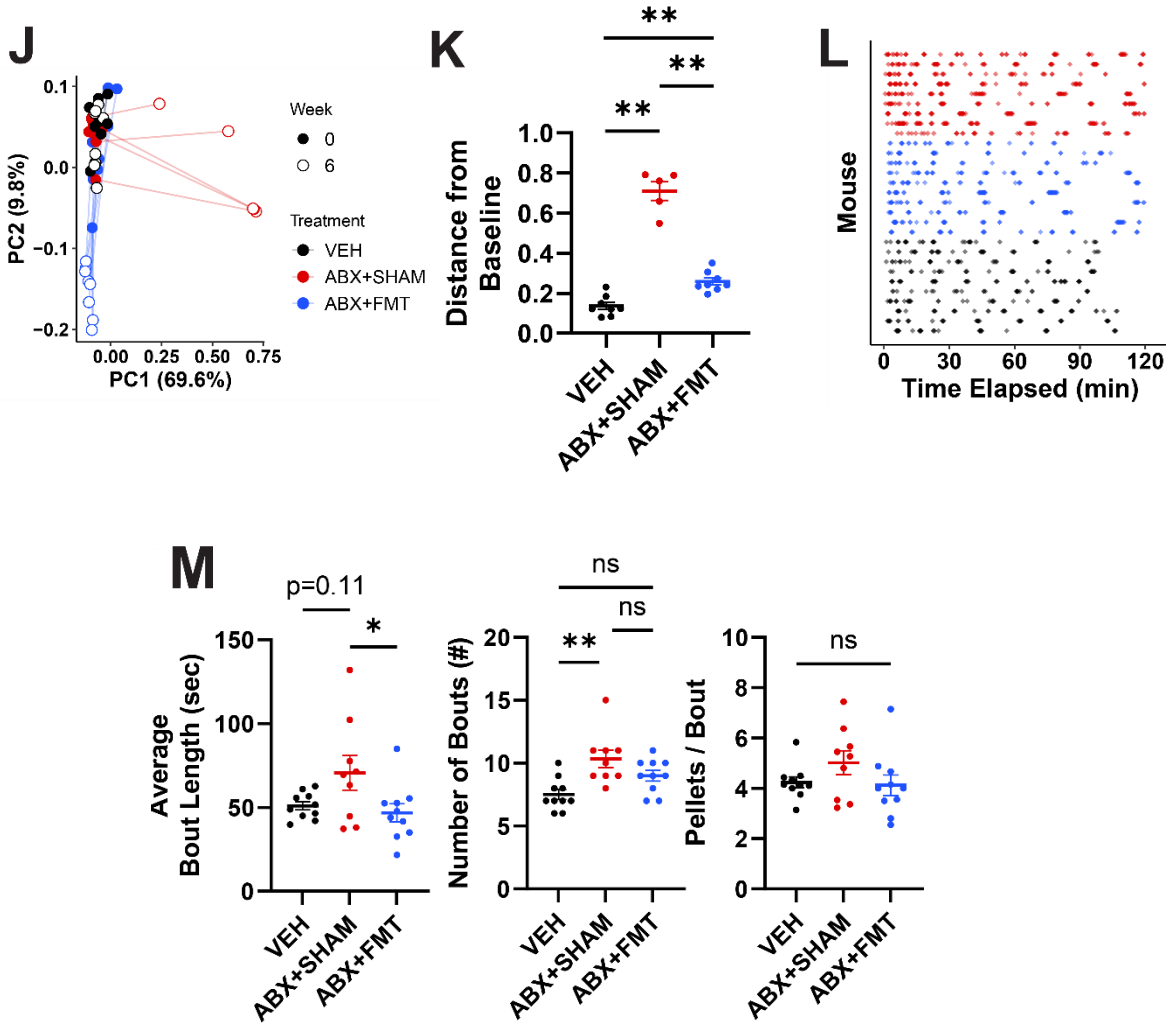

Figure S2. Additional behavioral parameters from free-feeding and operant conditioning assays and microbiome diversity measurements of FMT recipient mice, Related to Figures 1 and 2.

(N) Cumulative retrieval of high-sucrose pellets of VEH, ABX, and ABX+SCFA (n=8/group) mice. Shown is the mean (± SEM) plotted every 5 minutes. Significance calculated via two-way repeated measures ANOVA using 30-minute timepoints followed by Tukey's multiple comparisons test (within timepoints). Red and blue asterisks denote ABX vs. VEH and ABX+SCFA vs. VEH comparison significance, respectively.

(O) Discrimination Indices (active pokes/total pokes), between VEH and ABX (n=12/group) mice during the first 7 days of FR1 training sessions. Shown is the mean (± SEM). Session × Treatment interaction effect significance calculated via two-way repeated measures ANOVA.

(P) Total active and inactive pokes in VEH (n=10) and ABX (n=12) mice during the progressive ratio breakpoint session. Shown is the mean (± SEM). Significance calculated via two-way repeated measures ANOVA followed by Šidák's multiple comparisons test

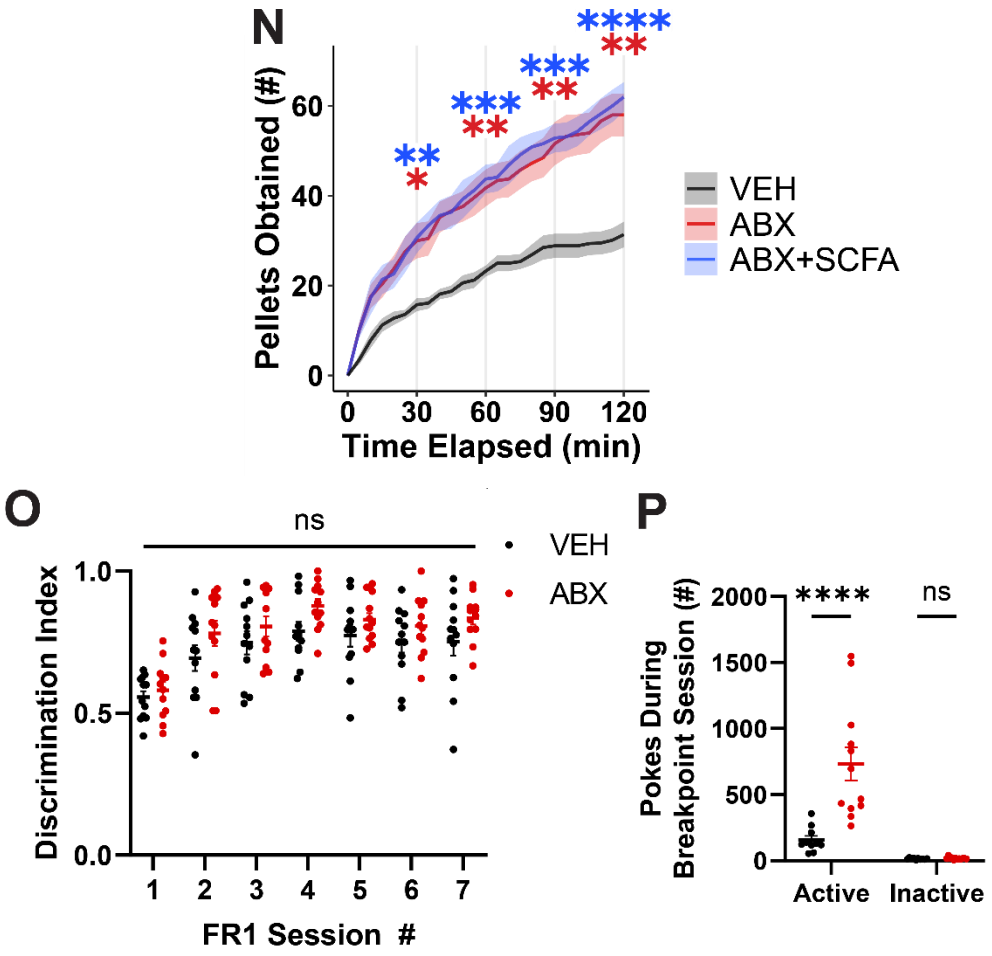

Figure 3. Certain microbial taxa correlate with suppression of high-sucrose pellet consumption.
(A) Cumulative retrieval of high-sucrose pellets between mice given vehicle (VEH), combined antibiotics (ABX), or individual antibiotics (A = ampicillin, V = vancomycin, N = neomycin, M = metronidazole) (n=8/group). Shown is the mean (± SEM) plotted every 5 minutes. Significance calculated via two-way repeated measures ANOVA using 30-minute timepoints followed by Dunnett's multiple comparisons test to VEH (within timepoints). VEH data reproduced in each panel for reference. See also Figure S4.
(B) Times at which mice in (A) had retrieved 50 high-sucrose pellets (1 gram). Significance calculated via one-way ANOVA Kruskal-Wallis followed by Dunn's multiple comparisons test to VEH.

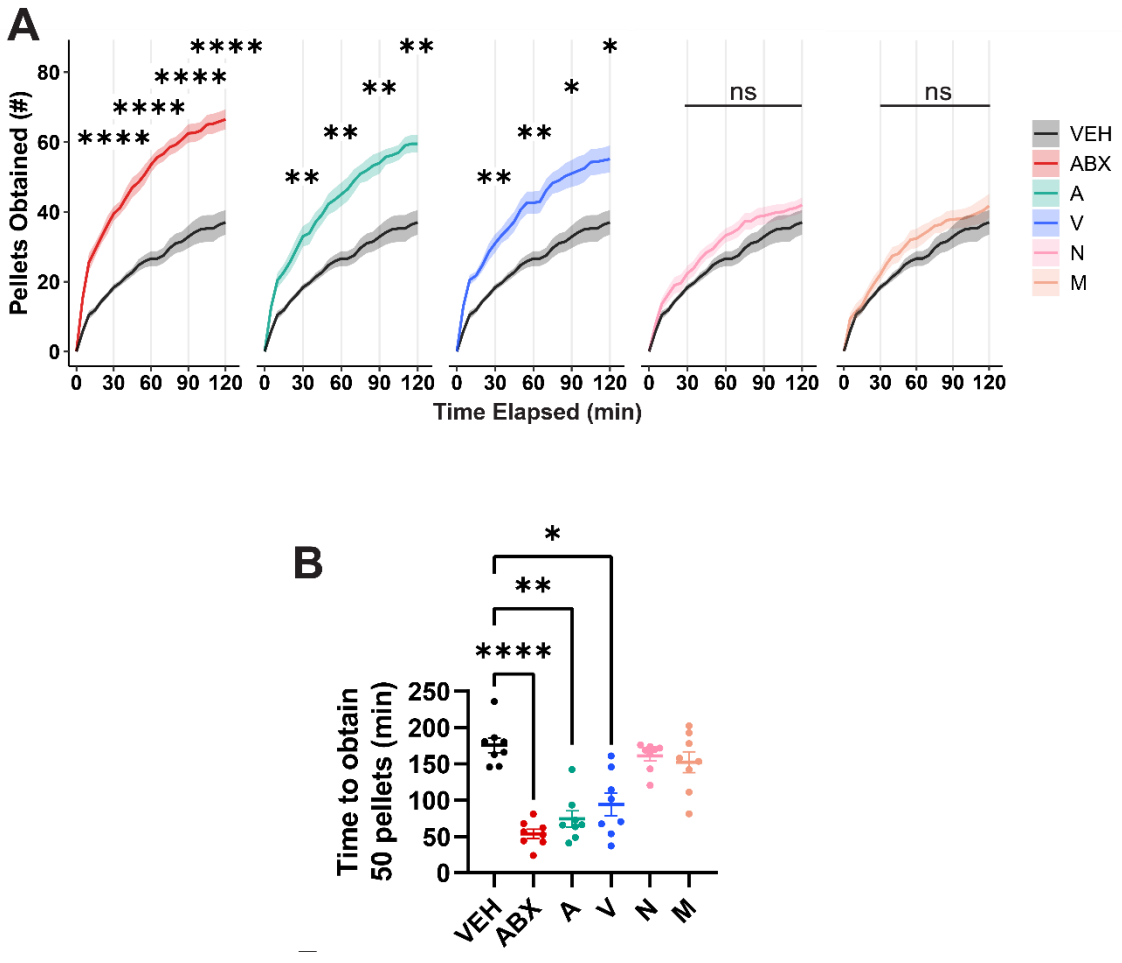

Figure 3. Certain microbial taxa correlate with suppression of high-sucrose pellet consumption.
(C) Cumulative retrieval of high-sucrose pellets between ABX-treated mice maintained on ABX or given FMT from animals administered no antibiotics or individual antibiotics (n=8/group). Shown is the mean (± SEM) plotted every 5 minutes. Significance calculated via two-way repeated measures ANOVA using 30-minute timepoints followed by Dunnett's multiple comparisons test to VEH-FMT (within timepoints). VEH-FMT data reproduced in each panel for reference. See also Figure S4.
(D) Times at which mice in (C) had retrieved 50 high-sucrose pellets (1 gram). Significance calculated via one-way ANOVA Kruskal-Wallis followed by Dunn's multiple comparisons test to VEH-FMT.

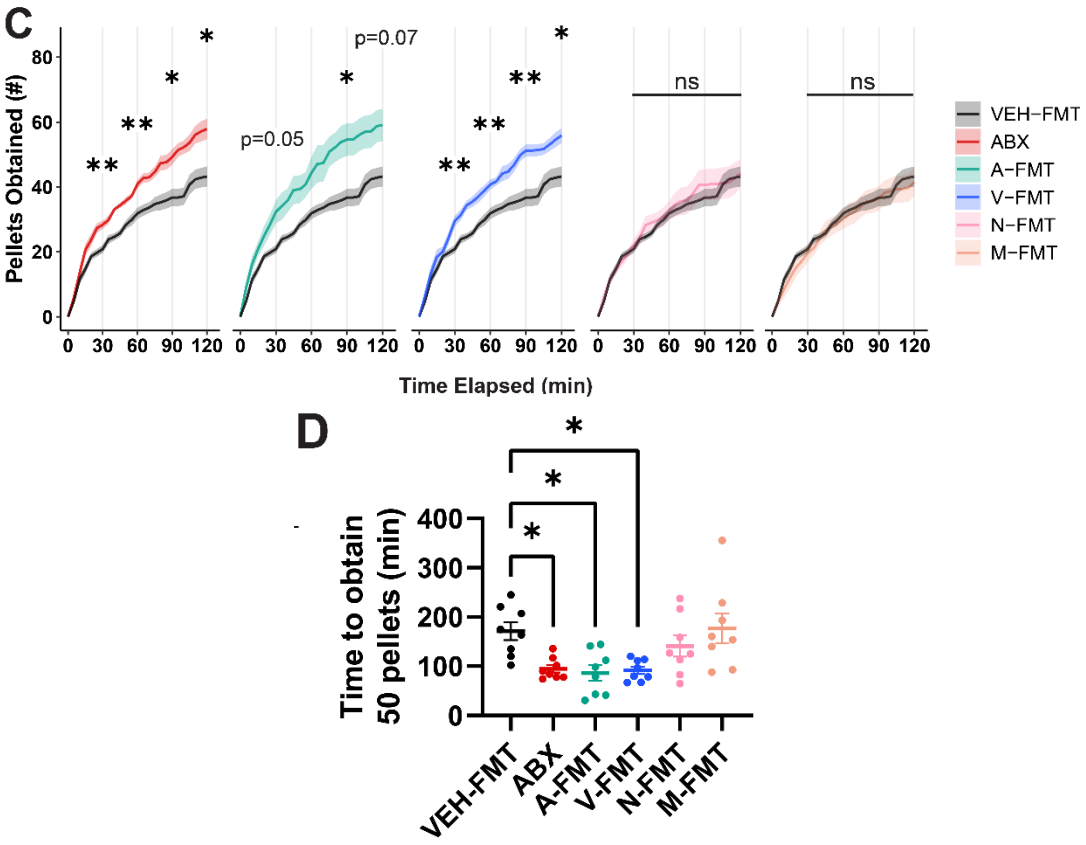

Figure 3. Certain microbial taxa correlate with suppression of high-sucrose pellet consumption.
(E–F) PCoA and boxplot of pairwise comparisons of weighted UniFrac distances in VEH (n=8), ABX (n=2), A (n=4), V (n=8), N (n=8), M (n=8) animals. Significance calculated via PERMANOVA (Table S1). Asterisks in (F) denote significance of the PERMANOVA test of treatment groups compared to VEH. See also Figure S4.
(G) Summary of ASVs and the highest-resolution taxonomic classification of each that significantly associate with vancomycin treatment in all three comparisons against metronidazole-, neomycin-, and vehicle-treated animals, filtered for those with a >0.01 absolute MaAsLin2 effect coefficient. The ASV corresponding to *Lactobacillus* sp. is denoted with an asterisk (*). Significance calculated using a general linear model in MaAsLin2 with antibiotic as a fixed effect and cage as a random effect. False discovery rate threshold was set to 0.1. Significance values are reported in Table S2.
(H) Relative abundances of select taxa that significantly negatively (S24-7 Family and *Lactobacillus* sp.) and positively (*A. muciniphila*) associate with vancomycin across all three comparisons as determined by MaAsLin2 analysis. Shown is the mean (± SEM). Significance illustrated via one-way ANOVA followed by Dunnett's multiple comparisons test to V.

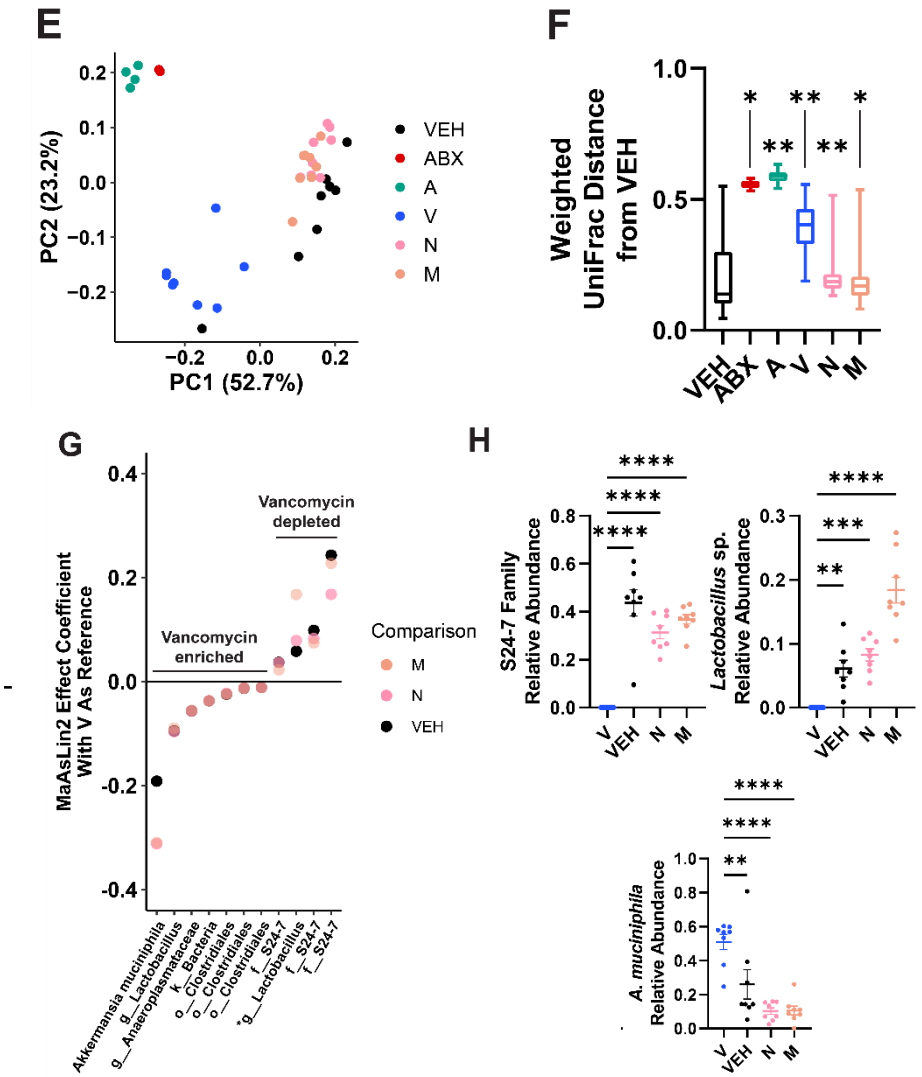

Figure S3. High-sucrose pellet-induced neural activity in reward-related brain regions and characterization of homeostatic feeding signals in VEH and ABX mice, Related to Figure 2.
(A) Representative images of the nucleus accumbens (NAc) and ventral tegmental area (VTA) in VEH and ABX mice without access to high-sucrose pellets, with c-Fos intensity represented in green. Scale bar is 100 microns. Images are cropped to emphasize the region of interest.
(B) Density of c-Fos+ neurons in the NAc shell, NAc core, and VTA (n=5/group) without access to high-sucrose pellets. Shown is the mean (± SEM). Significance calculated via two-way ANOVA with microbiota status and access to high-sucrose pellets as factors, followed by Bonferroni's multiple comparisons test (within brain regions). Data for mice given access to high-sucrose pellets is shown in Figures 2D and 2E.
(C) Representative images of c-Fos+ neurons in the dorsal striatum, lateral hypothalamus (LH), and basolateral amygdala (BLA) with (+Stimulus) and without (-Stimulus) 1 hour of access to high-sucrose pellets. Images have been cropped to aid cell body visualization. Scale bar is 100 microns.
(D) Density of c-Fos+ neurons in the dorsal striatum, LH, and BLA with (dorsal striatum: n=8/group, LH and BLA: n=8 VEH, n=7 ABX) and without (all regions: n=5/group) 1 hour of access to high-sucrose pellets. Shown is the mean (± SEM). Within-brain region Treatment × Stimulus interaction significance calculated via two-way ANOVA with microbiota status and access to high-sucrose pellets as factors.

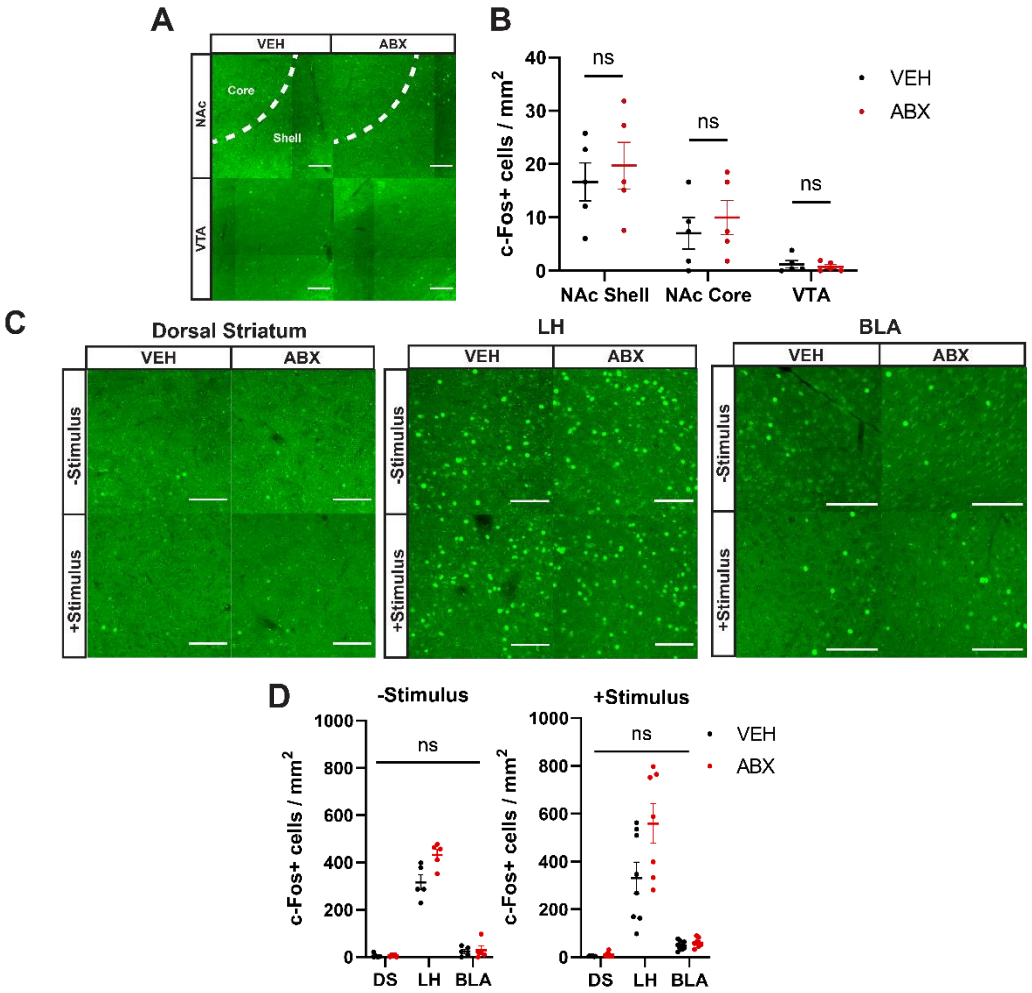

Figure S3. High-sucrose pellet-induced neural activity in reward-related brain regions and characterization of homeostatic feeding signals in VEH and ABX mice, Related to Figure 2.
(E–F) Representative images (E) and quantification (F) of c-Fos+ NPY+ neurons in the arcuate nucleus of the hypothalamus of VEH, ABX, or fasted (n=3/group) *NPY-hrGFP* transgenic mice. Shown is the mean (± SEM). Significance calculated via one-way ANOVA followed by Tukey's multiple comparisons test. Images have been cropped to aid cell body visualization. Scale bar is 100 microns.
(G) Hypothalamic neuropeptide expression as measured by qPCR in VEH (n=8) and ABX (n=7) mice. Shown is the mean (± SEM). Significance calculated via two-tailed Student's t-test followed by Holm-Šidák's correction for multiple comparisons.

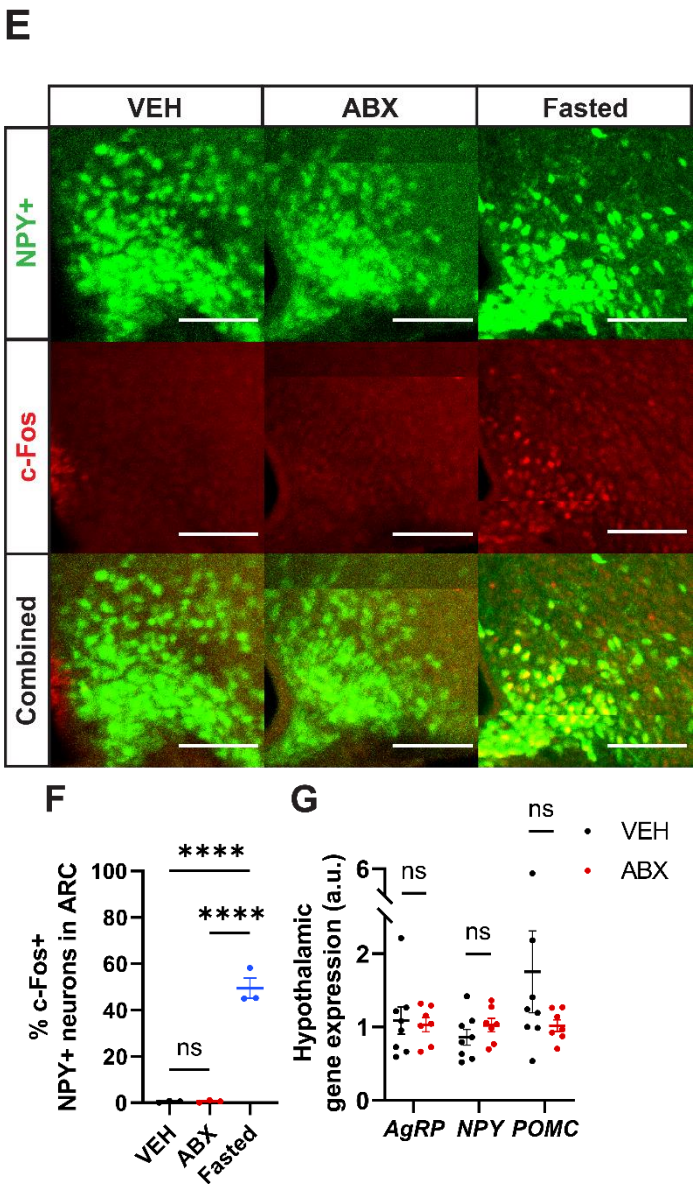

Figure 4. Family S24-7 and *L. johnsonii* functionally alter feeding in an induced model of binge-like intake.
(A) Schematic illustrating timeline of vehicle (VEH) or vancomycin (V) treatment and removal, treatment with saline vehicle (V+Sal), autologous FMT (V+Auto), or FMT from an SPF donor (V+SPF), and testing of binge intake. VEH mice received saline gavages.
(B) Total 1-hour intake of high-sucrose pellets in VEH, V+Sal, V+Auto, and V+SPF mice (n=20/group). Shown is the mean (± SEM). Significance calculated via one-way ANOVA followed by Tukey's multiple comparisons test.
(C) Relative abundances of S24-7 Family, *Lactobacillus* sp., and *A. muciniphila* in VEH, V+Sal, V+Auto, and V+SPF mice (n=8/group). Shown is the mean (± SEM). Significance calculated via one-way ANOVA followed by Tukey's multiple comparisons test. See also Figure S4.

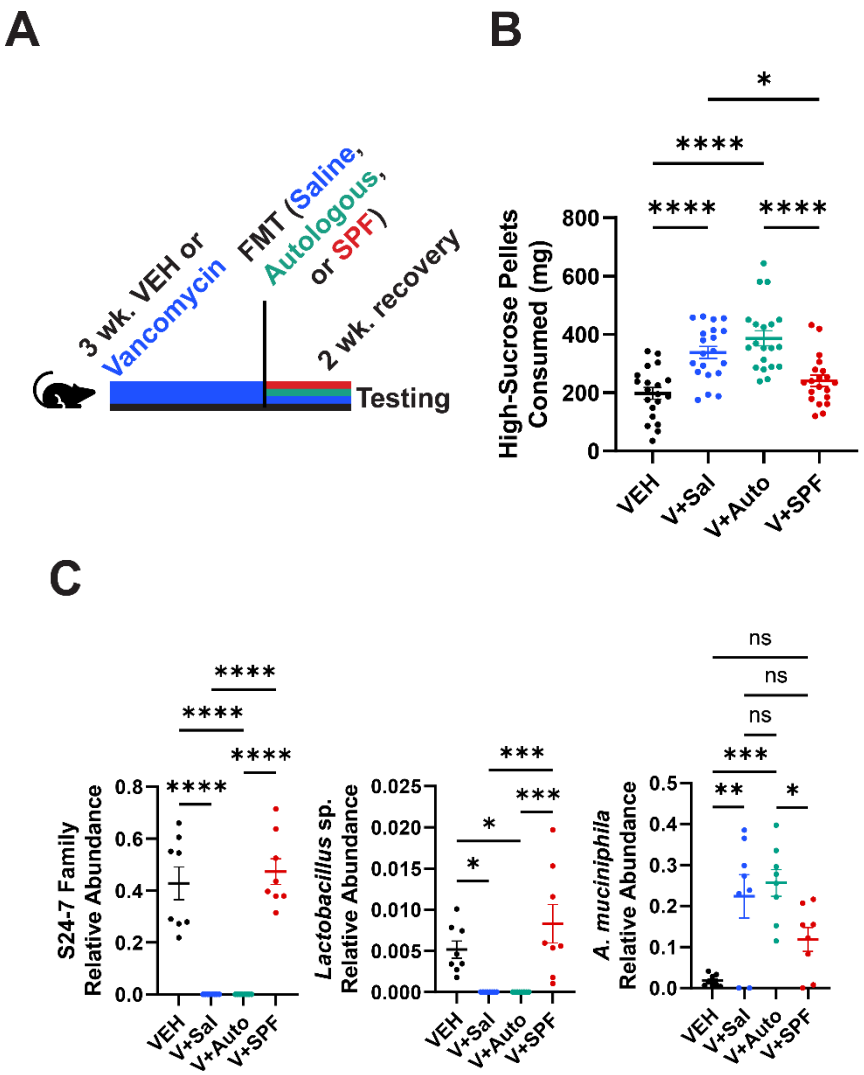

Figure 4. Family S24-7 and *L. johnsonii* functionally alter feeding in an induced model of binge-like intake.
(D) Schematic illustrating timeline of vehicle (VEH) or vancomycin treatment and removal, microbial treatment with an SPF microbiota (V+SPF), *A. muciniphila* (V+*A. muc*), or a mixture of three S24-7 family members and *Lactobacillus johnsonii* (V+4-mix), and testing of binge intake. VEH mice received saline gavages.
(E) Total 1-hour intake of high-sucrose pellets in VEH, V+SPF, V+*A. muc*, and V+4-mix mice (n=15/group). Shown is the mean (± SEM). Significance calculated via one-way ANOVA followed by Tukey's multiple comparisons test.
(F) Relative abundances of S24-7 Family, *Lactobacillus* sp., and *A. muciniphila* in V+*A. muc* and V+4-mix mice (n=8/group). Shown is the mean (± SEM). Significance calculated via two-tailed Student's t-tests. See also Figure S4.

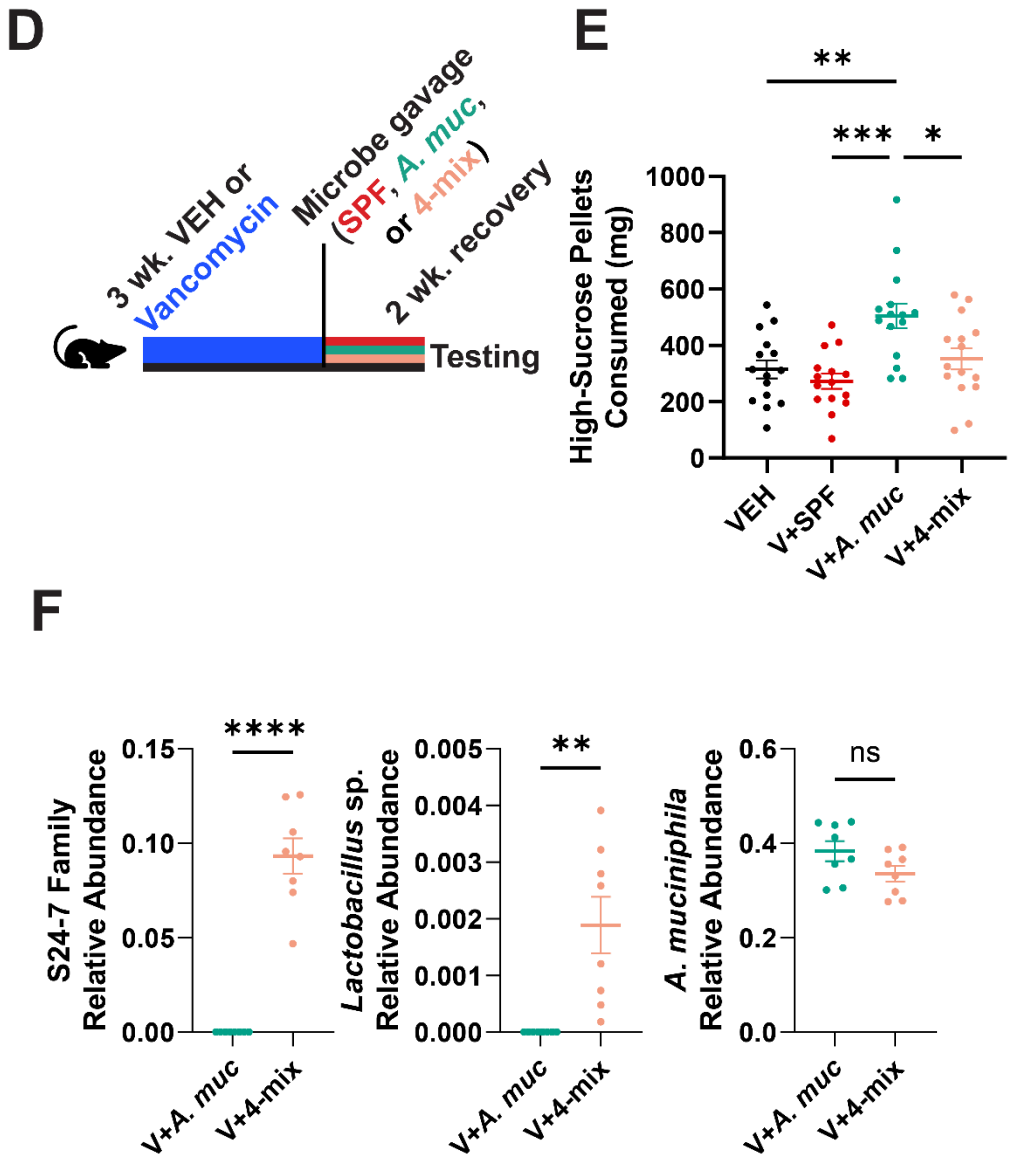

Figure S4. Differential antibiotic administration and microbial treatment has distinct effects on microbial abundance and diversity, Related to Figures 3 and 4.
(A) Microbial load in fecal samples relative to VEH mice (n=8/group) as calculated by qPCR with universal bacterial primers. Shown is the mean (± SEM). Significance calculated via one-way ANOVA followed by Dunnett's multiple comparisons test to VEH.
(B) Microbial load in fecal samples relative to VEH - FMT mice (n=8/group) as calculated by qPCR with universal bacterial primers. Shown is the mean (± SEM). Significance calculated via one-way ANOVA followed by Dunnett's multiple comparisons test to VEH - FMT.
(C–D) PCoA and boxplot of pairwise comparisons of unweighted UniFrac distances in VEH (n=8), ABX (n=2), A (n=4), V (n=8), N (n=8), M (n=8) animals. Significance calculated by PERMANOVA. Asterisks in (D) denote significance of the PERMANOVA test of treatment groups compared to VEH. See also Table S1.
(E) EMBOSS matcher alignment of the 16S rRNA DNA sequence of a *L. johnsonii* isolate cultured from SPF feces (top) to the significantly differentially abundant ASV aligning to *Lactobacillus* sp. (bottom).

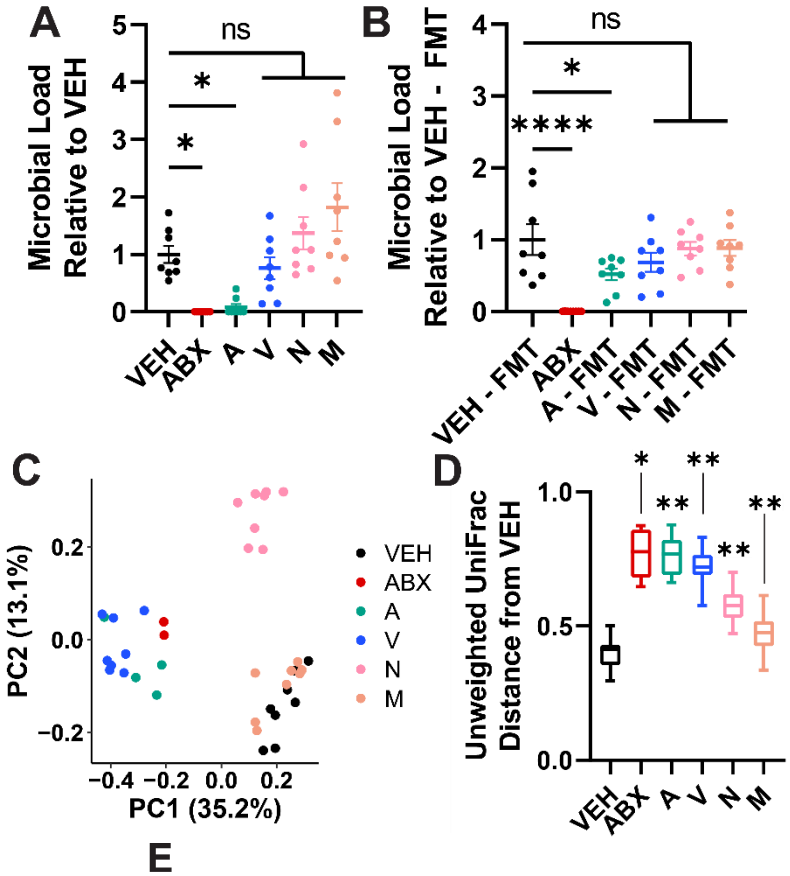

Figure S4. Differential antibiotic administration and microbial treatment has distinct effects on microbial abundance and diversity, Related to Figures 3 and 4.
(F–G) PCoA of weighted (F) and unweighted (G) UniFrac distances of fecal microbiomes from vehicle (VEH) or vancomycin-pretreated mice that received treatment with saline vehicle (V+Sal), autologous FMT (V+Auto), or FMT from an SPF donor (V+SPF). Significance calculated via within-timepoint one-way ANOVA Kruskal-Wallis of within-subject distance comparisons to baseline followed by Mann-Whitney U tests subject to FDR correction as implemented in QIIME2 (n=8/group). See also Table S1.
(H–I) PCoA of weighted (H) and unweighted (I) UniFrac distances of fecal microbiomes from VEH, V+SPF, V+*A. muc*, and V+4-mix (n=8/group) mice. Significance calculated via PERMANOVA. See also Table S1.

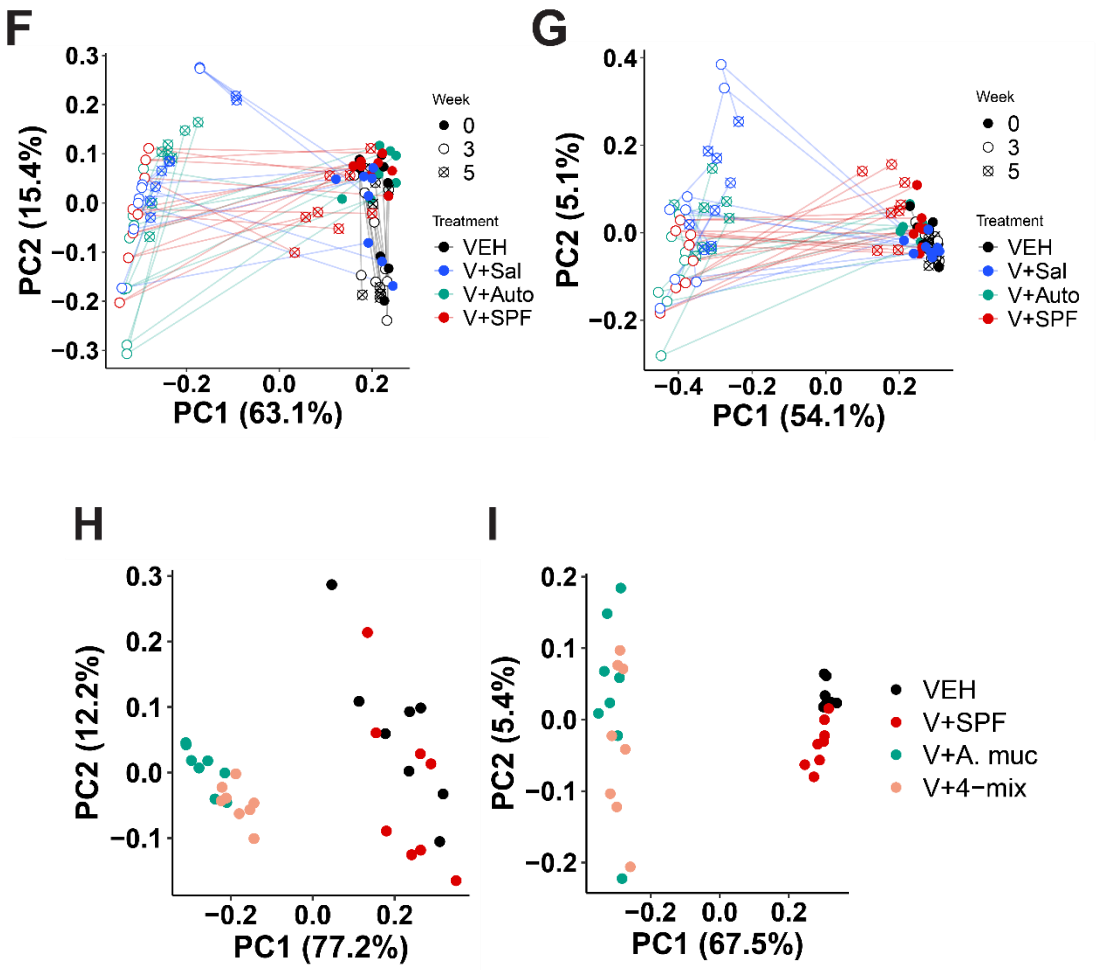

ACKNOWLEDGEMENTS

The authors thank Dr. Gil Sharon for help with animal behavioral testing and analysis of sequencing data. We are grateful to Drs. Yuki Oka, Viviana Gradinaru, and Scott Kanoski for scientific discussion. We thank Taren Thron, Yvette Garcia-Flores, Mark Adame, and Nikki Cruz for technical and logistical assistance. We thank the Caltech Office of Laboratory Animal Resources (OLAR) and the Institutional Animal Care and Use Committee (IACUC). We acknowledge the Caltech Biological Imaging Facility for microscopy assistance and the Caltech Neurotechnology Laboratory and Caltech TechLab 3D Printing Facility for behavioral equipment fabrication. We thank Dr. Catherine Oikonomou and all members of the Mazmanian Lab for critical evaluation of the manuscript. This work was supported by the National Science Foundation Graduate Research Fellowship under Grant No. DGE-1745301 to J.O., the Gates Millennium Scholarship Program to J.O., and funding from the Heritage Medical Research Institute to S.K.M.

Author Contributions

Conceptualization, J.O. and S.K.M.; investigation, J.O.; formal analysis, J.O. and J.B.; writing, J.O.; review, all authors.

Declaration of Interests

The authors declare no competing interests.

METHODS

Resource availability

Lead Contact

Further information and requests for resources and reagents should be directed to and will be fulfilled by the lead contact, Sarkis K. Mazmanian (sarkis@caltech.edu).

Materials availability

No new reagents were generated in this study.

Data and code availability

Microbial sequencing data have been deposited at the Sequence Read Archive (SRA) under BioProject PRJNA789557 and are publicly available as of the date of publication. All other experimental data used to generate the figures reported in this paper can be found in the CaltechDATA Repository (https://doi.org/10.22002/s8tfx-hwq49), publicly available as of the date of publication.

This paper does not report original code.

Any additional information required to reanalyze the data reported in this paper is available from the lead contact upon request.

Key Resources Table

REAGENT or RESOURCE	SOURCE	IDENTIFIER
Antibodies		
Rabbit anti-c-Fos 9F6 mAb	Cell Signaling Technologies	Cat#2250
Donkey anti-Rabbit IgG (H+L) Secondary Antibody Alexa Fluor 568	ThermoFisher Scientific	Cat#A10042
Bacterial and virus strains		
Muribaculum intestinale YL7	Leibniz Institute German Collection of Microorganisms and Cell Cultures GmbH (DSMZ)	Cat#100746
Muribaculum intestinale YL27	Leibniz Institute German Collection of Microorganisms and Cell Cultures GmbH (DSMZ)	Cat#28989
Paramuribaculum intestinale B1404	Leibniz Institute German Collection of Microorganisms and Cell Cultures GmbH (DSMZ)	Cat#100764
Akkermansia muciniphila BAA-835	American Type Culture Collection (ATCC)	Cat#BAA-835
Lactobacillus johnsonii	This study	N/A
Chemicals, peptides, and recombinant proteins		
Ampicillin sodium salt	Patterson Veterinary	Cat#07-893-3819
Vancomycin hydrochloride	Almaject Inc.	Cat#72611-765-10
Neomycin sulfate	Fisher Scientific	Cat#BP266925
Metronidazole	Acros Organics	Cat#210340050
Sodium acetate	Millipore Sigma	Cat#S2889
Sodium propionate	Millipore Sigma	Cat#P5436
Sodium butyrate	Millipore Sigma	Cat#303410
Critical commercial assays		
Quick-DNA Fecal/Soil Microbe Miniprep Kit	Zymo Research	Cat#D6010
Quick-RNA Miniprep Kit	Zymo Research	Cat#R1055
MoBio PowerSoil DNA Isolation Kit	Qiagen	Cat#12888
PowerUp SYBR Green Master Mix	ThermoFisher Scientific	Cat#A25742
Apex Taq RED Master Mix	Genesee Scientific	Cat#42-138B
iScript cDNA Synthesis Kit	Bio-Rad	Cat#1708891
Deposited data		
Raw sequencing data from 16S profiling	This study	NCBI SRA: BioProject PRJNA789557
All data to reproduce figures	This study	CaltechDATA Repository (https://doi.org/10.22002/s8tfx-hwq49)
Experimental models: Organisms/strains		
Mus musculus: C57BL/6J	The Jackson Laboratory	Cat#000664

Mus musculus: Gnotobiotic C57BL/6J	Caltech Gnotobiotic Facility	N/A
Mus musculus: B6.FVB-Tg(Npy-hrGFP)1Lowl/J	The Jackson Laboratory	Cat#006417
Oligonucleotides		
See Table S3	[93,98,99,102,103]	N/A
Software and algorithms		
R (Version 3.6.3)	[116]	https://www.r-project.org/
RStudio (Version 1.4.1106)	[115]	https://www.rstudio.com/
QIIME2 (Version 2019.10)	[96]	https://www.qiime2.org/
Ethovision XT 10	[117]	https://www.noldus.com/
Fiji/ImageJ (Version 1.53f51)	[118]	https://www.imagej.net/software/fiji/
MaAsLin2	[97]	https://huttenhower.sph.harvard.edu/maaslin/
Chromas (2.6.6)	Technelysium	https://technelysium.com.au/wp/chromas/
BLAST	[101]	https://blast.ncbi.nlm.nih.gov/Blast.cgi/
BORIS (7.13)	[108]	https://boris.unito.it/
GraphPad Prism (9.1.0)	GraphPad Software	https://www.graphpad.com/
Other		
Laboratory Autoclavable Rodent Diet	LabDiet	Cat#5010
High-Sucrose Purified Rodent Tablet (5TUL)	Test Diets	Cat#1811142
Calorie-Free Cellulose Reward Tablet (5TUW)	Test Diets	Cat#1812939
Custom Cellulose-Substituted Purified Rodent Tablet	Test Diets	N/A
Custom Sucralose-Substituted Purified Rodent Tablet	Test Diets	N/A
Custom AIN-76A 5 gram Purified Rodent Tablet	Test Diets	N/A
Rodent Diet with 60% kcal% Fat (High-Fat Diet)	Research Diets, Inc.	Cat#D12492
Chocolate Flavor Ensure®	Abbott Nutrition	Cat#53623
Bacto Brain Heart Infusion Broth	BD	Cat#237500
Chopped Meat Tubes	Anaerobe Systems	Cat#AS-811
Lactobacilli MRS Broth	BD	Cat#288130
Brucella Agar Plates with 5% Sheep's Blood	Teknova	Cat#B0150
Feeding Experimentation Device 2.0 (FED2)	[42]	https://hackaday.io/project/72964-feeding-experimentation-device-fed-20
Feeding Experimentation Device 3.0 (FED3)	[58]	https://hackaday.io/project/106885-feeding-experimentation-device-3-fed3

Experimental model and subject details

Mice

Wild-type C57BL/6J (The Jackson Laboratory, Cat#000664) and B6.FVB-Tg(Npy-hrGFP)1Lowl/J (The Jackson Laboratory, Cat#006417) mice were obtained from Jackson Laboratory at 8 weeks of age. Germ-free C57BL/6J mice were obtained from the Caltech gnotobiotic facility. All experiments were performed with male mice. Animals were group housed (2–5 mice per cage) unless otherwise specified. No statistical methods were used to predetermine sample size. For behavioral experiments, investigators were not blinded to treatment group unless otherwise specified.

Experimental mice were housed in sterilized microisolator cages and maintained on ad libitum autoclaved 5010 PicoLab Rodent Diet (LabDiet, Cat#5010) and sterilized water. Ambient temperature in the animal housing facilities was maintained at 21-24°C, 30-70% humidity, with a cycle of 13 hours light, 11 hours dark. All experiments were performed with approval from the Caltech Institutional Animal Care and Use Committee (IACUC).

Bacterial culture conditions

Akkermansia muciniphila (ATCC BAA-835), *Muribaculum intestinale* YL7 (DSM 100746), *Muribaculum intestinale* YL27 (DSM 28989), *Paramuribaculum intestinale* (DSM 100764), and the isolated strain of *L. johnsonii* were cultured, unshaken, under anaerobic conditions (10% CO_2, 10% H_2, 80% N_2) at 37°C. *M. intestinale* strains and *P. intestinale* were cultured in Chopped Meat Broth (Anaerobe Systems, Cat#AS-811), *A. muciniphila* was cultured in Bacto Brain Heart Infusion broth (BD Cat#237500),

supplemented with 5 mg hemin and 0.1 mg menadione per liter, and the *L. johnsonii* isolate was cultured in BD Difco Lactobacilli MRS Broth (BD Cat#288130).

Method Details

Antibiotic (ABX) treatment

Gut microbiota depletion with oral antibiotics (ABX) was performed by administration of ampicillin as sodium salt (1 g ampicillin/L, Patterson Veterinary, Cat#07-893-3819), vancomycin as hydrochloride salt (0.5 g vancomycin/L, Almaject Inc., Cat#72611-765-10), neomycin sulfate (1 g/L, Fisher Scientific, Cat#BP266925), and metronidazole (0.5 g/L, Acros Organics, Cat#210340050) to 8-week-old mice for a period of 4 weeks.[38,40] To encourage antibiotic uptake, ABX and VEH water was supplemented to 1% (w/v) with sucrose vehicle before filter sterilization (0.22 µm). Drinking water was replaced weekly. Administration of individual antibiotics was conducted using the same antibiotic concentrations and vehicle conditions. Animals removed from ABX for experimental reasons were switched to vehicle, which was maintained throughout behavioral testing.

For intragastric gavage administration of ABX, 200 µL of a filter-sterilized (0.22 µm) solution of ampicillin as sodium salt (15 mg ampicillin/mL), vancomycin as hydrochloride salt (7.5 mg vancomycin/mL), neomycin sulfate (15 mg/mL), and metronidazole (7.5 mg/mL) in water was administered once-daily to 8-week-old mice for a period of 10 days. Concentrated ABX solution was stored at 4°C for the treatment duration. Due to precipitation, ABX was briefly sonicated prior to daily gavage. VEH –

i.g. animals were given an equal volume daily gavage of sterile water. The final ABX/VEH gavage occurred 2 hours prior to behavioral testing.

For subcutaneous administration of ABX, 200 uL of a filter-sterilized (0.22 μm) and sonicated solution of ampicillin as sodium salt (15 mg ampicillin/mL) and metronidazole (7.5 mg/mL) in saline were injected into the loose skin over the shoulders of the mouse 1 hour prior to behavioral testing. Neomycin and vancomycin were not included in the subcutaneous antibiotic cocktail as these antibiotics undergo negligible absorption when administered orally.[90] VEH – s.c. animals were given an equal-volume subcutaneous injection of saline.

Germ-free (GF) C57BL/6J mice were removed from gnotobiotic isolators under sterile conditions and transferred to sterilized microisolator cages 3 days prior to behavioral testing.

Microbiota transplant and microbial treatment

Fecal samples were collected from experimental mice, weighed, and resuspended in a 10-fold volume of sterile filtered (0.22 μm) reduced phosphate buffered saline (PBS) containing 1.5% (w/v) sodium bicarbonate under anaerobic conditions. The sample was mashed with a pipette tip to create a fecal slurry, which was centrifuged at 250 x g for 5 minutes to separate fecal solids. The bacterial supernatant was collected and 200 μL was administered by intragastric gavage to recipient mice. This procedure occurred once-daily for 3 days following antibiotic removal. Mice were rehoused in a new sterile cage on the

first day receiving FMT. Non-FMT receiving control animals received gavages of reduced PBS with 1.5% (w/v) sodium bicarbonate. For autologous fecal microbiota transplants, mice from the same cage were assumed to share the same microbiota, and therefore samples from one cage would be collected and used for FMT in a given cage. Animals were given 2 weeks from the first day of FMT to allow for microbiota recovery prior to behavioral testing.

In the gut microbiota reconstitution experiment comparing the microbial diversity and bacterial loads between VEH, ABX+FMT, and ABX+SHAM mice, 3/4 ABX+SHAM mice in one cage were found dead during the 2-week recovery period between saline gavage and behavioral testing. We tentatively ascribe this phenomenon to opportunistic expansion of a gut pathobiont.

For experiments involving the supplementation of *A. muciniphila* or the mixture of S24-7 strains and *Lactobacillus johnsonii* (4-mix), autologous fecal bacterial supernatants were used to resuspend pelleted turbid bacterial cultures (2,400 x g for 20 minutes) for a final microbial density of 10^8-10^9 CFU/mL per microbe.[81] The S24-7 mixture consisted of equal bacterial culture volumes of *Muribaculum intestinale* YL7, *Muribaculum intestinale* YL27, and *Paramuribaculum intestinale* B1404. Resulting microbial suspensions were administered to recipient mice according to the same timeline as FMT administration.

Short-chain fatty acid treatment

SCFAs were administered as dissolved sodium salts (67.5 mM sodium acetate (Millipore Sigma, Cat#S2889), 25 mM sodium propionate (Millipore Sigma, Cat#P5436), 40 mM sodium butyrate (Millipore Sigma, Cat#303410)) in the drinking water before filter sterilization.[91,92] Control animals were placed on sodium- and pH-matched drinking water. Drinking water was replaced weekly and SCFA or sodium-matched treatment occurred throughout the entire course of ABX depletion and through behavioral testing.

Colony forming unit (CFU) analyses

Fecal material from mice was collected, weighed, and resuspended in a 10-fold volume of aerobic or anaerobic PBS in a sterile 1.5-mL microcentrifuge tube. Aerobic and anaerobic samples were briefly centrifuged at 250 x g for 5 minutes and the bacterial supernatants were serially diluted in aerobic or anaerobic PBS, respectively. Samples were plated in quadruplicate on both Brain Heart Infusion (BD, Cat#237500) agar supplemented with 5 mg hemin and 0.1 mg menadione per liter (BHIS), and Brucella agar plates supplemented with 5% (v/v) defibrinated sheep's blood (Teknova, Cat#B0150). Aerobic and anaerobic supernatants were cultured at 37°C aerobically and anaerobically, respectively, for 48 hours before counting of colony forming units. Plates where no colonies grew were given a measurement of 0 CFU/mg feces for purposes of statistical testing.

Analysis of fecal microbial load

Fecal samples were collected from experimental mice and immediately snap-frozen in liquid nitrogen before storage at -80°C. Samples were weighed and total fecal DNA was

extracted using either a Qiagen PowerMag Soil DNA Isolation Kit (Qiagen, Cat#12888) or a Zymo Quick-DNA Fecal/Soil Microbe Miniprep Kit (Zymo Research, Cat#D6010), according to the manufacturer's protocol. DNA concentrations were determined via spectrophotometer. Extracted DNA was used as template for triplicate qPCR reactions (ThermoFisher Scientific, Cat#A25742) using universal bacterial primers (200 nM forward and reverse) against the microbial 16S rRNA (515F: 5'-GTGCCAGCMGCCGCGGTAA-3', 806R: 5'-GGACTACHVGGGTWTCTAAT-3').[93] qPCR signal was normalized to fecal DNA content and sample weight.

Fecal microbiome community profiling

Bacterial 16S rRNA genes from extracted fecal DNA were PCR-amplified with barcoded primers targeting the V4 region. Sequencing was performed by either Microbiome Insights, Inc. (Vancouver, BC), or Laragen, Inc (Culver City, CA). For sequences prepared by Microbiome Insights, amplicons were sequenced with an Illumina MiSeq using the 300-bp paired-end kit (v.3) according to the protocol of Kozich et al. (2013).[94] For sequences prepared by Laragen, amplicons were sequenced according to the Earth Microbiome Protocol.[95] Sequences were analyzed using the QIIME2 (2019.10) software package.[96]

Demultiplexed reads were filtered for quality and denoised using the q2-deblur package. Sequences were trimmed to different lengths based on the quality scores of separate sequencing runs. These trim lengths are 147 bp, 220 bp, 151 bp, and 151 bp for the VEH/ABX+SHAM/ABX+FMT, individual antibiotic administration, SPF and

autologous FMT, and microbial rescue experiments, respectively. Taxonomic classification of amplicon sequence variants (ASVs) was performed in QIIME2 using classify-sklearn with a classifier pre-trained on the Greengenes database (13_8 release). Phylogenetic diversity metrics were generated from ASV feature tables using q2-phylogeny and q2-diversity plugins. Within-subject diversity comparisons across multiple timepoints were generated using the q2-longitudinal plugin. Sampling depth was chosen based on manual analysis of the reads per sample in a given experiment. These sampling depths are 8836, 1147, 14785, and 22785 reads, for the VEH/ABX+SHAM/ABX+FMT, individual antibiotic administration (6/8 ABX and 4/8 Ampicillin samples did not meet rarefaction threshold), SPF and autologous FMT, and microbial rescue experiments, respectively. Weighted and unweighted UniFrac diversity metrics, alpha-diversity metrics, and Principal Coordinate Analyses (PCoAs) of diversity metrics were generated as implemented in QIIME2. Hypothesis tests for differences in diversity were tested using PERMANOVA as implemented in QIIME2. Differential abundance analysis of ASVs was performed using the MaAsLin2 R package to identify features that associate with treatment conditions.[97] In the individual antibiotic treatment experiment, the vancomycin condition was used as the reference level in a one-versus-all comparison. Differential abundance analysis based on relative abundances was restricted to the vancomycin condition given the significant reduction of microbial load in ABX and ampicillin-treated mice. For this analysis, cage was included as a random effect and treatment group was included as a fixed effect. Features were normalized by total sum scaling, and an FDR-corrected significance threshold was set at 0.1. Significant results from the differential abundance analysis are in Table S2.

Isolation of *Lactobacillus johnsonii*

Fecal samples from a mouse from the VEH experimental condition were collected and resuspended in a 10-fold volume of anaerobic Lactobacilli MRS Broth (BD, Cat#288130) in a sterile 10-mL microcentrifuge tube. Serial 10-fold dilutions in MRS broth were plated on MRS agar plates and cultured for 48 hours under anaerobic conditions (10% CO_2, 10% H_2, 80% N_2) at 37°C. Single colonies were re-streaked on MRS agar plates and colony PCR Sanger sequencing was conducted by Laragen, Inc. using universal 16S ribosomal RNA primers. *16S:* (27F: 5'- AGAGTTTGATCMTGGCTCAG-3', 1492R: 5'-GGTTACCTTGTTACGACTT-3').[98,99] Chromatogram traces were analyzed using Chromas (2.6.6) (Technelysium) and sequence alignment visualization to the differentially abundant *Lactobacillus* sp. ASV (100% match) was performed using EMBOSS Matcher.[100] The sequenced 16S rRNA was used as a query sequence for a BLASTN analysis (NCBI) and found to have >99.8% sequence identity to cultured strains of *Lactobacillus johnsonii*.[101]

Hypothalamic neuropeptide expression

VEH and ABX animals were euthanized by cervical dislocation and hypothalami were extracted and snap-frozen in TRIzol reagent. Hypothalamic RNA was isolated using a Zymo Quick-RNA Miniprep Kit (Zymo Research, Cat#R1055) and reverse transcribed into cDNA using an iScript cDNA Synthesis Kit (Bio-Rad, Cat#1708891). Both steps were performed according to the manufacturer's directions. Triplicate qPCR reactions (ThermoFisher Scientific, Cat#A25742) were run using the following primer sets: *AgRP*:

(5’-TGCTACTGCCGCTTCTTCAA-3’ and 5’-CTTTGCCCAAACAACATCCA-3’), *NPY*: (5’-TAACAAGCGAATGGGGCTGT-3’ and 5’-ATCTGGCCATGTCCTCTGCT-3’), *POMC*: (5’-AGGCCTGACACGTGGAAGAT and 5’-AGGCACCAGCTCCACACAT-3’).[102] qPCR signal was normalized to the expression of the 18S eukaryotic rRNA *18S*: (5’-TTCCGATAACGAACGAGACTCT-3’ and 5’-TGGCTGAACGCCACTTGTC-3’).[103]

Brain sample collection

For c-Fos analysis of *NPY*+ neurons in the ARC, VEH, ABX, and overnight fasted mice were taken from their home cages and euthanized. For c-Fos analysis of reward-related brain regions, single-housed VEH and ABX mice were euthanized 60 minutes after the introduction of either an empty glass dish (-Stimulus) or a glass dish containing approximately 2 grams of high-sucrose pellets (5TUL, Test Diets, Cat#1811142) (+Stimulus) into their home cage. Treatment groups were given prior exposure to the glass dish and previously acclimated to the high-sucrose pellets (100 mg provided in the home cage the day before) to reduce effects of novelty. Euthanasia was conducted via a 150 µL intraperitoneal injection of a 1:10 saline dilution of Euthasol (Virbac, Cat#PVS111), a solution of sodium pentobarbital and sodium phenytoin. Mice were transcardially perfused with chilled PBS followed by chilled 4% paraformaldehyde in PBS. Brains were harvested and stored in 4% paraformaldehyde in PBS for 2 days at 4°C before transfer to a solution of 0.02% sodium azide in PBS at 4°C prior to sectioning.

Brain sectioning and c-Fos measurement

Brains were embedded in 2% (w/v) UltraPure low melting point agarose (ThermoFisher Scientific, Cat#16520100) in PBS containing 0.02% sodium azide and 50-µm-thick coronal sections were sectioned using a vibratome (Leica Biosystems, Cat#VT1000). Every third slice was collected and stored at 4°C in 0.02% sodium azide in PBS until staining. Coronal brain sections were incubated with primary antibody (1:500 rabbit anti-cFos (9F6), CST Cat#2250) in blocking buffer (10% horse serum, 0.3% Triton X-100, 0.02% sodium azide in PBS) and placed on a benchtop rocker overnight at room temperature. Primary antibody-stained slices underwent three 45-minute room temperature washes in PBS containing 0.3% Triton X-100. Secondary antibody (1:1000 donkey anti-rabbit Alexa Fluor 568, ThermoFisher Scientific, Cat#A10042) in blocking buffer was incubated with the washed slices for 2 hours rocking at room temperature protected from light. Slices underwent three washes, 2 hours each, in sterile PBS at room temperature, before mounting on Superfrost Plus microscope slides (Fisher Scientific, Cat#12-550-15). Slices were drained of excess liquid using a Kimwipe (Fisher Scientific) and Prolong Diamond Antifade Mountant with DAPI (ThermoFisher Scientific, Cat#P36962) was used to adhere the coverslip. Slides were left at room temperature overnight protected from light to solidify the mountant prior to imaging.

Microscopic imaging and cell quantification

Imaging was performed using a Zeiss LSM 880 confocal laser scanning microscope using Zen software. All images shown and quantified are maximum intensity projections in the z-direction of z-stacks of mounted 50-µm-thick coronal slices using a 10X objective lens. Tile-scans with stitching were employed to capture brain regions larger than a single field

of view. c-Fos+ and *NPY*+ cell bodies unambiguously brighter than background signal were quantified manually in Fiji/ImageJ (1.53f51) by a researcher blinded to treatment group and stimulus status. All images were minimally processed for brightness and contrast. Regions of interest (ROI) for quantification of cell density were defined using anatomical landmarks. For each mouse, the slice with greatest correspondence to the anterior-posterior coordinates of the target brain region was used for quantification.

Anterior-posterior coordinates for imaging were +1.0 mm to +1.3 mm (nucleus accumbens, dorsal striatum), -1.7 to -1.3 mm (lateral hypothalamus), -1.8 to -1.5 (arcuate nucleus of the hypothalamus) -3.7 to -3.4 mm (ventral tegmental area), -1.2 to -0.9 mm (basolateral amygdala).[104]

Free-feeding intake of high-sucrose pellets

Experimental mice were single-housed the day prior to behavioral testing. To reduce effects of neophobia, mice were housed overnight with an automated pellet dispenser[42] (Feeding Experimentation Device 2.0, (FED2)) in the "off" state and acclimated to 100 mg (five pellets) of the high-sucrose pellets (5TUL, Test Diets, Cat#1811142) in their home cage. This palatable food is a pelleted formulation of the widely studied AIN-76A complete diet, frequently used as a high-sugar stimulus for binge behavior in rodent studies, and is reported to be preferred at a ratio of >9:1 compared to standard chow in food choice assays.[19,69,105–107] The morning of behavioral testing, cages were manually checked to ensure the five acclimation pellets were consumed. Mice were provided ad lib chow and treatment water during the acclimation period. The unfasted mice, FED2, and

treatment water were moved into a new cage without chow and the FED2 was stocked with high-sucrose pellets and placed in the "on" state. Mice were left to consume pellets from the FED2, which records occurrences of pellet retrieval events to an internal memory card, for at least 2 hours or until 50 pellets had been retrieved. In the sucralose substitution experiment, the sucrose in the high-sucrose pellets was replaced with a mixture of microcrystalline cellulose and sucralose for a final diet concentration of 48% (w/w) cellulose and 2% (w/w) sucralose (Test Diets). Intake rate was modeled using RStudio running R (3.6.3) by fitting an exponential function[25] with a fixed y-intercept of zero to each trace of cumulative 2-hour intake. The derivative of this function was taken and calculated at each minute.

To confirm that the FED2s provided an accurate representation of pellet consumption, a cohort of VEH and ABX mice (n=5/group) were tested for free-feeding intake as above but with simultaneous video recording during the 2-hour test session. Pellet consumption events over the 2-hour test session were manually recorded using BORIS[108] (7.13) by an experienced researcher blinded to animal treatment status. The average FED accuracy, calculated as (Pellets Eaten / FED Retrieval Events) of all tested mice was 1.00 when rounded to the nearest hundredth place (mean=1.0019, standard deviation=0.0154). On five occasions, representing ~1% of all recorded retrieval events for this cohort (5/493, 3 VEH and 2 ABX), the FED2s were observed to dispense two pellets instead of one, in line with the previously reported accuracy of the FED2s,[42] and enabling values of FED accuracy >1. On four occasions, representing <1% of all recorded retrieval events for this cohort (4/493, 2 VEH and 2 ABX), mice were observed to retrieve a pellet from the

FED2 without having consumed it by the end of the 2-hour session. To test if the comparisons of time-series pellet retrieval data could be considered representative of time-series pellet consumption data, we performed within-mouse Kolmogorov-Smirnov comparisons (R, 3.6.3) of cumulative probability distributions of FED-recorded retrieval events and manually determined pellet consumption events. In all mice (10/10), the p-value was >0.995 and the KS statistics were <0.08 (mean = 0.0478, standard deviation = 0.0187), suggesting that FED-based pellet retrieval metrics are reflective of consumption events. Full information regarding comparisons to pellet consumption data can be found in Table S1.

Free-feeding intake of a high-fat diet

Experimental mice were single-housed the day prior to behavioral testing. To reduce effects of neophobia, mice were housed with 200 mg of the high-fat diet (HFD) (Research Diets, Cat#D12492) provided in a glass dish. The HFD chosen has previously been shown to induce binge-like consumption responses in mice.[55] The morning of behavioral testing, cages were manually checked to ensure the 200 mg of HFD was consumed. Mice were provided ad lib chow and treatment water during the acclimation period. The unfasted mice and treatment water were moved into a new cage without chow containing a pre-weighed amount of HFD (~2 g). Mice were free to consume for 2 hours. Every 30 minutes, the HFD was briefly removed from the cage, weighed, and returned to the cage. The difference in HFD weight from baseline was taken as intake.

Free-feeding intake of Ensure®

Experimental mice were single-housed the day prior to behavioral testing. To reduce effects of neophobia, mice were housed with 1 mL of chocolate Ensure® (Abbott Nutrition, Cat#53623) provided in a glass dish. Ensure® is a palatable liquid diet known to induce binge-like consumption responses in mice.[56] The morning of behavioral testing, cages were manually checked to confirm the 1 mL of Ensure® was consumed. Mice were provided ad lib chow and treatment water during the acclimation period. The unfasted mice and treatment water were moved into a new cage without chow containing an Ensure®-filled graduated 10-mL pipet outfitted with a ball-bearing sipper tube to allow for controlled consumption.[109] The end of the ball-bearing sipper was primed with chocolate Ensure® to assist in induction of consumption. Mice were free to consume for 2 hours and recorded with a video camera. Recordings were analyzed for drinking activity using BORIS by an experienced researcher blinded to treatment condition. The levels of Ensure® were measured visually at 30-minute timepoints. Differences in Ensure® volume from baseline were taken as intake. Cages were visually examined after the experiment for any evidence of Ensure® leakage and no leakage was observed.

Bout structure analyses

For measurements of FED bout length, pellets per bout, and number of bouts, a feeding bout was defined as at least two pellet retrieval events occurring within 60 seconds of each other.[58,110] A bout was considered terminated when at least 60 seconds have passed between pellet retrieval events.[58] Analysis of time-series data was performed in RStudio running R (3.6.3).

For measurements of Ensure® drinking bout length, drinking events within 60 seconds of one another were defined as being within the same bout.[111]

Operant conditioning

Custom-built acrylic arenas (10”x10”x12”) equipped with an operant conditioning unit with programmable active and inactive nose-poke ports (FED3) were used for fixed-ratio 1 (FR1) training and progressive ratio (PR) testing.[28,58] The assignment of active and inactive ports was reversed for half of the mice within a given treatment group to account for potential arena effects. Experimental mice were single-housed and acclimated to 100 mgs of high-sucrose pellets the day prior to beginning FR1 training. During FR1 training, mice were placed on a restricted feeding schedule of 2–3 g chow/day, given as a single bolus after the daily training session, to maintain ~95% of their starting body weight. FR1 training sessions, where a single nose-poke in the active port resulted in the delivery of a single high-sucrose pellet, lasted for 60 minutes and proceeded for at least 7 days. Mice unable to reach the training criterion, defined as 3 consecutive days of ≥75% correct port discrimination with at least 20 pellets retrieved, were trained up to maximum of 7 additional days, or until the criterion was met. 12/12 ABX mice and 10/12 VEH mice successfully reached the training criteria.

Successfully trained mice were returned to an ad libitum feeding schedule for 3 days before proceeding to PR testing. Mice underwent daily 90-minute PR breakpoint sessions, where the number of active pokes, N, required to obtain pellet n+1 is increased after each successful pellet retrieval event, based on the formula $N_{n+1} = 5e^{(0.2n)} - 5$,

rounded to the nearest integer.[112] The breakpoint is defined as the final ratio completed by the mouse in the PR session. Unfasted animals were tested daily until breakpoints were considered stabilized (either within ±10% variance in the number of pellets obtained or ±1 pellet when <10 pellets are obtained, over 3 consecutive days).[28,113] Performance in the final PR assay was taken as the breakpoint for comparisons between treatment groups.

Brief-access dietary selection assay

Unfasted experimental mice were habituated to the testing chamber (an empty cage with no bedding) for 10 minutes prior to the introduction of a bolus of pre-weighed edible stimuli in a glass dish—either standard chow, pure microcrystalline cellulose pellets (5TUW, Test Diets, Cat#1812939), a custom formulation of the high-sucrose pellets in which the sucrose was replaced by microcrystalline cellulose (Test Diets), or the high-sucrose pellets used throughout the study (5TUL, Test Diets, Cat#1811142). The stimuli were tested in the order listed. Animals were left to freely consume the stimulus for 10 minutes and the difference in stimulus weight was measured as intake. To reduce neophobia, the day prior to testing the mice were given a small amount of each edible stimulus in their home cage (100 mg/mouse) and housed with a glass dish overnight. The morning of behavioral testing, cages were checked to ensure the acclimation stimulus was consumed. Mice were given 1 day of rest between assays.

High-sucrose pellet binge-like consumption assay

To reduce anxiety and neophobia, animals were habituated to the testing chamber (an empty cage with no bedding) for 1 hour and given free access to ~1 gram of the high-sucrose pellets (5TUL, Test Diets, Cat#1811142) in a glass dish.[70,114] This habituation step occurred prior to antibiotic removal to reduce potential environmental contamination of antibiotic-treated mice.

For behavioral testing, habituated mice were placed in the testing chamber for 10 minutes prior to being given a pre-weighed bolus of approximately 1.5 grams of high-sucrose pellets in a glass dish and allowed to consume freely for 1 hour. The uneaten pellets were weighed, and the difference was recorded.

Fasting-refeeding assays

Single-housed experimental mice were fasted overnight for 16 hours with access to treatment water. To reduce neophobia, the day prior to fasting, animals refed with high-sucrose pellets were given access to 100 mg (five pellets) of high-sucrose pellets, and during the fast, were housed with a FED2 in the “off” state. For chow refeeding, a pre-weighed amount of chow was returned to the cage and weighed at 30-minute intervals. The difference in chow weight over time was taken as intake. For refeeding with the high-sucrose pellets, the FED2 was stocked with pellets and placed into the “on” state.

Homeostatic food intake measurements

Experimental mice were single-housed and provided with ad lib chow for the duration of VEH/ABX treatment. The difference in chow weight was measured and taken as intake.

For home-cage AIN-76A intake, custom-manufactured 5-gram tablets of AIN-76A were provided as the exclusive food source to VEH/ABX mice for 1 week, starting after 4 weeks of VEH/ABX. The difference in AIN-76A weight compared to baseline was measured and taken as intake.

Baited and unbaited hole board assay

Experimental mice were placed in a hole board apparatus (40 cm x 40 cm x 35 cm, 3 cm hole diameter, Stoelting, Cat#62015) with 16 holes arranged in a 4 x 4 grid and left to explore for 10 minutes. In the unbaited assay, the holes were empty, mice were video recorded, and the number of spontaneous head dips was measured by a researcher blinded to treatment group as a metric for exploratory behavior. In the stimulus-baited assay, each apparatus hole was baited with a single high-sucrose pellet, and the number of pellets consumed after 10 minutes was used as a readout.[46]

Anxiety assays

Open field assays were conducted in white acrylic arenas (50 x 50 x 30 cm). Mice were recorded via an overhead camera for 10 minutes. The time spent in the center (30 x 30 cm) zone was measured and quantified using Ethovision XT 10 (Noldus Information Technology).

Elevated plus maze assays were conducted on a white EPM apparatus (28-cm arm length, 9 x 9 cm center zone) with black acrylic walls (16 cm). Mice were placed in the center

and recorded via an overhead camera for 5 minutes. The time spent in the exposed open arms was measured and quantified using Ethovision XT 10.

Quantification and statistical analysis

Statistical tests and data visualization were performed in GraphPad Prism (9.1.0), QIIME2 (2019.10),[96] and RStudio[115] running R (3.6.3)[116] using the ggplot2 package. Statistical tests and replicate numbers are indicated in the respective figure legends and exact p-values for all comparisons made are reported in Table S1. Significantly different features as detected by MaAsLin2 analysis[97] are reported in Table S2. Error bars represent the standard error of the mean. For box-and-whisker plots, the whiskers represent the minimum and maximum values, the box extends from the 25th to the 75th percentile of the data, and the line within the box denotes the median. ****$p<0.0001$, ***$p<0.001$, **$p<0.01$, *$p<0.05$, ns: not significant.

Supplemental Information

Document S1. Figures S1–S4 and Table S3.

Table S1. Statistical tests and exact p-values for all comparisons made.

Table S2. Significantly differentially abundant ASVs in vancomycin-treated mice, related to Figure 3.

References

1. Coll, A.P., Farooqi, I.S., and O'Rahilly, S. (2007). The Hormonal Control of Food Intake. Cell *129*, 251–262. 10.1016/j.cell.2007.04.001.

2. Watts, A.G., Kanoski, S.E., Sanchez-Watts, G., and Langhans, W. (2021). The Physiological Control of Eating: Signals, Neurons, and Networks. Physiol. Rev.

3. Saper, C.B., Chou, T.C., and Elmquist, J.K. (2002). The Need to Feed: Homeostatic and Hedonic Control of Eating. Neuron *36*, 199–211. 10.1016/S0896-6273(02)00969-8.

4. Cummings, D.E., and Overduin, J. (2007). Gastrointestinal regulation of food intake. J. Clin. Invest. *117*, 13–23. 10.1172/JCI30227.

5. Berthoud, H.-R., Albaugh, V.L., and Neuhuber, W.L. (2021). Gut-brain communication and obesity: understanding functions of the vagus nerve. J. Clin. Invest. *131*, e143770. 10.1172/JCI143770.

6. Yu, K.B., and Hsiao, E.Y. (2021). Roles for the gut microbiota in regulating neuronal feeding circuits. J. Clin. Invest. *131*, e143772. 10.1172/JCI143772.

7. Backhed, F., Ding, H., Wang, T., Hooper, L.V., Koh, G.Y., Nagy, A., Semenkovich, C.F., and Gordon, J.I. (2004). The gut microbiota as an environmental factor that regulates fat storage. Proc. Natl. Acad. Sci. *101*, 15718–15723. 10.1073/pnas.0407076101.

8. Zarrinpar, A., Chaix, A., Xu, Z.Z., Chang, M.W., Marotz, C.A., Saghatelian, A., Knight, R., and Panda, S. (2018). Antibiotic-induced microbiome depletion alters metabolic homeostasis by affecting gut signaling and colonic metabolism. Nat. Commun. *9*, 2872. 10.1038/s41467-018-05336-9.

9. de Wouters d'Oplinter, A., Rastelli, M., Van Hul, M., Delzenne, N.M., Cani, P.D., and Everard, A. (2021). Gut microbes participate in food preference alterations during obesity. Gut Microbes *13*, 1959242. 10.1080/19490976.2021.1959242.

10. Agustí, A., Campillo, I., Balzano, T., Benítez-Páez, A., López-Almela, I., Romaní-Pérez, M., Forteza, J., Felipo, V., Avena, N.M., and Sanz, Y. (2021). Bacteroides uniformis CECT 7771 Modulates the Brain Reward Response to Reduce Binge Eating and Anxiety-Like Behavior in Rat. Mol. Neurobiol. *58*, 4959–4979. 10.1007/s12035-021-02462-2.

11. Trevelline, B.K., and Kohl, K.D. (2022). The gut microbiome influences host diet selection behavior. Proc. Natl. Acad. Sci. *119*, e2117537119. 10.1073/pnas.2117537119.

12. Gabanyi, I., Lepousez, G., Wheeler, R., Vieites-Prado, A., Nissant, A., Wagner, S., Moigneu, C., Dulauroy, S., Hicham, S., Polomack, B., et al. (2022). Bacterial sensing via neuronal Nod2 regulates appetite and body temperature. Science *376*, eabj3986. 10.1126/science.abj3986.

13. Petrovich, G.D. (2018). Feeding behavior survival circuit: anticipation & competition. Curr. Opin. Behav. Sci. *24*, 137–142. 10.1016/j.cobeha.2018.09.007.

14. Johnson, A.W. (2013). Eating beyond metabolic need: how environmental cues influence feeding behavior. Trends Neurosci. *36*, 101–109. 10.1016/j.tins.2013.01.002.

15. Liu, C.M., and Kanoski, S.E. (2018). Homeostatic and non-homeostatic controls of feeding behavior: Distinct vs. common neural systems. Physiol. Behav. *193*, 223–231. 10.1016/j.physbeh.2018.02.011.

16. Rossi, M.A., and Stuber, G.D. (2018). Overlapping Brain Circuits for Homeostatic and Hedonic Feeding. Cell Metab. *27*, 42–56. 10.1016/j.cmet.2017.09.021.

17. Berridge, K.C. (1996). Food reward: Brain substrates of wanting and liking. Neurosci. Biobehav. Rev. *20*, 1–25. 10.1016/0149-7634(95)00033-B.

18. Yasoshima, Y., and Shimura, T. (2015). A mouse model for binge-like sucrose overconsumption: Contribution of enhanced motivation for sweetener consumption. Physiol. Behav. *138*, 154–164. 10.1016/j.physbeh.2014.10.035.

19. Babbs, R.K., Kelliher, J.C., Scotellaro, J.L., Luttik, K.P., Mulligan, M.K., and Bryant, C.D. (2018). Genetic differences in the behavioral organization of binge eating, conditioned food reward, and compulsive-like eating in C57BL/6J and DBA/2J strains. Physiol. Behav. *197*, 51–66. 10.1016/j.physbeh.2018.09.013.

20. Corwin, R.L.W., and Babbs, R.K. (2012). Rodent Models of Binge Eating: Are They Models of Addiction? ILAR J. *53*, 23–34. 10.1093/ilar.53.1.23.

21. Davis, J.D. (1989). The Microstructure of Ingestive Behavior. Ann. N. Y. Acad. Sci. *575*, 106–121. 10.1111/j.1749-6632.1989.tb53236.x.

22. Spector, A.C., and St. John, S.J. (1998). Role of taste in the microstructure of quinine ingestion by rats. Am. J. Physiol.-Regul. Integr. Comp. Physiol. *274*, R1687–R1703. 10.1152/ajpregu.1998.274.6.R1687.

23. Yeomans, M.R. (1998). Taste, palatability and the control of appetite. Proc. Nutr. Soc. *57*, 609–615. 10.1079/PNS19980089.

24. Davis, J.D., and Perez, M.C. (1993). Food deprivation- and palatability-induced microstructural changes in ingestive behavior. Am. J. Physiol.-Regul. Integr. Comp. Physiol. *264*, R97–R103. 10.1152/ajpregu.1993.264.1.R97.

25. Davis, J.D., and Levine, M.W. (1977). A model for the control of ingestion. Psychol. Rev. *84*, 379–412. 10.1037/0033-295X.84.4.379.

26. Sclafani, A., and Ackroff, K. (2003). Reinforcement value of sucrose measured by progressive ratio operant licking in the rat. Physiol. Behav. *79*, 663–670. 10.1016/S0031-9384(03)00143-4.

27. Guttman, N. (1953). Operant conditioning, extinction, and periodic reinforcement in relation to concentration of sucrose used as reinforcing agent. J. Exp. Psychol. *46*, 213–224. 10.1037/h0061893.

28. Sharma, S., Hryhorczuk, C., and Fulton, S. (2012). Progressive-ratio Responding for Palatable High-fat and High-sugar Food in Mice. JoVE J. Vis. Exp., e3754.

29. Denis, R.G.P., Joly-Amado, A., Webber, E., Langlet, F., Schaeffer, M., Padilla, S., Cansell, C., Dehouck, B., Castel, J., Delbés, A.-S., et al. (2015). Palatability can drive feeding independent of AgRP neurons. Cell Metab. *22*, 646–657. 10.1016/j.cmet.2015.07.011.

30. Li, Z., Yi, C.-X., Katiraei, S., Kooijman, S., Zhou, E., Chung, C.K., Gao, Y., van den Heuvel, J.K., Meijer, O.C., Berbée, J.F.P., et al. (2018). Butyrate reduces appetite and activates brown adipose tissue via the gut-brain neural circuit. Gut *67*, 1269–1279. 10.1136/gutjnl-2017-314050.

31. Frost, G., Sleeth, M.L., Sahuri-Arisoylu, M., Lizarbe, B., Cerdan, S., Brody, L., Anastasovska, J., Ghourab, S., Hankir, M., Zhang, S., et al. (2014). The short-chain fatty acid acetate reduces appetite via a central homeostatic mechanism. Nat. Commun. *5*, 3611. 10.1038/ncomms4611.

32. Niimi, K., and Takahashi, E. (2019). New system to examine the activity and water and food intake of germ-free mice in a sealed positive-pressure cage. Heliyon *5*, e02176. 10.1016/j.heliyon.2019.e02176.

33. Moretti, C.H., Schiffer, T.A., Li, X., Weitzberg, E., Carlström, M., and Lundberg, J.O. (2021). Germ-free mice are not protected against diet-induced obesity and metabolic dysfunction. Acta Physiol. *231*, e13581. 10.1111/apha.13581.

34. Rabot, S., Membrez, M., Bruneau, A., Gérard, P., Harach, T., Moser, M., Raymond, F., Mansourian, R., and Chou, C.J. (2010). Germ-free C57BL/6J mice are resistant to high-fat-diet-induced insulin resistance and have altered cholesterol metabolism. FASEB J. *24*, 4948–4959. 10.1096/fj.10.164921.

35. Swartz, T.D., Duca, F.A., Wouters, T. de, Sakar, Y., and Covasa, M. (2012). Up-regulation of intestinal type 1 taste receptor 3 and sodium glucose luminal transporter-1 expression and increased sucrose intake in mice lacking gut microbiota. Br. J. Nutr. *107*, 621–630. 10.1017/S0007114511003412.

36. Muller, P.A., Schneeberger, M., Matheis, F., Wang, P., Kerner, Z., Ilanges, A., Pellegrino, K., del Mármol, J., Castro, T.B.R., Furuichi, M., et al. (2020). Microbiota modulate sympathetic neurons via a gut–brain circuit. Nature *583*, 441–446. 10.1038/s41586-020-2474-7.

37. Schieber, A.M.P., Lee, Y.M., Chang, M.W., Leblanc, M., Collins, B., Downes, M., Evans, R.M., and Ayres, J.S. (2015). Disease tolerance mediated by microbiome E. coli involves inflammasome and IGF-1 signaling. Science *350*, 558–563. 10.1126/science.aac6468.

38. Wu, W.-L., Adame, M.D., Liou, C.-W., Barlow, J.T., Lai, T.-T., Sharon, G., Schretter, C.E., Needham, B.D., Wang, M.I., Tang, W., et al. (2021). Microbiota regulate social behaviour via stress response neurons in the brain. Nature *595*, 409–414. 10.1038/s41586-021-03669-y.

39. Desbonnet, L., Clarke, G., Traplin, A., O'Sullivan, O., Crispie, F., Moloney, R.D., Cotter, P.D., Dinan, T.G., and Cryan, J.F. (2015). Gut microbiota depletion from early adolescence in mice: Implications for brain and behaviour. Brain. Behav. Immun. *48*, 165–173. 10.1016/j.bbi.2015.04.004.

40. Wu, J.-T., Sun, C.-L., Lai, T.-T., Liou, C.-W., Lin, Y.-Y., Xue, J.-Y., Wang, H.-W., Chai, L.M.X., Lee, Y.-J., Chen, S.-L., et al. (2022). Oral short-chain fatty acids administration regulates innate anxiety in adult microbiome-depleted mice. Neuropharmacology *214*, 109140. 10.1016/j.neuropharm.2022.109140.

41. Chu, C., Murdock, M.H., Jing, D., Won, T.H., Chung, H., Kressel, A.M., Tsaava, T., Addorisio, M.E., Putzel, G.G., Zhou, L., et al. (2019). The microbiota regulate neuronal function and fear extinction learning. Nature *574*, 543–548. 10.1038/s41586-019-1644-y.

42. Nguyen, K.P., O'Neal, T.J., Bolonduro, O.A., White, E., and Kravitz, A.V. (2016). Feeding Experimentation Device (FED): A flexible open-source device for measuring feeding behavior. J. Neurosci. Methods *267*, 108–114. 10.1016/j.jneumeth.2016.04.003.

43. Goulding, E.H., Schenk, A.K., Juneja, P., MacKay, A.W., Wade, J.M., and Tecott, L.H. (2008). A robust automated system elucidates mouse home cage behavioral structure. Proc. Natl. Acad. Sci. *105*, 20575–20582. 10.1073/pnas.0809053106.

44. Rathod, Y.D., and Fulvio, M.D. (2021). The feeding microstructure of male and female mice. PLOS ONE *16*, e0246569. 10.1371/journal.pone.0246569.

45. Crawley, J.N. (1985). Exploratory behavior models of anxiety in mice. Neurosci. Biobehav. Rev. *9*, 37–44. 10.1016/0149-7634(85)90030-2.

46. Burnett, C.J., Li, C., Webber, E., Tsaousidou, E., Xue, S.Y., Brüning, J.C., and Krashes, M.J. (2016). Hunger-driven motivational state competition. Neuron *92*, 187–201. 10.1016/j.neuron.2016.08.032.

47. Samuels, B.A., and Hen, R. (2011). Novelty-Suppressed Feeding in the Mouse. In Mood and Anxiety Related Phenotypes in Mice Neuromethods., T. D. Gould, ed. (Humana Press), pp. 107–121. 10.1007/978-1-61779-313-4_7.

48. Walf, A.A., and Frye, C.A. (2007). The use of the elevated plus maze as an assay of anxiety-related behavior in rodents. Nat. Protoc. *2*, 322–328. 10.1038/nprot.2007.44.

49. Gould, T.D., Dao, D.T., and Kovacsics, C.E. (2009). The Open Field Test. In Mood and Anxiety Related Phenotypes in Mice: Characterization Using Behavioral Tests Neuromethods., T. D. Gould, ed. (Humana Press), pp. 1–20.

50. Hoban, A.E., Moloney, R.D., Golubeva, A.V., McVey Neufeld, K.A., O'Sullivan, O., Patterson, E., Stanton, C., Dinan, T.G., Clarke, G., and Cryan, J.F. (2016). Behavioural and neurochemical consequences of chronic gut microbiota depletion during adulthood in the rat. Neuroscience *339*, 463–477. 10.1016/j.neuroscience.2016.10.003.

51. Fröhlich, E.E., Farzi, A., Mayerhofer, R., Reichmann, F., Jačan, A., Wagner, B., Zinser, E., Bordag, N., Magnes, C., Fröhlich, E., et al. (2016). Cognitive impairment by antibiotic-induced gut dysbiosis: Analysis of gut microbiota-brain communication. Brain. Behav. Immun. *56*, 140–155. 10.1016/j.bbi.2016.02.020.

52. McDougle, M., Quinn, D., Diepenbroek, C., Singh, A., de la Serre, C., and de Lartigue, G. (2021). Intact vagal gut-brain signalling prevents hyperphagia and excessive weight gain in response to high-fat high-sugar diet. Acta Physiol. *231*, e13530. 10.1111/apha.13530.

53. Chambers, A.P., Sandoval, D.A., and Seeley, R.J. (2013). Integration of Satiety Signals by the Central Nervous System. Curr. Biol. *23*, R379–R388. 10.1016/j.cub.2013.03.020.

54. Siemian, J.N., Arenivar, M.A., Sarsfield, S., Borja, C.B., Russell, C.N., and Aponte, Y. (2021). Lateral hypothalamic LEPR neurons drive appetitive but not consummatory behaviors. Cell Rep. *36*, 109615. 10.1016/j.celrep.2021.109615.

55. Jones, S.R., and Fordahl, S.C. (2021). Bingeing on High-Fat Food Enhances Evoked Dopamine Release and Reduces Dopamine Uptake in the Nucleus Accumbens. Obesity *29*, 721–730. 10.1002/oby.23122.

56. Campos, C.A., Bowen, A.J., Schwartz, M.W., and Palmiter, R.D. (2016). Parabrachial CGRP Neurons Control Meal Termination. Cell Metab. *23*, 811–820. 10.1016/j.cmet.2016.04.006.

57. Le Roy, T., Debédat, J., Marquet, F., Da-Cunha, C., Ichou, F., Guerre-Millo, M., Kapel, N., Aron-Wisnewsky, J., and Clément, K. (2019). Comparative Evaluation of Microbiota Engraftment Following Fecal Microbiota Transfer in Mice Models: Age, Kinetic and Microbial Status Matter. Front. Microbiol. *9*, 3289. 10.3389/fmicb.2018.03289.

58. Matikainen-Ankney, B.A., Earnest, T., Ali, M., Casey, E., Wang, J.G., Sutton, A.K., Legaria, A.A., Barclay, K.M., Murdaugh, L.B., Norris, M.R., et al. (2021). An open-source device for measuring food intake and operant behavior in rodent home-cages. eLife *10*, e66173. 10.7554/eLife.66173.

59. Kutlu, M.G., Zachry, J.E., Melugin, P.R., Cajigas, S.A., Chevee, M.F., Kelly, S.J., Kutlu, B., Tian, L., Siciliano, C.A., and Calipari, E.S. (2021). Dopamine release in the nucleus accumbens core signals perceived saliency. Curr. Biol. *31*, 4748–4761. 10.1016/j.cub.2021.08.052.

60. Hsu, T.M., McCutcheon, J.E., and Roitman, M.F. (2018). Parallels and Overlap: The Integration of Homeostatic Signals by Mesolimbic Dopamine Neurons. Front. Psychiatry *9*, 410. 10.3389/fpsyt.2018.00410.

61. Berridge, K.C. (2007). The debate over dopamine's role in reward: the case for incentive salience. Psychopharmacology (Berl.) *191*, 391–431. 10.1007/s00213-006-0578-x.

62. Hahn, T.M., Breininger, J.F., Baskin, D.G., and Schwartz, M.W. (1998). Coexpression of Agrp and NPY in fasting-activated hypothalamic neurons. Nat. Neurosci. *1*, 271–272. 10.1038/1082.

63. Augustine, V., Lee, S., and Oka, Y. (2020). Neural Control and Modulation of Thirst, Sodium Appetite, and Hunger. Cell *180*, 25–32. 10.1016/j.cell.2019.11.040.

64. Mizuno, T.M., and Mobbs, C.V. (1999). Hypothalamic Agouti-Related Protein Messenger Ribonucleic Acid Is Inhibited by Leptin and Stimulated by Fasting. Endocrinology *140*, 814–817. 10.1210/endo.140.2.6491.

65. Sanacora, G., Kershaw, M., Finkelstein, J.A., and White, J.D. (1990). Increased Hypothalamic Content of Preproneuropeptide Y Messenger Ribonucleic Acid in Genetically

Obese Zucker Rats and Its Regulation by Food Deprivation. Endocrinology *127*, 730–737. 10.1210/endo-127-2-730.

66. Perello, M., Stuart, R.C., and Nillni, E.A. (2007). Differential effects of fasting and leptin on proopiomelanocortin peptides in the arcuate nucleus and in the nucleus of the solitary tract. Am. J. Physiol.-Endocrinol. Metab. *292*, E1348–E1357. 10.1152/ajpendo.00466.2006.

67. Donaldson, G.P., Lee, S.M., and Mazmanian, S.K. (2016). Gut biogeography of the bacterial microbiota. Nat. Rev. Microbiol. *14*, 20–32. 10.1038/nrmicro3552.

68. Ormerod, K.L., Wood, D.L.A., Lachner, N., Gellatly, S.L., Daly, J.N., Parsons, J.D., Dal'Molin, C.G.O., Palfreyman, R.W., Nielsen, L.K., Cooper, M.A., et al. (2016). Genomic characterization of the uncultured Bacteroidales family S24-7 inhabiting the guts of homeothermic animals. Microbiome *4*, 36. 10.1186/s40168-016-0181-2.

69. Kirkpatrick, S.L., Goldberg, L.R., Yazdani, N., Babbs, R.K., Wu, J., Reed, E.R., Jenkins, D.F., Bolgioni, A.F., Landaverde, K.I., Luttik, K.P., et al. (2017). Cytoplasmic FMR1-Interacting Protein 2 Is a Major Genetic Factor Underlying Binge Eating. Biol. Psychiatry *81*, 757–769. 10.1016/j.biopsych.2016.10.021.

70. Castro, D.C., Oswell, C.S., Zhang, E.T., Pedersen, C.E., Piantadosi, S.C., Rossi, M.A., Hunker, A.C., Guglin, A., Morón, J.A., Zweifel, L.S., et al. (2021). An endogenous opioid circuit determines state-dependent reward consumption. Nature *598*, 646–651.

71. Cordain, L., Eaton, S.B., Sebastian, A., Mann, N., Lindeberg, S., Watkins, B.A., O'Keefe, J.H., and Brand-Miller, J. (2005). Origins and evolution of the Western diet: health implications for the 21st century. Am. J. Clin. Nutr. *81*, 341–354. 10.1093/ajcn.81.2.341.

72. Duca, F.A., Swartz, T.D., Sakar, Y., and Covasa, M. (2012). Increased Oral Detection, but Decreased Intestinal Signaling for Fats in Mice Lacking Gut Microbiota. PLoS ONE *7*, e39748. 10.1371/journal.pone.0039748.

73. García-Cabrerizo, R., Carbia, C., O´Riordan, K.J., Schellekens, H., and Cryan, J.F. (2021). Microbiota-gut-brain axis as a regulator of reward processes. J. Neurochem. *157*, 1495–1524. 10.1111/jnc.15284.

74. Crumeyrolle-Arias, M., Jaglin, M., Bruneau, A., Vancassel, S., Cardona, A., Daugé, V., Naudon, L., and Rabot, S. (2014). Absence of the gut microbiota enhances anxiety-like behavior and neuroendocrine response to acute stress in rats. Psychoneuroendocrinology *42*, 207–217. 10.1016/j.psyneuen.2014.01.014.

75. Heijtz, R.D., Wang, S., Anuar, F., Qian, Y., Bjorkholm, B., Samuelsson, A., Hibberd, M.L., Forssberg, H., and Pettersson, S. (2011). Normal gut microbiota modulates brain development and behavior. Proc. Natl. Acad. Sci. *108*, 3047–3052. 10.1073/pnas.1010529108.

76. Nishino, R., Mikami, K., Takahashi, H., Tomonaga, S., Furuse, M., Hiramoto, T., Aiba, Y., Koga, Y., and Sudo, N. (2013). Commensal microbiota modulate murine behaviors in a strictly contamination-free environment confirmed by culture-based methods. Neurogastroenterol. Motil. *25*, 521-e371. 10.1111/nmo.12110.

77. Manca, C., Shen, M., Boubertakh, B., Martin, C., Flamand, N., Silvestri, C., and Di Marzo, V. (2020). Alterations of brain endocannabinoidome signaling in germ-free mice. Biochim. Biophys. Acta BBA - Mol. Cell Biol. Lipids *1865*, 158786. 10.1016/j.bbalip.2020.158786.

78. Bercik, P., Denou, E., Collins, J., Jackson, W., Lu, J., Jury, J., Deng, Y., Blennerhassett, P., Macri, J., McCoy, K.D., et al. (2011). The Intestinal Microbiota Affect Central Levels of Brain-Derived Neurotropic Factor and Behavior in Mice. Gastroenterology *141*, 599-609.e3. 10.1053/j.gastro.2011.04.052.

79. Valladares, R., Sankar, D., Li, N., Williams, E., Lai, K.-K., Abdelgeliel, A.S., Gonzalez, C.F., Wasserfall, C.H., Iii, J.L., Schatz, D., et al. (2010). Lactobacillus johnsonii N6.2 Mitigates the Development of Type 1 Diabetes in BB-DP Rats. PLOS ONE *5*, e10507. 10.1371/journal.pone.0010507.

80. Kang, J.-H., Yun, S.-I., Park, M.-H., Park, J.-H., Jeong, S.-Y., and Park, H.-O. (2013). Anti-Obesity Effect of Lactobacillus gasseri BNR17 in High-Sucrose Diet-Induced Obese Mice. PLOS ONE *8*, e54617. 10.1371/journal.pone.0054617.

81. Chagwedera, D.N., Ang, Q.Y., Bisanz, J.E., Leong, Y.A., Ganeshan, K., Cai, J., Patterson, A.D., Turnbaugh, P.J., and Chawla, A. (2019). Nutrient Sensing in CD11c Cells Alters the Gut Microbiota to Regulate Food Intake and Body Mass. Cell Metab. *30*, 364-373.e7. 10.1016/j.cmet.2019.05.002.

82. Armougom, F., Henry, M., Vialettes, B., Raccah, D., and Raoult, D. (2009). Monitoring Bacterial Community of Human Gut Microbiota Reveals an Increase in Lactobacillus in Obese Patients and Methanogens in Anorexic Patients. PLOS ONE *4*, e7125. 10.1371/journal.pone.0007125.

83. Morita, C., Tsuji, H., Hata, T., Gondo, M., Takakura, S., Kawai, K., Yoshihara, K., Ogata, K., Nomoto, K., Miyazaki, K., et al. (2015). Gut Dysbiosis in Patients with Anorexia Nervosa. PLOS ONE *10*, e0145274. 10.1371/journal.pone.0145274.

84. Mack, I., Cuntz, U., Grämer, C., Niedermaier, S., Pohl, C., Schwiertz, A., Zimmermann, K., Zipfel, S., Enck, P., and Penders, J. (2016). Weight gain in anorexia nervosa does not ameliorate the faecal microbiota, branched chain fatty acid profiles and gastrointestinal complaints. Sci. Rep. *6*, 26752. 10.1038/srep26752.

85. Prochazkova, P., Roubalova, R., Dvorak, J., Kreisinger, J., Hill, M., Tlaskalova-Hogenova, H., Tomasova, P., Pelantova, H., Cermakova, M., Kuzma, M., et al. (2021). The intestinal microbiota and metabolites in patients with anorexia nervosa. Gut Microbes *13*, 1902771. 10.1080/19490976.2021.1902771.

86. Leyrolle, Q., Cserjesi, R., Mulders, M.D.G.H., Zamariola, G., Hiel, S., Gianfrancesco, M.A., Rodriguez, J., Portheault, D., Amadieu, C., Leclercq, S., et al. (2021). Specific gut microbial, biological, and psychiatric profiling related to binge eating disorders: A cross-sectional study in obese patients. Clin. Nutr. *40*, 2035–2044. 10.1016/j.clnu.2020.09.025.

87. Breton, J., Tirelle, P., Hasanat, S., Pernot, A., L'Huillier, C., do Rego, J.-C., Déchelotte, P., Coëffier, M., Bindels, L.B., and Ribet, D. (2021). Gut microbiota alteration in a mouse model of Anorexia Nervosa. Clin. Nutr. Edinb. Scotl. *40*, 181–189. 10.1016/j.clnu.2020.05.002.

88. Bernard, A., Ancel, D., Neyrinck, A.M., Dastugue, A., Bindels, L.B., Delzenne, N.M., and Besnard, P. (2019). A Preventive Prebiotic Supplementation Improves the Sweet Taste Perception in Diet-Induced Obese Mice. Nutrients *11*, 549. 10.3390/nu11030549.

89. Lyte, M., Fodor, A.A., Chapman, C.D., Martin, G.G., Perez-Chanona, E., Jobin, C., and Dess, N.K. (2016). Gut Microbiota and a Selectively Bred Taste Phenotype: A Novel Model of Microbiome-Behavior Relationships. Psychosom. Med. *78*, 610–619. 10.1097/PSY.0000000000000318.

90. Kim, S., Covington, A., and Pamer, E.G. (2017). The intestinal microbiota: Antibiotics, colonization resistance, and enteric pathogens. Immunol. Rev. *279*, 90–105. 10.1111/imr.12563.

91. Smith, P.M., Howitt, M.R., Panikov, N., Michaud, M., Gallini, C.A., Bohlooly-Y, M., Glickman, J.N., and Garrett, W.S. (2013). The Microbial Metabolites, Short-Chain Fatty Acids, Regulate Colonic Treg Cell Homeostasis. Science *341*, 569–573. 10.1126/science.1241165.

92. Erny, D., Hrabě de Angelis, A.L., Jaitin, D., Wieghofer, P., Staszewski, O., David, E., Keren-Shaul, H., Mahlakoiv, T., Jakobshagen, K., Buch, T., et al. (2015). Host microbiota constantly control maturation and function of microglia in the CNS. Nat. Neurosci. *18*, 965–977. 10.1038/nn.4030.

93. Caporaso, J.G., Lauber, C.L., Walters, W.A., Berg-Lyons, D., Lozupone, C.A., Turnbaugh, P.J., Fierer, N., and Knight, R. (2011). Global patterns of 16S rRNA diversity at a depth of millions of sequences per sample. Proc. Natl. Acad. Sci. *108*, 4516–4522. 10.1073/pnas.1000080107.

94. Kozich, J.J., Westcott, S.L., Baxter, N.T., Highlander, S.K., and Schloss, P.D. (2013). Development of a Dual-Index Sequencing Strategy and Curation Pipeline for Analyzing Amplicon Sequence Data on the MiSeq Illumina Sequencing Platform. Appl. Environ. Microbiol. *79*, 5112–5120. 10.1128/AEM.01043-13.

95. Thompson, L.R., Sanders, J.G., McDonald, D., Amir, A., Ladau, J., Locey, K.J., Prill, R.J., Tripathi, A., Gibbons, S.M., Ackermann, G., et al. (2017). A communal catalogue reveals Earth's multiscale microbial diversity. Nature *551*, 457–463. 10.1038/nature24621.

96. Bolyen, E., Rideout, J.R., Dillon, M.R., Bokulich, N.A., Abnet, C.C., Al-Ghalith, G.A., Alexander, H., Alm, E.J., Arumugam, M., Asnicar, F., et al. (2019). Reproducible, interactive, scalable and extensible microbiome data science using QIIME 2. Nat. Biotechnol. *37*, 852–857. 10.1038/s41587-019-0209-9.

97. Mallick, H., Rahnavard, A., McIver, L.J., Ma, S., Zhang, Y., Nguyen, L.H., Tickle, T.L., Weingart, G., Ren, B., Schwager, E.H., et al. (2021). Multivariable association discovery in population-scale meta-omics studies. PLOS Comput. Biol. *17*, e1009442. 10.1371/journal.pcbi.1009442.

98. Lane, D.J. (1991). 16S/23S rRNA sequencing. In Nucleic acid techniques in bacterial systematics., E. Stackebrandt and M. Goodfellow, eds. (John Wiley and Sons), pp. 115–175.

99. Turner, S., Pryer, K.M., Miao, V.P., and Palmer, J.D. (1999). Investigating deep phylogenetic relationships among cyanobacteria and plastids by small subunit rRNA sequence analysis. J. Eukaryot. Microbiol. *46*, 327–338. 10.1111/j.1550-7408.1999.tb04612.x.

100. Madeira, F., Park, Y.M., Lee, J., Buso, N., Gur, T., Madhusoodanan, N., Basutkar, P., Tivey, A.R.N., Potter, S.C., Finn, R.D., et al. (2019). The EMBL-EBI search and sequence analysis tools APIs in 2019. Nucleic Acids Res. *47*, W636–W641. 10.1093/nar/gkz268.

101. Altschul, S.F., Gish, W., Miller, W., Myers, E.W., and Lipman, D.J. (1990). Basic local alignment search tool. J. Mol. Biol. *215*, 403–410. 10.1016/S0022-2836(05)80360-2.

102. Piper, M.L., Unger, E.K., Myers, M.G., and Xu, A.W. (2008). Specific Physiological Roles for Signal Transducer and Activator of Transcription 3 in Leptin Receptor-Expressing Neurons. Mol. Endocrinol. *22*, 751–759. 10.1210/me.2007-0389.

103. Reichenbach, A., Mequinion, M., Bayliss, J.A., Lockie, S.H., Lemus, M.B., Mynatt, R.L., Stark, R., and Andrews, Z.B. (2018). Carnitine Acetyltransferase in AgRP Neurons Is Required for the Homeostatic Adaptation to Restricted Feeding in Male Mice. Endocrinology *159*, 2473–2483. 10.1210/en.2018-00131.

104. Paxinos, G., and Franklin, K.B.J. (2019). Paxinos and Franklin's the Mouse Brain in Stereotaxic Coordinates (Academic Press).

105. Rouibi, K., and Contarino, A. (2012). Increased motivation to eat in opiate-withdrawn mice. Psychopharmacology (Berl.) *221*, 675–684. 10.1007/s00213-011-2612-x.

106. Blasio, A., Steardo, L., Sabino, V., and Cottone, P. (2014). Opioid system in the medial prefrontal cortex mediates binge-like eating. Addict. Biol. *19*, 652–662. 10.1111/adb.12033.

107. Babbs, R.K., Beierle, J.A., Yao, E.J., Kelliher, J.C., Medeiros, A.R., Anandakumar, J., Shah, A.A., Chen, M.M., Johnson, W.E., and Bryant, C.D. (2020). The effect of the demyelinating agent cuprizone on binge-like eating of sweetened palatable food in female and male C57BL/6 substrains. Appetite *150*, 104678. 10.1016/j.appet.2020.104678.

108. Friard, O., and Gamba, M. (2016). BORIS: a free, versatile open-source event-logging software for video/audio coding and live observations. Methods Ecol. Evol. *7*, 1325–1330. 10.1111/2041-210X.12584.

109. Thiele, T.E., Crabbe, J.C., and Boehm, S.L. (2014). "Drinking in the Dark" (DID): A Simple Mouse Model of Binge-Like Alcohol Intake. Curr. Protoc. Neurosci. Editor. Board Jacqueline N Crawley Al *68*, 9.49.1-9.49.12. 10.1002/0471142301.ns0949s68.

110. Strohmayer, A.J., and Smith, G.P. (1987). The meal pattern of genetically obese (ob/ob) mice. Appetite *8*, 111–123. 10.1016/S0195-6663(87)80004-1.

111. Ford, M.M., Steele, A.M., McCracken, A.D., Finn, D.A., and Grant, K.A. (2013). The relationship between adjunctive drinking, blood ethanol concentration and plasma corticosterone across fixed-time intervals of food delivery in two inbred mouse strains. Psychoneuroendocrinology *38*, 2598–2610. 10.1016/j.psyneuen.2013.06.011.

112. Richardson, N.R., and Roberts, D.C.S. (1996). Progressive ratio schedules in drug self-administration studies in rats: a method to evaluate reinforcing efficacy. J. Neurosci. Methods *66*, 1–11. 10.1016/0165-0270(95)00153-0.

113. Devarakonda, K., Nguyen, K.P., and Kravitz, A.V. (2016). ROBucket: A low cost operant chamber based on the Arduino microcontroller. Behav. Res. Methods *48*, 503–509. 10.3758/s13428-015-0603-2.

114. Goldberg, L.R., Kirkpatrick, S.L., Yazdani, N., Luttik, K.P., Lacki, O.A., Keith Babbs, R., Jenkins, D.F., Evan Johnson, W., and Bryant, C.D. (2017). Casein kinase 1-epsilon deletion increases mu opioid receptor-dependent behaviors and binge eating. Genes Brain Behav. *16*, 725–738. 10.1111/gbb.12397.

115. RStudio Team (2020). RStudio: Integrated Development for R. http://www.rstudio.com/.

116. R Core Team (2018). R: A language and environment for statistical computing. R Found. Stat. Comput. https://www.R-project.org/.

117. Noldus, L.P.J.J., Spink, A.J., and Tegelenbosch, R.A.J. (2001). EthoVision: A versatile video tracking system for automation of behavioral experiments. Behav. Res. Methods Instrum. Comput. *33*, 398–414. 10.3758/BF03195394.

118. Schindelin, J., Arganda-Carreras, I., Frise, E., Kaynig, V., Longair, M., Pietzsch, T., Preibisch, S., Rueden, C., Saalfeld, S., Schmid, B., et al. (2012). Fiji: an open-source platform for biological-image analysis. Nat. Methods *9*, 676–682. 10.1038/nmeth.2019.

Supplemental Tables

Table S1. Statistical tests and exact p-values for all comparisons made.

Figure	Statistical test	Test statistics and P values
1A	Two-way RM ANOVA Šidák's multiple comparisons test	Time x Treatment (F(4,124) = [22.59], P<0.0001) Time (F(2.423,75.12) = [574.8], P<0.0001) Treatment (F(1,31) = [34.94], P<0.0001) Subject (F(31,124) = [8.629], P<0.0001) 0 30 t=4.963, df=31.00, p-adj.=0.0001 60 t=4.979, df=30.42, p-adj.=0.0001 90 t=5.699, df=28.90, p-adj.<0.0001 120 t=6.276, df=30.38, p-adj.<0.0001
1B	Mann-Whitney	Mann-Whitney U=10, P<0.0001
1C	Two-way RM ANOVA Šidák's multiple comparisons test	Time x Treatment (F(4,124) = [15.12], P<0.0001) Time (F(1.045,32.40) = [158.8], P<0.0001) Treatment (F(1,31) = [33.15], P<0.0001) Subject (F(31,124) = [1.071], P<0.3824) 0 t=4.403, df=27.24, p-adj.=0.0007 30 t=6.248, df=30.96, p-adj.<0.0001 60 t=2.817, df=30.69, p-adj.=0.0413 90 t=0.2559, df=26.95, p-adj.=0.9997 120 t=0.8750, df=21.76, p-adj.=0.9163
1E	Two-tailed Student's t-test	Pellets / Bout t=3.466, df=31, P=0.0016 Average Bout Length (sec) t=5.049, df=31, P<0.0001
1F	Two-tailed Student's t-test	t=4.690, df=19, P=0.0002

1G	Two-way RM ANOVA, Tukey's multiple comparisons test (within timepoints)	Time x Treatment (F(8,104) = [8.708], P<0.0001) Time (F(2.638,68.58) = [506.7], P<0.0001) Treatment (F(2,26) = [14.89], P<0.0001) Subject (F(26,104) =[6.849], P<0.0001) 0 30 VEH vs. ABX+SHAM q=4.807, df=10.91, p-adj.=0.0152 VEH vs. ABX+FMT q=2.175, df=17.42, p-adj.=0.2983 ABX+SHAM vs. ABX+FMT q=3.781, df=10.04, p-adj.=0.0557 60 VEH vs. ABX+SHAM q=5.359, df=11.79, p-adj.=0.0069 VEH vs. ABX+FMT q=1.050, df=17.81, p-adj.=0.7419 ABX+SHAM vs. ABX+FMT q=4.562, df=12.54, p-adj.=0.0176 90 VEH vs. ABX+SHAM q=5.156, df=12.31, p-adj.=0.0084 VEH vs. ABX+FMT q=0.372, df=15.68, p-adj.=0.9627 ABX+SHAM vs. ABX+FMT q=4.284, df=15.77, p-adj.=0.0208 120 VEH vs. ABX+SHAM q=8.129, df=11.04, p-adj.=0.0003 VEH vs. ABX+FMT q=1.526, df=15.49, p-adj.=0.5404 ABX+SHAM vs. ABX+FMT q=6.343, df=14.31, p-adj.=0.0013
1H	One-way ANOVA Kruskal-Wallis, Dunn's multiple comparisons test	KW statistic: 16.82, P=0.0002 VEH vs. ABX+SHAM Z=4.064, p-adj.=0.0001 VEH vs. ABX+FMT Z=1.497, p-adj.=0.4033 ABX+SHAM vs. ABX+FMT Z=2.607, p-adj.=0.0274

1I	Two-way RM ANOVA, Tukey's multiple comparisons test (within timepoints)	Time x Treatment (F(8,104) = [4.109], P=0.0003) Time (F(1.040,27.04) = [112.9], P<0.0001) Treatment (F(2,26) = [14.88], P<0.0001) Subject (F(26,104) =[1.290], P=0.1839) 0 VEH vs. ABX+SHAM q=4.661, df=11.93, p-adj.=0.0164 VEH vs. ABX+FMT q=2.176, df=17.99, p-adj.=0.2972 ABX+SHAM vs. ABX+FMT q=3.245, df=12.07, p-adj.=0.0950 30 VEH vs. ABX+SHAM q=5.670, df=10.47, p-adj.=0.0059 VEH vs. ABX+FMT q=0.6618, df=17.37, p-adj.=0.8871 ABX+SHAM vs. ABX+FMT q=5.128, df=11.55, p-adj.=0.0095 60 VEH vs. ABX+SHAM q=4.228, df=12.62, p-adj.=0.0270 VEH vs. ABX+FMT q=0.9741, df=12.48, p-adj.=0.7742 ABX+SHAM vs. ABX+FMT q=3.870, df=16.62, p-adj.=0.0361 90 VEH vs. ABX+SHAM q=1.335, df=15.96, p-adj.=0.6214 VEH vs. ABX+FMT q=1.206, df=15.28, p-adj.=0.6770 ABX+SHAM vs. ABX+FMT q=2.189, df=16.43, p-adj.=0.2954 120 VEH vs. ABX+SHAM q=0.1707, df=16.33, p-adj.=0.9920 VEH vs. ABX+FMT q=1.236, df=17.24, p-adj.=0.6635 ABX+SHAM vs. ABX+FMT q=1.315, df=17.00, p-adj.=0.6294
2B	Two-way RM ANOVA, Šidák's multiple comparisons test	Time x Treatment (F(6,132) = [0.5929], P=0.7355) Time (F(6,132) = [17.52], P<0.0001) Treatment (F(1,22) = [33.70], P<0.0001) Subject (F(22,132) = [4.566], P<0.0001) 1 t=2.761, df=154.0, p-adj.=0.0444 2 t=3.394, df=154.0, p-adj.=0.0061 3 t=4.590, df=154.0, p-adj.<0.0001 4 t=3.939, df=154.0, p-adj.=0.0009 5 t=4.273, df=154.0, p-adj.=0.0002 6 t=3.535, df=154.0, p-adj.=0.0038 7 t=4.220, df=154.0, p-adj.=0.0003
2C	Two-tailed Student's t-test	t=3.956, df=20, P=0.0008

2E, S3B	Two-way ANOVAs, Bonferroni's multiple comparisons test (within region)	NAc Shell Treatment x Stimulus (F(1,22)=[8.128], P=0.0093) Stimulus (F(1,22)=[63.65], P<0.0001) Treatment (F(1,22)=[10.61], P=0.0036) -Stimulus, VEH vs. ABX t=0.2588, df=22.00, p-adj.>0.9999 +Stimulus, VEH vs. ABX t=4.924, df=22.00, p-adj.=0.0001 NAc Core Treatment x Stimulus (F(1,22)=[5.531], P=0.0280) Stimulus (F(1,22)=[26.17], P<0.0001) Treatment (F(1,22)=[7.238], P=0.0134) -Stimulus, VEH vs. ABX t=0.2157, df=22.00, p-adj.>0.9999 +Stimulus, VEH vs. ABX t=4.065, df=22.00, p-adj.=0.0010 VTA Treatment x Stimulus (F(1,22)=[11.69], P=0.0025) Stimulus (F(1,22)=[61.99], P<0.0001) Treatment (F(1,22)=[11.35], P=0.0028) -Stimulus, VEH vs. ABX t=0.03228, df=22.00, p-adj.>0.9999 +Stimulus, VEH vs. ABX t=5.473, df=22.00, p-adj.<0.0001
3A	Two-way RM ANOVA, Dunnett's multiple comparisons test to VEH (within timepoints)	Time x Treatment (F(20,168) = [8.733], P<0.0001) Time (F(2.415, 101.4) = [909.2], P<0.0001) Treatment (F(5,42) = [16.98], P<0.0001) Subject (F(42,168) = [7.409], P<0.0001) 0 30 vs. ABX q=9.449, df=9.771, p-adj.<0.0001 vs. A q=4.737, df=8.366, p-adj.=0.0051 vs. V q=4.505, df=8.685, p-adj.=0.0063 vs. N q=1.746, df=9.626, p-adj.=0.3400 vs M q=1.766, df=10.35, p-adj.=0.3272 60 vs. ABX q=8.787, df=13.98, p-adj.<0.0001 vs. A q=4.636, df=11.84, p-adj.=0.0025 vs. V q=4.167, df=12.15, p-adj.=0.0052 vs. N q=2.279, df=13.94, p-adj.=0.1373 vs M q=1.650, df=13.12, p-adj.=0.3725 90 vs. ABX q=7.159, df=13.44, p-adj.<0.0001 vs. A q=4.747, df=13.98, p-adj.=0.0014 vs. V q=3.624, df=13.58, p-adj.=0.0118 vs. N q=1.476, df=13.20, p-adj.=0.4699 vs M q=1.210, df=13.42, p-adj.=0.6384 120 vs. ABX q=6.550, df=13.48, p-adj.<0.0001 vs. A q=5.221, df=12.79, p-adj.=0.0008 vs. V q=3.469, df=13.83, p-adj.=0.0154 vs. N q=1.219, df=11.70, p-adj.=0.6345 vs M q=0.9712, df=14.00, p-adj.=0.7922

3B	One-way ANOVA Kruskal-Wallis, Dunn's multiple comparisons test to VEH	KW statistic: 32.78, P<0.0001 vs. ABX Z=4.286, p-adj<0.0001 vs. A Z=3.607, p-adj.=0.0015 vs. V Z=2.929, p-adj.=0.0170 vs. N Z=0.500, p-adj.>0.9999 vs. M Z=0.7857, p-adj.>0.9999
3C	Two-way RM ANOVA, Dunnett's multiple comparisons test to VEH - FMT (within timepoints)	Time x Treatment (F(20,168) = [3.097], P<0.0001) Time (F(1.862,78.19) = [664.2], P<0.0001) Treatment (F(5,42) = [5.676], P=0.0004) Subject (F(42,168) = [7.177], P<0.0001) 0 30 vs. ABX q=4.175, df=13.99, p-adj.=0.0039 vs. A - FMT q=3.022, df=8.781, p-adj.=0.0536 vs. V - FMT q=4.091, df=13.15, p-adj.=0.0052 vs. N - FMT q=0.5943, df=13.17, p-adj.=0.9608 vs M - FMT q=0.4231, df=10.11, p-adj.=0.9901 60 vs. ABX q=4.179, df=12.95, p-adj.=0.0045 vs. A - FMT q=2.413, df=8.722, p-adj.=0.1347 vs. V - FMT q=3.794, df=13.89, p-adj.=0.0082 vs. N - FMT q=0.2564, df=11.30, p-adj.=0.9986 vs M - FMT q=0.5038, df=11.15, p-adj.=0.9795 90 vs. ABX q=3.493, df=13.85, p-adj.=0.0147 vs. A - FMT q=3.148, df=10.64, p-adj.=0.0364 vs. V - FMT q=4.486, df=12.46, p-adj.=0.0028 vs. N - FMT q=0.7089, df=10.95, p-adj.=0.9232 vs M - FMT q=0.05443, df=12.62, p-adj.>0.9999 120 vs. ABX q=3.317, df=13.99, p-adj.=0.0203 vs. A - FMT q=2.718, df=11.72, p-adj.=0.0699 vs. V - FMT q=3.323, df=12.70, p-adj.=0.0223 vs. N - FMT q=0.1942, df=12.97, p-adj.=0.9997 vs M - FMT q=0.3277, df=12.61, p-adj.=0.9967
3D	One-way ANOVA Kruskal-Wallis, Dunn's multiple comparisons test to VEH - FMT	KW statistic: 19.01, P=0.0019 vs. ABX Z=2.857, p-adj=0.0214 vs. A Z=2.929, p-adj.=0.0170 vs. V Z=2.982, p-adj.=0.0143 vs. N Z=1.179, p-adj.>0.9999 vs. M Z=0.3393, p-adj.>0.9999
3E	PERMANOVA, 999 permutations	pseudo-F=24.6428, P=0.001

3F	Pairwise PERMANOVA, 999 permutations	VEH vs. ABX pseudo-F=16.058 q=0.030 VEH vs. A pseudo-F=25.467 q=0.008 VEH vs. V pseudo-F=16.462 q=0.006 VEH vs. N pseudo-F=5.715 q=0.005 VEH vs. M pseudo-F=3.388 q=0.012 ABX vs. A pseudo-F=7.070 q=0.085 ABX vs. V pseudo-F=16.857 q=0.026 ABX vs. N pseudo-F=126.981 q=0.025 ABX vs. M pseudo-F=57.546 q=0.027 A vs. V pseudo-F=18.418 q=0.008 A vs. N pseudo-F=66.127 q=0.008 A vs. M pseudo-F=51.221 q=0.008 V vs. N pseudo-F=51.202 q=0.005 V vs. M pseudo-F=36.243 q=0.006 N vs. M pseudo-F=18.202 q=0.005
3H	One-way ANOVA, Dunnett's multiple comparisons test to V	S24-7 Family F[3,28]=[36.67] P<0.0001 V vs. VEH q=9.680, p-adj.<0.0001 V vs. N q=6.963, p-adj.<0.0001 V vs. M q=8.166, p-adj.<0.0001 *Lactobacillus* sp. F[3,28]=34.93 P<0.0001 V vs. VEH q=3.320, p-adj.=0.0069 V vs. N q=4.508, p-adj.=0.0003 V vs. M q=10.05, p-adj.<0.0001 *A. muciniphila* F[3,28]=13.76 P<0.0001 V vs. VEH q=3.420, p-adj.=0.0054 V vs. N q=5.580, p-adj.<0.0001 V vs. M q=5.532, p-adj.<0.0001
4B	One-way ANOVA, Tukey's multiple comparisons test	F(3,76)=[16.39] P<0.0001 VEH vs. V+Sal q=6.543, df=76, p-adj.<0.0001 VEH vs. V+Auto q=8.827, df=76, p-adj.<0.0001 VEH vs. V+SPF q=2.026, df=76, p-adj.=0.4833 V+Sal vs. V+Auto q=2.283, df=76, p-adj.=0.3767 V+Sal vs. V+SPF q=4.517, df=76, p-adj.=0.0108 V+Auto vs. V+SPF q=6.801, df=76, p-adj.<0.0001

4C	One-way ANOVA, Tukey's multiple comparisons test	S24-7 Family F(3, 28)=[42.12] P<0.0001 VEH vs. V+Sal q=10.65, p-adj.<0.0001 VEH vs. V+Auto q=10.65, p-adj.<0.0001 VEH vs. V+SPF q=1.124, p-adj.=0.8560 V+Sal vs. V+Auto q=0.001062, p-adj.>0.9999 V+Sal vs. V+SPF q=11.78, p-adj.<0.0001 V+Auto vs. V+SPF q=11.78, p-adj.<0.0001 *Lactobacillus* sp. F[3,28]=10.22 P=0.0001 VEH vs. V+Sal q=4.041, p-adj.=0.0377 VEH vs. V+Auto q=4.041, p-adj.=0.0377 VEH vs. V+SPF q=2.442, p-adj.=0.3294 V+Sal vs. V+Auto q=0.000, p-adj.>0.9999 V+Sal vs. V+SPF q=6.482, p-adj.=0.0005 V+Auto vs. V+SPF q=6.482, p-adj.=0.0005 *A. muciniphila* F[3,28]=9.939 P=0.0001 VEH vs. V+Sal q=5.998, p-adj.=0.0012 VEH vs. V+Auto q=6.945, p-adj.=0.0002 VEH vs. V+SPF q=2.924, p-adj.=0.1883 V+Sal vs. V+Auto q=0.9648, p-adj.=0.9077 V+Sal vs. V+SPF q=3.074, p-adj.=0.1555 V+Auto vs. V+SPF q=4.020, p-adj.=0.0389
4E	One-way ANOVA, Tukey's multiple comparisons test	F(3,56)=[8.124] P=0.0001 VEH vs. V+SPF q=1.208, df=56, p-adj.=0.8283 VEH vs. V+A. muc q=5.340, df=56, p-adj.=0.0021 VEH vs. V+4-mix q=1.039, df=56, p-adj.=0.8827 V+SPF vs. V+A. muc q=6.548, df=56, p-adj.=0.0001 V+SPF vs. V+4-mix q=2.247, df=56, p-adj.=0.3932 V+A. muc vs. V+4-mix q=4.301, df=56, p-adj.=0.0183
4F	Two-tailed Student's t-tests	S24-7 Family t=9.975, df=14, P<0.0001 *Lactobacillus* sp. t=3.798, df=14, P=0.0020 *A. muciniphila* t=1.790, df=14, P=0.0950
S1A	Two-tailed Student's t-tests	Brain Heart Infusion Aerobic t=5.647, df=8.0, P=0.000483 Anaerobic t=5.842, df=8.0, P=0.000386 Brucella + Sheep's Blood Aerobic t=4.622, df=8.0, P=0.001706 Anaerobic t=4.051, df=8.0, P=0.003679
S1B	Two-tailed Student's t-test	t=7.954, df=14, P<0.0001
S1C	Two-way RM ANOVA	Time x Treatment (F(1,22) = [0.4014], P=0.5329) Time (F(1,22) = [306.2], P<0.0001) Treatment (F(1, 22) = [2.060], P=0.1653) Subject (F(22, 22) = [15.06], P<0.0001)

S1D	Two-tailed Student's t-test	t=0.3815, df=18, P=0.7073
S1E, S1F	Descriptive Statistics and Kolmogorov-Smirnov tests	(Pellets Eaten / FED Retrieval Events) VEH1:(33/33) VEH2:(46/45) VEH3:(38/39) VEH4:(42/42) VEH5:(55/54) ABX1:(55/55) ABX2:(62/62) ABX3:(53/53) ABX4:(52/51) ABX5:(58/59) mean=1.0016, std. dev. = 0.0154 KS-tests VEH1: KS Statistic=0.0303, P=1 VEH2: KS Statistic=0.0628, P=0.9998 VEH3: KS Statistic=0.0540, P=1 VEH4: KS Statistic=0.0476, P=1 VEH5: KS Statistic=0.0525, P=1 ABX1: KS Statistic=0.0182, P=1 ABX2: KS Statistic=0.0322, P=1 ABX3: KS Statistic=0.0755, P=0.9985 ABX4: KS Statistic=0.0701, P=0.9975 ABX5: KS Statistic=0.0351, P=1 mean, KS Statistic = 0.0478, std. dev., KS Statistic = 0.0187 mean, P = 0.9996, std. dev., P = 0.0009
S1G	Two-tailed Student's t-test	t=0.3705, df=31, P=0.7135
S1H	Two-tailed Student's t-test	t=1.979, df=31, P=0.0568
S1I	Two-tailed Student's t-test	t=3.273, df=8, P=0.0113
S1J	Two-way RM ANOVA, Šidák's multiple comparisons test	Time x Treatment (F(4,64) = [7.645], P<0.0001) Time (F(1.892,30.28) = [262.9], P<0.0001) Treatment (F(1,16) = [19.32], P=0.0005) Subject (F(16, 64) = [5.854], P<0.0001) 0 30 t=7.049, df=14.50, p-adj.<0.0001 60 t=4.694, df=14.90, p-adj.=0.0015 90 t=3.085, df=15.56, p-adj.=0.0359 120 t=2.776, df=15.95, p-adj.=0.0658
S1K	Two-way RM ANOVA	Time x Treatment (F(4,56) = [1.562], P=0.1972) Time (F(2.177,30.48) = [381.3], P<0.0001) Treatment (F(1,14) = [0.9646], P=0.3426) Subject (F(14, 56) = [5.649], P<0.0001)
S1L	Two-way RM ANOVA, Šidák's multiple comparisons test	Time x Treatment (F(4,72) = [6.016], P=0.0003) Time (F(2.668,48.02) = [567.2], P<0.0001) Treatment (F(1,18) = [4.728], P=0.0433) Subject (F(18,72) = [5.371], P<0.0001) 0 30 t=0.9488, df=16.60, p-adj.=0.8895 60 t=0.1412, df=17.87, p-adj.>0.9999 90 t=3.570, df=17.90, p-adj.=0.0110 120 t=2.926, df=15.91, p-adj.=0.0487

S1M	Mann-Whitney	Mann-Whitney U=15, P=0.0068
S1N	Two-tailed Student's t-test	t=1.793, df=18, P=0.0898
S1O	Two-tailed Student's t-test	t=0.7280, df=18, P=0.4760
S1P	Two-tailed Student's t-test	t=0.1089, df=18, P=0.9145
S1Q	Two-way RM ANOVA	Time x Treatment (F(4,52) = [1.774], P=0.1481) Time (F(2.168,28.19) = [388.4], P<0.0001) Treatment (F(1,13) = [0.1332], P=0.7210) Subject (F(13,52) = [3.483], P=0.0006)
S1R	Two-way RM ANOVA, Šidák's multiple comparisons test	Time x Treatment (F(4,44) = [13.81], P<0.0001) Time (F(1.923,21.16) = [191.2], P<0.0001) Treatment (F(1, 11) = [29.28], P=0.0002) Subject (F(11, 44) = [6.588], P<0.0001) 0 30 t=4.747, df=8.511, p-adj.=0.0061 60 t=6.000, df=7.046, p-adj.=0.0026 90 t=4.634, df=10.97, p-adj.=0.0036 120 t=4.941, df=10.91, p-adj.=0.0023
S1S	Two-way RM ANOVA, Šidák's multiple comparisons test	Stimulus x Treatment (F(3,66) = [32.18], P<0.0001) Stimulus (F(1.263,27.79) = [164.0], P<0.0001) Treatment (F(1,22) = [19.62], P=0.0002) Subject (F(22,66) = [1.846], P=0.0295) Chow t=1.113, df=13.84, p-adj.=0.7380 Cellulose t=0.9121, df=17.58, p-adj.=0.8465 Novel Pellet (50% Cellulose) t=1.239, df=16.73, p-adj.=0.6531 Novel Pellet (50% Sucrose) t=5.719, df=16.78, p-adj.=0.0001
S1T	Two-way RM ANOVA, Šidák's multiple comparisons test	Time x Treatment (F(4,48) = [6.063], P=0.0005) Time (F(4,48) = [141.1], P<0.0001) Treatment (F(1,12) = [15.01], P=0.0022) Subject (F(12, 48) = [5.815], P<0.0001) 0 30 t=2.919, df=60.00, p-adj.=0.0245 60 t=3.518, df=60.00, p-adj.=0.0042 90 t=4.142, df=60.00, p-adj.=0.0005 120 t=4.333, df=60.00, p-adj.=0.0003
S2A	Two-way RM ANOVA, Šidák's multiple comparisons test	Time x Treatment (F(4,72) = [1.967], P=0.1088) Time (F(2.371,42.67) = [207.1], P<0.0001) Treatment (F(1,18) = [5.810], P=0.0268) Subject (F(18, 72) = [5.190], P<0.0001) 0 30 t=2.283, df=15.65, p-adj.=0.1709 60 t=2.474, df=17.83, p-adj.=0.1129 90 t=2.587, df=17.57, p-adj.=0.0908 120 t=1.330, df=17.51, p-adj.=0.6735

S2B	Two-way RM ANOVA, Šidák's multiple comparisons test	Time x Treatment (F(4,72) = [9.303], P<0.0001) Time (F(1.468,26.42) = [221.2], P<0.0001) Treatment (F(1,18) = [14.62], P=0.0012) Subject (F(18,72) = [9.435], P<0.0001) 0 30 t=4.386, df=16.30, p-adj.=0.0022 60 t=3.964, df=12.89, p-adj.=0.0082 90 t=3.330, df=12.51, p-adj.=0.0281 120 t=3.392, df=12.94, p-adj.=0.0240
S2C	Two-way RM ANOVA, Šidák's multiple comparisons test	Time x Treatment (F(4,72) = [7.930], P<0.0001) Time (F(1.556,28.00) = [213.1], P<0.0001) Treatment (F(1,18) = [10.64], P=0.0043) Subject (F(18,72) = [10.33], P<0.0001) 0 30 t=2.629, df=17.49, p-adj.=0.0836 60 t=14.001, df=17.73, p-adj.=0.0043 90 t=2.944, df=17.99, p-adj.=0.0427 120 t=3.074, df=17.96, p-adj.=0.0324
S2D	Two-way RM ANOVA, Šidák's multiple comparisons test	Time x Treatment (F(3,54) = [8.676], P<0.0001) Time (F(2.449,44.09) = [7.541], P=0.0008) Treatment (F(1,18) = [11.51], P=0.0032) Subject (F(18,54) = [2.027], P=0.0238) 0-30 t=4.386, df=16.30, p-adj.=0.0018 30-60 t=1.095, df=17.53, p-adj.=0.7438 60-90 t=0.8045, df=16.70, p-adj.=0.8962 90-120 t=1.166, df=16.76, p-adj.=0.7000
S2F	Two-tailed Student's t-test	Number of Bouts t=1.642, df=18, P=0.1179 Average Bout Length t=0.7122, df=18, P=0.4855

S2G	Mixed-effects analysis, Tukey's multiple comparisons test (within timepoints)	Aerobic BHIS Fixed Effects Time P=0.0014 Treatment P=0.0906 Time X Treatment P=0.245 Aerobic Brucella Fixed Effects Time P=0.0685 Treatment P=0.0775 Time X Treatment P=0.1044 Anaerobic BHIS Fixed Effects Time P=0.0010 Treatment P=0.0229 Time X Treatment P=0.3236 0 VEH vs. ABX+SHAM q=1.042, df=13.12, p-adj.=0.7464 VEH vs. ABX+FMT q=0.03121, df=13.90, p-adj.=0.9997 ABX+SHAM vs. ABX+FMT q=1.133, df=13.57, p-adj.=0.7087 4 VEH vs. ABX+SHAM q=7.661, df=7.000, p-adj.=0.0025 VEH vs. ABX+FMT q=7.661, df=7.000, p-adj.=0.0025 6 VEH vs. ABX+SHAM q=2.961, df=7.242, p-adj.=0.1586 VEH vs. ABX+FMT q=0.01245, df=9.962, p-adj.>0.999 ABX+SHAM vs. ABX+FMT q=6.075, df=8.056, p-adj.=0.0065 Anaerobic Brucella Fixed Effects Time P=0.0003 Treatment P=0.0150 Time X Treatment P=0.0121 0 VEH vs. ABX+SHAM q=0.1198, df=12.92, p-adj.=0.9961 VEH vs. ABX+FMT q=0.2194, df=12.22, p-adj.=0.9869 ABX+SHAM vs. ABX+FMT q=0.1148, df=13.85, p-adj.=0.9964 4 VEH vs. ABX+SHAM q=3.303 df=7.000, p-adj.=0.1155 VEH vs. ABX+FMT q=3.303, df=7.000, p-adj.=0.1155 6 VEH vs. ABX+SHAM q=6.263, df=7.709, p-adj.=0.0060 VEH vs. ABX+FMT q=0.5190, df=10.36, p-adj.=0.9289 ABX+SHAM vs. ABX+FMT q=10.54, df=9.450, p-adj.<0.0001

S2H	One-way ANOVA, Tukey's multiple comparisons test	F(2,18)=[17.16] P<0.0001 VEH vs. ABX+SHAM q=8.217, df=18, p-adj.<0.0001 VEH vs. ABX+FMT q=4.557, df=18, p-adj.=0.0125 ABX+SHAM vs. ABX+FMT q=4.220, df=18, p-adj.=0.0207
S2I	Mixed-effects analysis, Tukey's multiple comparisons test (within timepoints)	Fixed Effects Time P=<0.0001 Treatment P<0.0001 Time X Treatment P<0.0001 4 VEH vs. ABX+SHAM q=1.988, df=39.00, p-adj.=0.3479 VEH vs. ABX+FMT q=0.6486, df=39.00, p-adj.=0.8909 ABX+SHAM vs. ABX+FMT q=2.637, df=39.00, p-adj.=0.1626 6 VEH vs. ABX+SHAM q=18.65, df=39.00, p-adj.<0.0001 VEH vs. ABX+FMT q=7.345, df=39.00, p-adj.<0.0001 ABX+SHAM vs. ABX+FMT q=12.20, df=39.00, p-adj.<0.0001
S2K	One-way ANOVA Kruskal-Wallis, Mann-Whitney U tests, FDR correction	KW statistic: 16.753247, P=0.00023 VEH vs.ABX+FMT U=2.0, p-adj.=0.00431 VEH vs. ABX+SHAM U=40.0, p-adj.=0.00431 ABX+SHAM vs. ABX+FMT U=40.0, p-adj.=0.00431
S2M	One-way ANOVA, Tukey's multiple comparisons test	Average Bout Length (sec) F(2,26)=[3.635] P=0.0405 VEH vs. ABX+SHAM q=2.971, df=26, p-adj.=0.1093 VEH vs. ABX+FMT q=0.6430, df=26, p-adj.=0.8928 ABX+SHAM vs. ABX+FMT q=3.597, df=26, p-adj.=0.0441 Number of Bouts: F(2,26)=[7.697] P=0.0024 VEH vs. ABX+SHAM q=5.537, df=26, p-adj.=0.0016 VEH vs. ABX+FMT q=3.012, df=26, p-adj.=0.1034 ABX+SHAM vs. ABX+FMT q=2.606, df=26, p-adj.=0.1759 Pellets / Bout: F(2,26)=[1.600] P=0.2212

S2N	Two-way RM ANOVA, Tukey's multiple comparisons test (within timepoints)	Time x Treatment (F(8,84) = [12.58], P<0.0001) Time (F(1.785,37.49) = [369.8], P<0.0001) Treatment (F(2,21) = [14.72], P=0.0001) Subject (F(21,84) =[10.54], P<0.0001) 0 30 VEH vs. ABX q=4.819, df=8.839, p-adj.=0.0197 VEH vs. ABX+SCFA q=5.690, df=9.412, p-adj.=0.0070 ABX vs. ABX+SCFA q=0.1700, df=13.73, p-adj.=0.9921 60 VEH vs. ABX q=6.109, df=8.229, p-adj.=0.0060 VEH vs. ABX+SCFA q=8.451, df=8.989, p-adj.=0.0005 ABX vs. ABX+SCFA q=0.5431, df=13.22, p-adj.=0.9224 90 VEH vs. ABX q=5.830, df=11.02, p-adj.=0.0044 VEH vs. ABX+SCFA q=8.098, df=13.58, p-adj.=0.0002 ABX vs. ABX+SCFA q=0.3373, df=12.25, p-adj.=0.9692 120 VEH vs. ABX q=6.810, df=11.49, p-adj.=0.0013 VEH vs. ABX+SCFA q=9.946, df=13.73, p-adj.<0.0001 ABX vs. ABX+SCFA q=0.9810, df=12.48, p-adj.=0.7714
S2O	Two-way RM ANOVA	Time x Treatment (F(6,132) = [0.3921], P=0.8831) Time (F(4.148,91.26) = [22.50], P<0.0001) Treatment (F(1,22) = [3.310], P=0.0825) Subject (F(22,132) = [6.554], P<0.0001)
S2P	Two-way RM ANOVA, Šidák's multiple comparisons test	Port x Treatment (F(1,20) = [16.24], P=0.0007) Time (F(1,20) = [36.69], P<0.0001) Treatment (F(1,20) = [16.51], P=0.0006) Subject (F(20,20) = [1.006], P=0.4944) Active t=5.723, df=40.00, p-adj.<0.0001 Inactive t=0.03321, df=40.00, p-adj.=0.9993
S3D	Two-way ANOVA	Dorsal Striatum Treatment x Stimulus (F(1,22)=[1.114], P=0.3026) Stimulus (F(1,22)=[0.1223], P=0.7298) Treatment (F(1,22)=[1.224], P=0.2804) Lateral Hypothalamus Treatment x Stimulus (F(1,21)=[0.6934], P=0.4144) Stimulus (F(1,21)=[1.129], P=0.3000) Treatment (F(1,21)=[6.627], P=0.0177) Basolateral Amygdala Treatment x Stimulus (F(1,21)=[0.06900], P=0.7954) Stimulus (F(1,21)=[7.608], P=0.0118) Treatment (F(1,21)=[0.7070], P=0.4099)
S3F	One-way ANOVA, Tukey's multiple comparisons test	F(2,6)=[123.5], P<0.0001 VEH vs. ABX q=0.03847, df=6, p-adj.=0.9996 VEH vs. Fasted q=19.27, df=6, p-adj.<0.0001 ABX vs. Fasted q=19.23, df=6, p-adj.<0.0001

S3G	Two-tailed Student's t-tests, Holm-Šidák multiple comparisons correction	AgRP: t=0.2823, df=10.51, p-adj.=0.783220 NPY: t=1.161, df=12.92, p-adj.=0.547806 POMC: t=1.302, df=7.286, p-adj.=0.547806
S4A	One-way ANOVA, Dunnett's multiple comparisons test to VEH	F(5,42)=[9.757] P<0.0001 vs. ABX q=3.087, df=42, p-adj.=0.0154 vs. A q=2.843, df=42, p-adj.=0.0288 vs. V q=0.7453, df=42, p-adj.=0.9135 vs. N q=1.142, df=42, p-adj.=0.6777 vs. M q=2.534, df=42, p-adj.=0.0601
S4B	One-way ANOVA, Dunnett's multiple comparisons test to VEH - FMT	F(5,42)=[8.751] P<0.0001 vs. ABX q=5.724, df=42, p-adj.<0.0001 vs. A – FMT q=2.760, df=42, p-adj.=0.0352 vs. V – FMT q=1.797, df=42, p-adj.=0.2687 vs. N – FMT q=0.7223, df=42, p-adj.=0.9229 vs. M – FMT q=0.6682, df=42, p-adj.=0.9424
S4C	PERMANOVA, 999 permutations	pseudo-F=10.171, P=0.001
S4D	Pairwise PERMANOVA, 999 permuations	VEH vs. ABX pseudo-F=7.224 q=0.027 VEH vs. A pseudo-F=9.382 q=0.006 VEH vs. V pseudo-F=24.403 q=0.002 VEH vs. N pseudo-F=10.144 q=0.002 VEH vs. M pseudo-F=3.182 q=0.002 ABX vs. A pseudo-F=2.067 q=0.064 ABX vs. V pseudo-F=7.496 q=0.026 ABX vs. N pseudo-F=7.348 q=0.027 ABX vs. M pseudo-F=6.768 q=0.027 A vs. V pseudo-F=4.483 q=0.006 A vs. N pseudo-F=9.273 q=0.006 A vs. M pseudo-F=7.899 q=0.002 V vs. N pseudo-F=22.889 q=0.002 V vs. M pseudo-F=21.717 q=0.002 N vs. M pseudo-F=8.119 q=0.002
S4F	One-way ANOVA Kruskal-Wallis, Mann-Whitney U tests, FDR correction	Week 3 (Within-Subject Distance to Week 0) KW statistic: 20.318182, P=0.000146 VEH vs. V+Sal U=0, p-adj.=0.001878 VEH vs. V+Auto U=0, p-adj.=0.001878 VEH vs. V+SPF U=0, p-adj.=0.001878 V+Sal vs. V+Auto U=14, p-adj.=0.079298 V+Sal vs. V+SPF U=26, p-adj.=0.563524 V+Auto vs. V+SPF U=14, p-adj.=0.079298 Week 5 (Within-Subject Distance to Week 0) KW statistic: 23.423295, P=0.000033 VEH vs. V+Sal U=0, p-adj.=0.001409 VEH vs. V+Auto U=0, p-adj.=0.001409 VEH vs. V+SPF U=30, p-adj.=0.874826 V+Sal vs. V+Auto U=25, p-adj.=0.593804 V+Sal vs. V+SPF U=64, p-adj.=0.001409 V+Auto vs. V+SPF U=0, p-adj.=0.001409

S4G	One-way ANOVA Kruskal-Wallis, Mann-Whitney U tests, FDR correction	Week 3 (Within-Subject Distance to Week 0) KW statistic: 17.628, P=0.000525 VEH vs. V+Sal U=0, p-adj.=0.001878 VEH vs. V+Auto U=0, p-adj.=0.001878 VEH vs. V+SPF U=0, p-adj.=0.001878 V+Sal vs. V+Auto U=35, p-adj.=0.874826 V+Sal vs. V+SPF U=34, p-adj.=0.874826 V+Auto vs. V+SPF U=38, p-adj.=0.845286 Week 5 (Within-Subject Distance to Week 0) KW statistic: 25.571023, P=0.000012 VEH vs. V+Sal U=0, p-adj.=0.001409 VEH vs. V+Auto U=0, p-adj.=0.001409 VEH vs. V+SPF U=4, p-adj.=0.004651 V+Sal vs. V+Auto U=37, p-adj.=0.636502 V+Sal vs. V+SPF U=64, p-adj.=0.001409 V+Auto vs. V+SPF U=0, p-adj.=0.001409
S4H	PERMANOVA, 999 permutations Pairwise PERMANOVA, 999 permutations	pseudo-F=34.711, P=0.001 VEH vs. V+SPF pseudo-F=1.861, q=0.158 VEH vs. V+A. muc pseudo-F=49.715, q=0.002 VEH vs. V+4-mix pseudo-F=38.692, q=0.002 V+SPF vs. V+A. muc pseudo-F=64.622, q=0.002 V+SPF vs. V+4-mix pseudo-F=50.165, q=0.002 V+A. muc vs. V+4-mix pseudo-F=11.950, q=0.002
S4I	PERMANOVA, 999 permutations Pairwise PERMANOVA, 999 permutations	pseudo-F=27.967, P=0.001 VEH vs. V+SPF pseudo-F=7.297, q=0.001 VEH vs. V+A. muc pseudo-F=43.678, q=0.001 VEH vs. V+4-mix pseudo-F=40.234, q=0.001 V+SPF vs. V+A. muc pseudo-F=40.058, q=0.001 V+SPF vs. V+4-mix pseudo-F=35.915, q=0.001 V+A. muc vs. V+4-mix pseudo-F=2.758, q=0.003

Table S2. Significantly differentially abundant ASVs from a one-versus-all comparison of vancomycin-treated mice to vehicle (VEH), neomycin (N), and metronidazole (M)- treated mice. Related to Figure 3E-3H.

feature	comparison	coef	stderr	pval	qval	taxonomic_classification	confidence
9d141f572d712cdd1d3d3e494bcd88a1	M	0.1676000992	0.01564525	3.18E-11	2.19E-08	k__Bacteria; p__Firmicutes; c__Bacilli; o__Lactobacillales; f__Lactobacillaceae; g__Lactobacillus; s__	0.999996935
1959ff04daf040b4984c26c51c00759e	VEH	0.0088037453	0.00091504	2.24E-10	7.74E-08	k__Bacteria; p__Firmicutes; c__Clostridia; o__Clostridiales; f__Clostridiaceae	0.999999996
26c2b38189d9a65f8c9944f409440b1a	M	-0.0004599978	5.67E-05	7.77E-09	1.07E-06	k__Bacteria; p__Firmicutes; c__Clostridia; o__Clostridiales; f__; g__; s__	0.989006425
26c2b38189d9a65f8c9944f409440b1a	N	-0.0004599978	5.67E-05	7.77E-09	1.07E-06	k__Bacteria; p__Firmicutes; c__Clostridia; o__Clostridiales; f__; g__; s__	0.989006425
26c2b38189d9a65f8c9944f409440b1a	VEH	-0.0004599978	5.67E-05	7.77E-09	1.07E-06	k__Bacteria; p__Firmicutes; c__Clostridia; o__Clostridiales; f__; g__; s__	0.989006425
fd4d5be53f7b770860c049540825b711	M	0.0004107478	5.35E-05	1.67E-08	1.92E-06	k__Bacteria; p__Bacteroidetes; c__Bacteroidia; o__Bacteroidales; f__Prevotellaceae; g__Prevotella; s__copri	0.999999289
bc8d534ccbe1f9478971dbcd8eefeb01	N	0.0002806724	3.89E-05	6.28E-08	5.83E-06	k__Bacteria; p__Bacteroidetes; c__Bacteroidia; o__Bacteroidales; f__Bacteroidaceae; g__Bacteroides; s__	0.999938616
41cae4bb4d6e804a5fdb6360b088e578	N	0.0005102854	6.99E-05	6.76E-08	5.83E-06	k__Bacteria; p__Firmicutes; c__Clostridia; o__Clostridiales; f__Lachnospiraceae; g__[Ruminococcus]; s__gnavus	0.999909657
c8f028d09d0f955b80de2167a958c0f9	VEH	0.2431192619	0.03368156	9.19E-08	7.05E-06	k__Bacteria; p__Bacteroidetes; c__Bacteroidia; o__Bacteroidales; f__S24-7; g__; s__	0.99999974
c8f028d09d0f955b80de2167a958c0f9	M	0.2275705132	0.03368156	2.96E-07	2.04E-05	k__Bacteria; p__Bacteroidetes; c__Bacteroidia; o__Bacteroidales; f__S24-7; g__; s__	0.999999974
bbad263c52eefa43d5b161f614dd09a8	VEH	0.0008266607	0.00013038	7.37E-07	4.62E-05	k__Bacteria; p__Firmicutes; c__Clostridia; o__Clostridiales; f__Clostridiaceae	0.999999994
07b3b3fd19823989e27dfa162390aea3	N	-0.3117622501	0.05055128	1.36E-06	7.84E-05	k__Bacteria; p__Verrucomicrobia; c__Verrucomicrobiae; o__Verrucomicrobiales; f__Verrucomicrobiaceae; g__Akkermansia; s__muciniphila	1
07b3b3fd19823989e27dfa162390aea3	M	-0.3093644143	0.05055128	1.54E-06	8.19E-05	k__Bacteria; p__Verrucomicrobia; c__Verrucomicrobiae; o__Verrucomicrobiales; f__Verrucomicrobiaceae; g__Akkermansia; s__muciniphila	1
ffff7e4c4459fb30cabc41dac23f233f	M	0.0021136637	0.00036461	3.17E-06	0.00016011	k__Bacteria; p__Firmicutes; c__Clostridia; o__Clostridiales; f__Ruminococcaceae; g__Oscillospira; s__	0.999588863
f5d4bb82a1ae3e8911685814c15ebde7	N	0.0029456744	0.00052181	5.39E-06	0.00024783 5	k__Bacteria; p__Firmicutes; c__Clostridia; o__Clostridiales; f__Lachnospiraceae; g__; s__	0.957803015
b7d839aa99a5ed92f7e573fe9b46f009	N	0.2068255273	0.03831673 8	1.05E-05	0.00045190 7	k__Bacteria; p__Bacteroidetes; c__Bacteroidia; o__Bacteroidales; f__Bacteroidaceae; g__Bacteroides	1
92d3f9294475c5db2c3938c62b98f56a	VEH	0.0087088538	0.00165340 7	1.34E-05	0.00054262 5	k__Bacteria; p__Firmicutes; c__Bacilli; o__Turicibacterales; f__Turicibacteraceae; g__Turicibacter; s__	0.999998257
3d8c0b2b90721080cb0e4aa33c0cbeaa	M	0.0004533407	8.65E-05	1.59E-05	0.00054836 1	k__Bacteria; p__Firmicutes; c__Clostridia; o__Clostridiales; f__; g__; s__	0.792621458
060cc5109df11770fc002cb0e5f6b45d	N	0.0015902303	0.00030496 1	1.68E-05	0.00054836 1	k__Bacteria; p__Firmicutes; c__Erysipelotrichi; o__Erysipelotrichales; f__Erysipelotrichaceae; g__Clostridium; s__cocleatum	0.977500483
989c30259d382002e27a9758d2360e5a	VEH	0.0034705552	0.00065721 7	1.43E-05	0.00054836 1	k__Bacteria; p__Firmicutes; c__Clostridia; o__Clostridiales; f__; g__; s__	0.996965753

2129ce20d170a8378d271211a3a0b373	N	0.03686884	0.00708105	1.75E-05	0.000548361	k__Bacteria; p__Bacteroidetes; c__Bacteroidia; o__Bacteroidales; f__S24-7; g__; s__	0.999999994
2129ce20d170a8378d271211a3a0b373	VEH	0.03721759	0.00708105	1.53E-05	0.000548361	k__Bacteria; p__Bacteroidetes; c__Bacteroidia; o__Bacteroidales; f__S24-7; g__; s__	0.999999994
abc42b844c4a0405b43af6899f595005	N	0.00094366	0.00018579	2.46E-05	0.000710325	k__Bacteria; p__Firmicutes; c__Clostridia; o__Clostridiales; f__Lachnospiraceae; g__; s__	0.8533011091
60e9eaffc8d9edf8f12a4aaefae6488c	M	0.00556184	0.00110304	2.47E-05	0.000710325	k__Bacteria; p__Firmicutes; c__Clostridia; o__Clostridiales; f__[Mogibacteriaceae]; g__; s__	0.999982687
9d141f572d712cdd1d3d3e494bcd88a1	N	0.07892522	0.01564525	2.70E-05	0.000745496	k__Bacteria; p__Firmicutes; c__Bacilli; o__Lactobacillales; f__Lactobacillaceae; g__Lactobacillus; s__	0.999996935
c8f028d09d0f955b80de2167a958c0f9	N	0.16789918	0.03368156	3.17E-05	0.000841721	k__Bacteria; p__Bacteroidetes; c__Bacteroidia; o__Bacteroidales; f__S24-7; g__; s__	0.99999974
67818b4c16e624fa3f4500bec8b20af1	VEH	0.02710340	0.00589449	8.97E-05	0.002292035	k__Bacteria; p__Actinobacteria; c__Coriobacteriia; o__Coriobacteriales; f__Coriobacteriaceae; g__; s__	0.988763924
574df1ca94b4a202fedd94b639c5552c	M	0.00081953	0.00018140	0.000103574	0.002552356	k__Bacteria; p__Firmicutes; c__Clostridia; o__Clostridiales; f__Lachnospiraceae; g__; s__	0.7771062823
97f75a60cec78a738cd2dc833940293a	M	0.00015088	3.40E-05	0.000127625	0.003036584	k__Bacteria; p__Firmicutes; c__Erysipelotrichi; o__Erysipelotrichales; f__Erysipelotrichaceae; g__Coprobacillus; s__	0.999940299
b436106131a799633256bcb5499c411a	N	-0.09607969	0.02275586	0.000245291	0.005369541	k__Bacteria; p__Firmicutes; c__Bacilli; o__Lactobacillales; f__Lactobacillaceae; g__Lactobacillus	0.99962255
8ea3133b817d442c58c048f706466eea	N	8.19E-05	1.94E-05	0.000249022	0.005369541	k__Bacteria; p__Bacteroidetes; c__Bacteroidia; o__Bacteroidales; f__[Paraprevotellaceae]; g__[Prevotella]; s__	1
bb19e961df38008bc9b54bb9333487d1	N	0.00139866	0.00033316	0.000246532	0.005369541	k__Bacteria; p__Firmicutes; c__Clostridia; o__Clostridiales; f__Lachnospiraceae; g__Coprococcus; s__	0.945601666
a98701cae3ad44e74bbd0e06f3abb303	N	0.00949039	0.00225824	0.000258047	0.005404372	k__Bacteria; p__Firmicutes; c__Clostridia; o__Clostridiales	0.999998695
edcd02445f2f1cb78eeff125d5246cd8	M	0.00601972	0.00143660	0.000267088	0.005420316	k__Bacteria; p__Firmicutes; c__Clostridia; o__Clostridiales; f__Ruminococcaceae; g__; s__	0.94790865
b436106131a799633256bcb5499c411a	VEH	-0.09496911	0.02275586	0.000279343	0.005507054	k__Bacteria; p__Firmicutes; c__Bacilli; o__Lactobacillales; f__Lactobacillaceae; g__Lactobacillus	0.99962255
ac7354881af0410ca3a857664158815e	VEH	-0.01297645	0.00313187	0.000302587	0.005581501	k__Bacteria; p__Firmicutes; c__Clostridia; o__Clostridiales; f__; g__; s__	0.995609779
ac7354881af0410ca3a857664158815e	M	-0.01294166	0.00313187	0.000311658	0.005581501	k__Bacteria; p__Firmicutes; c__Clostridia; o__Clostridiales; f__; g__; s__	0.995609779
5e0bdd5f7437ff72c342000a470bc2f8	N	0.0012539	0.00030376	0.000298014	0.005581501	k__Bacteria; p__Firmicutes; c__Clostridia; o__Clostridiales; f__; g__; s__	0.753773183
a855db6227e007e5e935c16e8acd9ee0	VEH	0.098444394	0.02384994	0.000315476	0.005581501	k__Bacteria; p__Bacteroidetes; c__Bacteroidia; o__Bacteroidales; f__S24-7; g__; s__	0.999999993
605d400401d55e3aec644ee88c78741e	N	0.00074238	0.00018475	0.000410663	0.007083938	k__Bacteria; p__Firmicutes; c__Clostridia; o__Clostridiales; f__; g__; s__	0.908331073
92d3f9294475c5db2c3938c62b98f56a	M	0.00656376	0.00165340	0.000455571	0.007666922	k__Bacteria; p__Firmicutes; c__Bacilli; o__Turicibacterales; f__Turicibacteraceae; g__Turicibacter; s__	0.999998257
ac7354881af0410ca3a857664158815e	N	-0.01243597	0.00313187	0.000479079	0.007870585	k__Bacteria; p__Firmicutes; c__Clostridia; o__Clostridiales; f__; g__; s__	0.995609779

b436106131a799633256bcb5499c411a	M	-0.089446439	0.02275586 4	0.000531473	0.008481859	k__Bacteria; p__Firmicutes; c__Bacilli; o__Lactobacillales; f__Lactobacillaceae; g__Lactobacillus	0.99962255
d7753f037c8da436987cad841ef6ca9d	M	0.000567545	0.000144853	0.000549476	0.008481859	k__Bacteria; p__Firmicutes; c__Clostridia; o__Clostridiales	0.99999977
571c692660207ca06c720e4c4519d1f9	N	0.001303303	0.000335057	0.000565457	0.008481859	k__Bacteria; p__Firmicutes; c__Clostridia; o__Clostridiales	0.99998558
be586859fe1ea2a5c447dee2351580d3	M	0.025992429	0.006645478	0.000559366	0.008481859	k__Bacteria; p__Tenericutes; c__Mollicutes; o__RF39; f__; g__; s__	0.99999979
f8c24848ab290d4a5a56361ed29bbb85	VEH	0.005608786	0.001454883	0.000618804	0.009084562	k__Bacteria; p__Firmicutes; c__Clostridia; o__Clostridiales; f__; g__; s__	0.998831407
26a55b2799d49c0ffce3b27ccc2dc970	M	9.70E-05	2.52E-05	0.000673815	0.009686086	k__Bacteria; p__Firmicutes; c__Clostridia; o__Clostridiales; f__Dehalobacteriaceae; g__Dehalobacterium; s__	0.99997329
f9f7f7a25f22662142a2ee53aff04a28	VEH	0.000248178	6.48E-05	0.000698262	0.009832674	k__Bacteria; p__Tenericutes; c__Mollicutes; o__RF39; f__; g__; s__	1
07b3b3fd19823989e27dfa162390aea3	VEH	-0.191447672	0.05055128	0.000774 98	0.010629139	k__Bacteria; p__Verrucomicrobia; c__Verrucomicrobiae; o__Verrucomicrobiales; f__Verrucomicrobiaceae; g__Akkermansia; s__muciniphila	1
af6d79235faf126f819839464 39da2ed	N	0.000294702	7.79E-05	0.000785632	0.010629139	k__Bacteria; p__Firmicutes; c__Clostridia; o__Clostridiales; f__Ruminococcaceae; g__Oscillospira; s__	0.958986447
e21e4f5d7b199d7a9c8b36856b4d76b1	VEH	0.000410725	0.000109661	0.000828009	0.010815054	k__Bacteria; p__Tenericutes; c__Mollicutes; o__RF39; f__; g__; s__	1
d746cd769789b8b79c9ffd37ca5947e2	VEH	0.000797257	0.000212	0.000830722	0.010815054	k__Bacteria; p__Firmicutes; c__Clostridia; o__Clostridiales; f__Ruminococcaceae; g__; s__	0.99732839
45aa4d2ff6bff48528a46a10a9fc3157	N	0.004754483	0.001270941	0.000874706	0.011176796	k__Bacteria; p__Firmicutes; c__Clostridia; o__Clostridiales; f__; g__; s__	0.975882135
9d141f572d712cdd1d3d3e494bcd88a1	VEH	0.058406936	0.015645252	0.000892499	0.011196809	k__Bacteria; p__Firmicutes; c__Bacilli; o__Lactobacillales; f__Lactobacillaceae; g__Lactobacillus; s__	0.999996935
fff5d9fdfc56850decb391acd351670b	M	9.46E-05	2.56E-05	0.000947185	0.011465927	k__Bacteria; p__Firmicutes; c__Clostridia; o__Clostridiales; f__Lachnospiraceae; g__Dorea; s__	0.849588411
9e1960b8bb909981d74154e2967fdbff	N	0.019636056	0.005285643	0.000935976	0.011465927	k__Bacteria; p__Firmicutes; c__Clostridia; o__Clostridiales; f__Ruminococcaceae; g__Ruminococcus; s__	0.991842242
4807c543021fb97583c4871d279585cc	M	0.000316964	8.67E-05	0.001092588	0.012752296	k__Bacteria; p__Firmicutes; c__Clostridia; o__Clostridiales; f__Ruminococcaceae; g__Oscillospira; s__	0.998759969
351fc33b80d474c64cafac95ad2f7a4d	M	0.002717061	0.000742149	0.001077025	0.012752296	k__Bacteria; p__Firmicutes; c__Clostridia; o__Clostridiales; f__Lachnospiraceae; g__[Ruminococcus]; s__gnavus	0.821492578
4b6303da7e96e5499e102ccc83736a99	M	0.003217951	0.000881666	0.001081895	0.012752296	k__Bacteria; p__Bacteroidetes; c__Bacteroidia; o__Bacteroidales; f__S24-7; g__; s__	0.999999982
a877702090ae1fb8be2be1425e5f6569	VEH	6.06E-05	1.68E-05	0.001153688	0.013049914	k__Bacteria; p__Firmicutes; c__Clostridia; o__Clostridiales; f__Lachnospiraceae; g__[Ruminococcus]; s__gnavus	0.999514257
c7b74aaa97725cd24c96e841569ca06c	M	0.000150033	4.15E-05	0.001212 69	0.013306246	k__Bacteria; p__Firmicutes; c__Clostridia; o__Clostridiales; f__Lachnospiraceae; g__; s__	0.933636595
ab337549a20731139dffeb15baa65a18	N	0.000290452	8.04E-05	0.001214918	0.013306246	k__Bacteria; p__Firmicutes; c__Clostridia; o__Clostridiales; f__Lachnospiraceae; g__[Ruminococcus]; s__gnavus	0.886213443
4b6303da7e96e5499e102ccc83736a99	N	0.003157771	0.000881666	0.001323 76	0.014271789	k__Bacteria; p__Bacteroidetes; c__Bacteroidia; o__Bacteroidales; f__S24-7; g__; s__	0.999999982

01d3992491f1546cbcac742fc5368d18	VEH	8.61E-05	2.42E-05	0.001394358	0.014801648	k__Bacteria; p__Firmicutes; c__Clostridia; o__Clostridiales; f__Lachnospiraceae	0.715312555
cce64cd1a0bd124d73acaeaf350ebb01	VEH	-0.024067952	0.00681706	0.001509982	0.015786179	k__Bacteria; p__Firmicutes; c__Clostridia; o__Clostridiales; f__; g__; s__	0.993927202
cce64cd1a0bd124d73acaeaf350ebb01	M	-0.024000157	0.00681706	0.001549166	0.015954098	k__Bacteria; p__Firmicutes; c__Clostridia; o__Clostridiales; f__; g__; s__	0.993927202
cf63a715ea3e04c6f553579b5721fdbd	N	0.000165838	4.77E-05	0.001677507	0.017021766	k__Bacteria; p__Firmicutes; c__Clostridia; o__Clostridiales; f__Ruminococcaceae; g__Oscillospira; s__	0.999908002
a855db6227e007e5e935c16e8acd9ee0	N	0.082929037	0.02384994 5	0.001732398	0.017323977	k__Bacteria; p__Bacteroidetes; c__Bacteroidia; o__Bacteroidales; f__S24-7; g__; s__	0.999999993
54da53d77e0434198446f9d51cb6a1d0	N	0.000254639	7.35E-05	0.001780481	0.017550046	k__Bacteria; p__Firmicutes; c__Clostridia; o__Clostridiales; f__Lachnospiraceae; g__; s__	0.825343903
519cfad250326c65c6e5e63160b9d74e	N	0.000545877	0.00015779 3	0.001812652	0.017615919	k__Bacteria; p__Firmicutes; c__Clostridia; o__Clostridiales; f__Lachnospiraceae; g__; s__	0.76344238
33d2969004a35481ca0d7f729b2389f4	M	0.000180685	5.26E-05	0.001928446	0.018480941	k__Bacteria; p__Firmicutes; c__Clostridia; o__Clostridiales; f__; g__; s__	0.986680802
c2d9c54fd3c95008ae2421ef5deab402	N	0.000558649	0.00016316 3	0.001985534	0.018767376	k__Bacteria; p__Firmicutes; c__Clostridia; o__Clostridiales; f__Ruminococcaceae; g__Oscillospira; s__	0.999987119
ab337549a20731139dffeb15baa65a18	M	0.000272124	8.04E-05	0.002183881	0.020233324	k__Bacteria; p__Firmicutes; c__Clostridia; o__Clostridiales; f__Lachnospiraceae; g__[Ruminococcus]; s__gnavus	0.886213443
6f0ec8e4e488fd4085da50803578ad53	N	0.002009493	0.00059385 4	0.002199274	0.020233324	k__Bacteria; p__Firmicutes; c__Clostridia; o__Clostridiales; f__Lachnospiraceae; g__Coprococcus; s__	0.852668124
ccd4e8a2ae4b9f5ebe74142821795ffe	VEH	5.68E-05	1.70E-05	0.002438521	0.021339955	k__Bacteria; p__Firmicutes; c__Clostridia; o__Clostridiales; f__; g__; s__	0.998504104
916264c2f350a35362097038b9320cda	N	0.000132509	3.98E-05	0.002474198	0.021339955	k__Bacteria; p__Firmicutes; c__Clostridia; o__Clostridiales; f__Lachnospiraceae	0.981909032
13f57ee6354ddc1a682c4e766e0c3362	N	0.000614014	0.00018378 8	0.002452941	0.021339955	k__Bacteria; p__Firmicutes; c__Clostridia; o__Clostridiales; f__Ruminococcaceae; g__; s__	0.982101112
c90786514fd5c6029ccf4a1f8f5fd179	M	0.000658126	0.00019655	0.002406611	0.021339955	k__Bacteria; p__Firmicutes; c__Clostridia; o__Clostridiales; f__; g__; s__	0.999321062
462668fc68ae632701005af6bb8165db	VEH	0.009361009	0.00279783 3	0.002422492	0.021339955	k__Bacteria; p__Firmicutes; c__Clostridia; o__Clostridiales; f__; g__; s__	0.999404342
cce64cd1a0bd124d73acaeaf350ebb01	N	-0.022659901	0.00681706 3	0.002561176	0.021817429	k__Bacteria; p__Firmicutes; c__Clostridia; o__Clostridiales; f__; g__; s__	0.993927202
83c56ecf0f4731dcc2d596d4ba39899d	VEH	9.21E-05	2.81E-05	0.002846936	0.023955921	k__Bacteria; p__Firmicutes; c__Clostridia; o__Clostridiales; f__Ruminococcaceae; g__; s__	0.893183147
cbcbb326008cb2e6b6a07e1bee028688	M	-0.001321578	0.00040714	0.003030097	0.024597256	k__Bacteria; p__Firmicutes; c__Clostridia; o__Clostridiales; f__; g__; s__	0.986861691
cbcbb326008cb2e6b6a07e1bee028688	VEH	-0.001321578	0.00040714	0.003030097	0.024597256	k__Bacteria; p__Firmicutes; c__Clostridia; o__Clostridiales; f__; g__; s__	0.986861691
08d59d38820658776cc356af59cdbe6f	VEH	0.000127477	3.91E-05	0.002986397	0.024597256	k__Bacteria; p__Firmicutes; c__Clostridia; o__Clostridiales	0.999999901
29e4519433f7d508de27587e5aa088f2	M	-0.000132579	4.12E-05	0.003253482	0.025223626	k__Bacteria; p__Firmicutes; c__Clostridia; o__Clostridiales; f__; g__; s__	0.931736665

29e4519433f7d508de27587e5aa088f2	N	-0.00013	4.12E-05	0.003253482	0.025223626	k__Bacteria; p__Firmicutes; c__Clostridia; o__Clostridiales; f__; g__; s__	0.931736665
29e4519433f7d508de27587e5aa088f2	VEH	-0.00013	4.12E-05	0.003253482	0.025223626	k__Bacteria; p__Firmicutes; c__Clostridia; o__Clostridiales; f__; g__; s__	0.931736665
b0fb6fa031a0fc6667650358bd2367a7	VEH	0.00301	0.0009324	0.003253	0.025223626	k__Bacteria; p__Firmicutes; c__Clostridia; o__Clostridiales; f__; g__; s__	0.999182766
f75f72b1e28326141cf8b3afd87e5f5c	VEH	6.70E-05	2.09E-05	0.003341	0.025325627	k__Bacteria; p__Firmicutes; c__Clostridia; o__Clostridiales; f__Lachnospiraceae; g__; s__	0.728254125
060cc5109df11770fc002cb0e5f6b45d	M	0.00098	0.0009649	0.003363	0.025325627	k__Bacteria; p__Firmicutes; c__Erysipelotrichi; o__Erysipelotrichales; f__Erysipelotrichaceae; g__Clostridium; s__cocleatum	0.977548 3
2129ce20d170a8378d271211a3a0b373	M	0.02276	0.00708105	0.003376	0.025325627	k__Bacteria; p__Bacteroidetes; c__Bacteroidia; o__Bacteroidales; f__S24-7; g__; s__	0.999999994
a1c122273fe2a77850eb1d31af2082f4	N	0.00013	4.12E-05	0.003432067	0.025463721	k__Bacteria; p__Firmicutes; c__Clostridia; o__Clostridiales; f__Lachnospiraceae; g__; s__	0.894603254
a5004df0b829b1dc8dcbc5f93f6f4a27	VEH	0.00029	9.37E-05	0.003735176	0.027417784	k__Bacteria; p__Firmicutes; c__Clostridia; o__Clostridiales; f__Lachnospiraceae; g__; s__	0.953066902
e2b96d3932a4d65463cde2e9967e15b4	M	-0.00217	0.0006915	0.003844	0.027632913	k__Bacteria; p__Firmicutes; c__Clostridia; o__Clostridiales; f__; g__; s__	0.948430036
e2b96d3932a4d65463cde2e9967e15b4	N	-0.00217	0.0006915	0.003844	0.027632913	k__Bacteria; p__Firmicutes; c__Clostridia; o__Clostridiales; f__; g__; s__	0.948430036
cbcbb326008cb2e6b6a07e1bee028688	N	-0.00128	0.00040714	0.003921	0.027898404	k__Bacteria; p__Firmicutes; c__Clostridia; o__Clostridiales; f__; g__; s__	0.986861691
7e477e438d4f13d4453b78de5b79fec5	N	-0.05298	0.0169880164	0.004179429	0.028097724	k__Bacteria; p__Proteobacteria; c__Betaproteobacteria; o__Burkholderiales; f__Alcaligenaceae; g__Sutterella; s__	0.999999991
ba21b8e11876506b6675e342a187eb2b	VEH	-0.03703	0.0118609734	0.004142368	0.028097724	k__Bacteria	0.999999999
ba21b8e11876506b6675e342a187eb2b	M	-0.03698	0.0118609733	0.004180296	0.028097724	k__Bacteria	0.999999999
ba21b8e11876506b6675e342a187eb2b	N	-0.03689	0.0118609733	0.004269043	0.028097724	k__Bacteria	0.999999999
52ddd479ba834b36445d547f90d2271a	M	-0.00252	0.0008083734	0.004286939	0.028097724	k__Bacteria; p__Firmicutes; c__Clostridia; o__Clostridiales; f__; g__; s__	0.996736226
52ddd479ba834b36445d547f90d2271a	N	-0.00252	0.0008083734	0.004286939	0.028097724	k__Bacteria; p__Firmicutes; c__Clostridia; o__Clostridiales; f__; g__; s__	0.996736226
e2b96d3932a4d65463cde2e9967e15b4	VEH	-0.00216	0.0006915	0.004060897	0.028097724	k__Bacteria; p__Firmicutes; c__Clostridia; o__Clostridiales; f__; g__; s__	0.948430036
b23ac4bfbb29c44e68a6193d80ef42ee	M	9.29E-05	2.98E-05	0.004316462	0.028097724	k__Bacteria; p__Firmicutes; c__Clostridia; o__Clostridiales; f__; g__; s__	0.790108862
a855db6227e007e5e935c16e8acd9ee0	M	0.07449	0.0239499345	0.004234667	0.028097724	k__Bacteria; p__Bacteroidetes; c__Bacteroidia; o__Bacteroidales; f__S24-7; g__; s__	0.999999993
52ddd479ba834b36445d547f90d2271a	VEH	-0.00250	0.0008083733	0.004489719	0.028952394	k__Bacteria; p__Firmicutes; c__Clostridia; o__Clostridiales; f__; g__; s__	0.996736226
bc367af0ef71afb4a205dfcca1925e38	M	0.00013	4.28E-05	0.005105702	0.032619761	k__Bacteria; p__Firmicutes; c__Clostridia; o__Clostridiales; f__Lachnospiraceae; g__Anaerostipes; s__	0.999766295

cf815c35c8c3 4a77847777c5 f7cf293c	N	0.00288 0248	0.000 94970 2	0.00 5301 073	0.03 3557 251	k__Bacteria; p__Firmicutes; c__Clostridia; o__Clostridiales; f__; g__; s__	0.8354 42968
2df3a48c79aa b2b3c9ef9e44 1d6cc8e4	M	0.00080 7422	0.000 26732 8	0.00 5465 918	0.03 4286 21	k__Bacteria; p__Tenericutes; c__Mollicutes; o__RF39; f__; g__; s__	0.9999 99999
60a3a677866a a0c98da35def 502a52b8	M	-0.01134 6994	0.003 79856	0.00 5928 974	0.03 5469 686	k__Bacteria; p__Firmicutes; c__Clostridia; o__Clostridiales; f__; g__; s__	0.9946 19347
60a3a677866a a0c98da35def 502a52b8	N	-0.01134 6994	0.003 79856	0.00 5928 974	0.03 5469 686	k__Bacteria; p__Firmicutes; c__Clostridia; o__Clostridiales; f__; g__; s__	0.9946 19347
60a3a677866a a0c98da35def 502a52b8	VEH	-0.01134 001	0.003 79856	0.00 5955 713	0.03 5469 686	k__Bacteria; p__Firmicutes; c__Clostridia; o__Clostridiales; f__; g__; s__	0.9946 19347
639241a700c5 0bc3efa14b61 4b7bd4df	N	0.00022 6748	7.59E -05	0.00 5908 794	0.03 5469 686	k__Bacteria; p__Firmicutes; c__Clostridia; o__Clostridiales; f__Lachnospiraceae	0.8204 30667
fbacd8769f7df 5b8e34bda9c9 8e973b3	N	0.00060 7507	0.000 20353 1	0.00 5963 02	0.03 5469 686	k__Bacteria; p__Firmicutes; c__Clostridia; o__Clostridiales; f__Lachnospiraceae	0.8456 62367
7fe285bd433f 880268c377dc 413a4510	VEH	0.00193 2554	0.000 6461	0.00 5872 291	0.03 5469 686	k__Bacteria; p__Firmicutes; c__Clostridia; o__Clostridiales; f__Ruminococcaceae	0.9998 01378
541e5e5bd24a 22cbed64c4ce 9d34a57d	M	0.00011 3064	3.80E -05	0.00 6023 593	0.03 5523 752	k__Bacteria; p__Actinobacteria; c__Coriobacteriia; o__Coriobacteriales; f__Coriobacteriaceae; g__Adlercreutzia; s__	0.9999 87984
802ab0f99337 ef1105db78a1 5919f1c1	N	5.86E-05	1.98E -05	0.00 6411 889	0.03 7493 252	k__Bacteria; p__Firmicutes; c__Clostridia; o__Clostridiales; f__Lachnospiraceae	0.9690 76108
13f57ee6354d dc1a682c4e76 6e0c3362	M	0.00053 6418	0.000 18378 8	0.00 7006 446	0.04 0287 064	k__Bacteria; p__Firmicutes; c__Clostridia; o__Clostridiales; f__Ruminococcaceae; g__; s__	0.9821 01112
8a591cb75aaa 58505d1443b dcd62b923	M	0.00569 8745	0.001 95722 7	0.00 6981 43	0.04 0287 064	k__Bacteria; p__Firmicutes; c__Clostridia; o__Clostridiales; f__; g__; s__	0.9998 22108
a9219af303a9 1c4985bfa7d0 f7e39d85	VEH	7.93E-05	2.72E -05	0.00 7092 621	0.04 0445 522	k__Bacteria; p__Firmicutes; c__Clostridia; o__Clostridiales; f__Lachnospiraceae; g__; s__	0.9532 79511
208e370f451d 50cce2012cf2 bce1829c	VEH	0.00049 2326	0.000 17131 7	0.00 7657 477	0.04 3308 68	k__Bacteria; p__Firmicutes; c__Clostridia; o__Clostridiales	0.9999 99994
c4962864a628 b9ba6f753f25 ba7fb957	N	0.00380 0148	0.001 34046 3	0.00 8414 049	0.04 7200 763	k__Bacteria; p__Firmicutes; c__Clostridia; o__Clostridiales	0.9999 99986
abf9251ced1f 7978c2c76914 ed911a2d	M	0.00022 2002	7.83E -05	0.00 8532 204	0.04 7477 587	k__Bacteria; p__Firmicutes; c__Clostridia; o__Clostridiales; f__; g__; s__	0.9056 51895
bf817ac9d4d8 35c4760dd02 7da63d990	N	-0.05688 0383	0.020 07883 3	0.00 8619 313	0.04 7578 607	k__Bacteria; p__Tenericutes; c__Mollicutes; o__Anaeroplasmatales; f__Anaeroplasmataceae; g__Anaeroplasma; s__	1
bf817ac9d4d8 35c4760dd02 7da63d990	VEH	-0.05641 5009	0.020 07883 3	0.00 9111 582	0.04 9503 87	k__Bacteria; p__Tenericutes; c__Mollicutes; o__Anaeroplasmatales; f__Anaeroplasmataceae; g__Anaeroplasma; s__	1
1152a0568f40 78bc6bb38fd5 3848bdd6	N	8.50E-05	3.02E -05	0.00 9056 908	0.04 9503 87	k__Bacteria; p__Firmicutes; c__Clostridia; o__Clostridiales; f__Lachnospiraceae; g__Coprococcus; s__	0.9950 80916
4a563f1fd9b4 f12bc12279b0 14819408	VEH	7.59E-05	2.71E -05	0.00 9230 184	0.04 9756 462	k__Bacteria; p__Bacteroidetes; c__Bacteroidia; o__Bacteroidales; f__S24-7; g__; s__	0.9999 99985
18f4f0fa87b2 d71da0960a0a 97789d8a	N	-6.22E-05	2.22E -05	0.00 9419 822	0.04 9997 517	k__Bacteria; p__Bacteroidetes; c__Bacteroidia; o__Bacteroidales; f__Bacteroidaceae; g__Bacteroides; s__	0.9387 94822
45aa4d2ff6bff 48528a46a10a 9fc3157	M	0.00355 6464	0.001 27094 1	0.00 9362 936	0.04 9997 517	k__Bacteria; p__Firmicutes; c__Clostridia; o__Clostridiales; f__; g__; s__	0.9758 82135

18f4f0fa87b2d71da0960a0a97789d8a	VEH	-6.19E-05	2.22E-05	0.009642832	0.050790487	k__Bacteria; p__Bacteroidetes; c__Bacteroidia; o__Bacteroidales; f__Bacteroidaceae; g__Bacteroides; s__	0.938794822
dac1bc8c7f49ddfecc8c4e1d45e23206	N	4.86E-05	1.75E-05	0.009993925	0.051563529	k__Bacteria; p__Firmicutes; c__Clostridia; o__Clostridiales; f__Lachnospiraceae	0.888277199
79da6a3fcaade334061ccdf878fcaa36	N	0.00011 9691	4.31E-05	0.009879137	0.051563529	k__Bacteria; p__Firmicutes; c__Clostridia; o__Clostridiales; f__Lachnospiraceae; g__Coprococcus; s__	0.995554693
7e477e438d4f13d4453b78de5b79fec5	M	0.04693 258	0.01698801 6	0.010013787	0.051563529	k__Bacteria; p__Proteobacteria; c__Betaproteobacteria; o__Burkholderiales; f__Alcaligenaceae; g__Sutterella; s__	0.999999991
bf817ac9d4d835c4760dd027da63d990	M	-0.05541 4989	0.02007883 3	0.010260405	0.052013716	k__Bacteria; p__Tenericutes; c__Mollicutes; o__Anaeroplasmatales; f__Anaeroplasmataceae; g__Anaeroplasma; s__	1
14ee3c3fb2a858c251c641843bdaec41	VEH	-0.00542 2175	0.00196658 9	0.010327018	0.052013716	k__Bacteria; p__Firmicutes; c__Clostridia; o__Clostridiales; f__; g__; s__	0.897782457
b6cb71bf3313dfb87b60655b69921b67	M	8.42E-05	3.06E-05	0.010327361	0.052013716	k__Bacteria; p__Firmicutes; c__Clostridia; o__Clostridiales; f__Dehalobacteriaceae; g__Dehalobacterium; s__	0.999997424
019ea2f3c4fc8fdb626be0b26602769e	M	0.00033 2122	0.0001208833	0.010567167	0.052835833	k__Bacteria; p__Firmicutes; c__Clostridia; o__Clostridiales; f__Lachnospiraceae; g__[Ruminococcus]; s__gnavus	0.997694395
cd6551dad60be8d58e630faf706f0560	VEH	-0.00354 6149	0.00129904 9	0.011018467	0.053722652	k__Bacteria; p__Firmicutes; c__Clostridia; o__Clostridiales; f__Christensenellaceae; g__; s__	0.785960521
d4526b1eae773cd79a544c989629ee78	M	0.00017 3815	6.36E-05	0.010937112	0.053722652	k__Bacteria; p__Firmicutes; c__Clostridia; o__Clostridiales; f__Lachnospiraceae	0.747207574
ffff7e4c4459fb30cabc41dac23f233f	N	0.00099 3052	0.0003646137	0.010995248	0.053722652	k__Bacteria; p__Firmicutes; c__Clostridia; o__Clostridiales; f__Ruminococcaceae; g__Oscillospira; s__	0.99588863
55e954fc0348add784d9a6a41e08232e	VEH	0.00432 0016	0.0017587518	0.011055966	0.053722652	k__Bacteria; p__Firmicutes; c__Clostridia; o__Clostridiales; f__Lachnospiraceae; g__Roseburia; s__	0.897322992
23165ce82a91829813bcc0ea8649c769	N	0.00014 9034	5.49E-05	0.011376127	0.054510608	k__Bacteria; p__Firmicutes; c__Clostridia; o__Clostridiales; f__Lachnospiraceae; g__[Ruminococcus]; s__gnavus	0.999779837
08a390e1234e21c707ce929d36e8de98	M	0.00030 9919	0.0001140113	0.011322966	0.054510608	k__Bacteria; p__Firmicutes; c__Clostridia; o__Clostridiales; f__Ruminococcaceae; g__Ruminococcus; s__	0.999034209
cd6551dad60be8d58e630faf706f0560	M	-0.00351 7409	0.00129904 9	0.011609457	0.055245004	k__Bacteria; p__Firmicutes; c__Clostridia; o__Clostridiales; f__Christensenellaceae; g__; s__	0.785960521
055ae6eb5b1d3805962e00ef18b64d37	VEH	0.00029 8437	0.0001106628	0.011908228	0.056278611	k__Bacteria; p__Firmicutes; c__Clostridia; o__Clostridiales; f__; g__; s__	0.999372577
d6e7dc3f148f492eebb3172524bd713a	M	-0.00401 4223	0.0014905732	0.012015696	0.056400204	k__Bacteria; p__Firmicutes; c__Clostridia; o__Clostridiales; f__; g__; s__	0.995333089
4c5774cb51800113bc527281f0f58f21	M	0.00051 9687	0.0001933885	0.012179385	0.056782267	k__Bacteria; p__Firmicutes; c__Clostridia; o__Clostridiales; f__; g__; s__	0.855773632
14ee3c3fb2a858c251c641843bdaec41	N	-0.00524 2064	0.00196658 9	0.012817482	0.059200 16	k__Bacteria; p__Firmicutes; c__Clostridia; o__Clostridiales; f__; g__; s__	0.897782457
d6e7dc3f148f492eebb3172524bd713a	VEH	-0.00397 0627	0.0014905732	0.012869 6	0.059200 16	k__Bacteria; p__Firmicutes; c__Clostridia; o__Clostridiales; f__; g__; s__	0.995333089
51d579d0981bb2d6c21c68177a599298	M	0.00023 2197	8.74E-05	0.013080872	0.059773 52	k__Bacteria; p__Firmicutes; c__Clostridia; o__Clostridiales; f__; g__; s__	0.796465994
fd1a5d85af366b86ec3c81c7d576bc56	N	7.09E-05	2.67E-05	0.013212429	0.059977475	k__Bacteria; p__Firmicutes; c__Clostridia; o__Clostridiales; f__Ruminococcaceae; g__; s__	0.837958667

c5cad9161104 5093b7795b6 2eeb0622b	VEH	0.00048 6883	0.000 18431 8	0.01 3558 276	0.06 1145 166	k__Bacteria; p__Firmicutes; c__Clostridia; o__Clostridiales; f__Lachnospiraceae; g__[Ruminococcus]; s__gnavus	0.9985 96209
659353e28aec 82bb6d68dba 560d6a84a	N	6.95E-05	2.67E -05	0.01 4486 83	0.06 4908 524	k__Bacteria; p__Proteobacteria; c__Gammaproteobacteria; o__Enterobacteriales; f__Enterobacteriaceae	0.9999 98852
e7340d907e73 2e1c6101911d ca684058	VEH	6.58E-05	2.52E -05	0.01 4584 445	0.06 4924 303	k__Bacteria; p__Firmicutes; c__Clostridia; o__Clostridiales; f__; g__; s__	0.9995 73838
298553b6407 bdc0b2a394f2 61747de37	M	0.00026 4004	0.000 10164 4	0.01 5025 885	0.06 6460 645	k__Bacteria; p__Firmicutes; c__Clostridia; o__Clostridiales; f__Lachnospiraceae	0.7726 87534
dcf2e9140af8 e0e7cbf68022 c9345740	M	0.00017 7836	6.91E -05	0.01 5888 347	0.06 9466 345	k__Bacteria; p__Firmicutes; c__Clostridia; o__Clostridiales; f__Ruminococcaceae; g__Ruminococcus; s__	0.8215 05589
9e1960b8bb9 09981d74154 e2967fdbff	VEH	0.01359 8425	0.005 28564 3	0.01 5906 786	0.06 9466 345	k__Bacteria; p__Firmicutes; c__Clostridia; o__Clostridiales; f__Ruminococcaceae; g__Ruminococcus; s__	0.9918 42242
04b9ab1fb2a2 dcb2807a9022 19255c5a	VEH	0.00016 4283	6.43E -05	0.01 6531 5	0.07 1740 473	k__Bacteria; p__Tenericutes; c__Mollicutes; o__RF39; f__; g__; s__	0.9999 99997
14ee3c3fb2a8 58c251c64184 3bdaec41	M	-0.00501 836	0.001 96658 9	0.01 6691 604	0.07 1976 555	k__Bacteria; p__Firmicutes; c__Clostridia; o__Clostridiales; f__; g__; s__	0.8977 82457
ae3a1d0052c7 7280ba3e1a82 feeccfc8	M	9.48E-05	3.72E -05	0.01 6898 843	0.07 1976 555	k__Bacteria; p__Firmicutes; c__Clostridia; o__Clostridiales; f__Ruminococcaceae; g__Ruminococcus; s__	0.9758 02817
42e1351b398 d79bc45f3219 c5085e37e	M	0.00012 3894	4.86E -05	0.01 6801 885	0.07 1976 555	k__Bacteria; p__Firmicutes; c__Clostridia; o__Clostridiales; f__Lachnospiraceae	0.9595 44716
08a723df8dea 49956daa1104 101a21e1	M	0.00027 7777	0.000 10947 7	0.01 7257 133	0.07 2926 401	k__Bacteria; p__Firmicutes; c__Clostridia; o__Clostridiales; f__; g__; s__	0.8389 53891
f80414c180b9 fce74a07e0ca 43c3e0dc	M	0.00036 3697	0.000 14344 8	0.01 7333 231	0.07 2926 401	k__Bacteria; p__Firmicutes; c__Clostridia; o__Clostridiales	0.9999 99669
13d377cbdf24 2c05bc1f9ab2 4a98f151	M	0.00070 1841	0.000 27899 8	0.01 7898 475	0.07 4848 17	k__Bacteria; p__Firmicutes; c__Clostridia; o__Clostridiales; f__; g__; s__	0.9999 2525
60edbe38920c 3e58ef2d7092 c3a94301	N	0.00018 7879	7.46E -05	0.01 8026 217	0.07 4928 253	k__Bacteria; p__Firmicutes; c__Clostridia; o__Clostridiales	0.9999 96163
6d8a7c658e19 8d633940ac32 f020335e	N	0.00015 3368	6.12E -05	0.01 8561 937	0.07 6693 032	k__Bacteria; p__Firmicutes; c__Clostridia; o__Clostridiales; f__Ruminococcaceae; g__; s__	0.9886 37989
0bcaade4441a 8a787e518607 f9f89850	VEH	5.07E-05	2.03E -05	0.01 8868 291	0.07 7118 551	k__Bacteria; p__Firmicutes; c__Clostridia; o__Clostridiales; f__; g__; s__	0.9163 39741
81d3c9402d8 173ff3e80b91 bf77997f4	N	0.01668 8594	0.006 6813	0.01 8888 457	0.07 7118 551	k__Bacteria; p__Firmicutes; c__Clostridia; o__Clostridiales; f__; g__; s__	0.7544 91008
a6dce86bee3a 572abc5c511b 8a35ec47	N	6.15E-05	2.47E -05	0.01 9282 486	0.07 8264 207	k__Bacteria; p__Firmicutes; c__Clostridia; o__Clostridiales; f__Ruminococcaceae; g__Ruminococcus; s__	0.8318 45432
85a70500228 4bcb1d4c3b83 7e9a11138	M	-0.00084 5567	0.000 34075 6	0.01 9604 894	0.07 8647 541	k__Bacteria; p__Firmicutes; c__Clostridia; o__Clostridiales; f__; g__; s__	0.9918 3172
1ecc0af434f8 2e6a5ffb7076 b4347ec6	VEH	0.00456 4866	0.001 83861 3	0.01 9545 729	0.07 8647 541	k__Bacteria; p__Firmicutes; c__Clostridia; o__Clostridiales; f__; g__; s__	0.9979 7946
3cbb809369be 53ed7cc98270 654d82d3	M	-6.35E-05	2.58E -05	0.02 0068 218	0.07 9580 864	k__Bacteria; p__Firmicutes; c__Clostridia; o__Clostridiales; f__; g__; s__	0.8107 62827
3cbb809369be 53ed7cc98270 654d82d3	N	-6.35E-05	2.58E -05	0.02 0068 218	0.07 9580 864	k__Bacteria; p__Firmicutes; c__Clostridia; o__Clostridiales; f__; g__; s__	0.8107 62827

6f0973d6d920e3cde21b5d84df989c22	M	4.03E-05	1.66E-05	0.021401571	0.084383335	k__Bacteria; p__Firmicutes; c__Clostridia; o__Clostridiales; f__Lachnospiraceae; g__; s__	0.723791424
079ebc100b40b55c01ba4159d2655823	VEH	-0.003726178	0.001531283	0.021597038	0.084462726	k__Bacteria; p__Firmicutes; c__Clostridia; o__Clostridiales; f__; g__; s__	0.997704622
85a705002284bcb1d4c3b837e9a11138	VEH	-0.000830514	0.000340756	0.021661525	0.084462726	k__Bacteria; p__Firmicutes; c__Clostridia; o__Clostridiales; f__; g__; s__	0.991803172
2db26663b691e5d36a6e85b369d686a5	VEH	6.32E-05	2.60E-05	0.022008849	0.085315202	k__Bacteria; p__Firmicutes; c__Clostridia; o__Clostridiales; f__Lachnospiraceae	0.876307665
640f6ad15d3a14bcdc7156744fda995a	N	0.001732533	0.00071403	0.022202817	0.085586277	k__Bacteria; p__Firmicutes; c__Clostridia; o__Clostridiales; f__Ruminococcaceae; g__Oscillospira; s__	0.999619069
079ebc100b40b55c01ba4159d2655823	M	-0.003691916	0.001531283	0.022718788	0.087088687	k__Bacteria; p__Firmicutes; c__Clostridia; o__Clostridiales; f__; g__; s__	0.997704622
2766e329ca430cca038dbfb571744e04	N	9.44E-05	3.93E-05	0.023035923	0.087816501	k__Bacteria; p__Firmicutes; c__Clostridia; o__Clostridiales; f__Ruminococcaceae; g__Clostridium; s__methylpentosum	0.963209332
85a705002284bcb1d4c3b837e9a11138	N	-0.000819335	0.000340756	0.023324054	0.087944986	k__Bacteria; p__Firmicutes; c__Clostridia; o__Clostridiales; f__; g__; s__	0.991803172
01e8f4b4988db96473ca011b3e35029a	VEH	0.000100684	4.19E-05	0.023324322	0.087944986	k__Bacteria; p__Firmicutes; c__Clostridia; o__Clostridiales; f__; g__; s__	0.999873758
c5cad91611045093b7795b62eeb0622b	N	0.000442658	0.000184318	0.023475094	0.088031604	k__Bacteria; p__Firmicutes; c__Clostridia; o__Clostridiales; f__Lachnospiraceae; g__[Ruminococcus]; s__gnavus	0.998596209
bb19e961df38008bc9b54bb9333487d1	M	0.000795598	0.000333168	0.023866557	0.089015809	k__Bacteria; p__Firmicutes; c__Clostridia; o__Clostridiales; f__Lachnospiraceae; g__Coprococcus; s__	0.945601666
16d6caac01e201b47778334ac1635095	N	0.002722744	0.001139857	0.024162733	0.089635944	k__Bacteria; p__Firmicutes; c__Clostridia; o__Clostridiales; f__; g__; s__	0.999810123
218117cc438d650049cc6e5f621901b3	VEH	-5.25E-05	2.21E-05	0.024798676	0.091503135	k__Bacteria; p__Firmicutes; c__Clostridia; o__Clostridiales; f__Ruminococcaceae; g__Faecalibacterium; s__prausnitzii	0.999970751
90cbcac5a96e88bf87fd642f3b471649	M	0.000287212	0.000120951	0.024933227	0.091510248	k__Bacteria; p__Firmicutes; c__Clostridia; o__Clostridiales; f__Lachnospiraceae; g__; s__	0.985129675
ee0e5ae38a54719c0fd6d3d3708fae52	M	0.000253194	0.000107708	0.026291674	0.095985476	k__Bacteria; p__Tenericutes; c__Mollicutes; o__RF39; f__; g__; s__	1
cd6551dad60be8d58e630faf706f0560	N	-0.003019369	0.001299049	0.027876765	0.099149317	k__Bacteria; p__Firmicutes; c__Clostridia; o__Clostridiales; f__Christensenellaceae; g__; s__	0.785960521
35c0febdaa87aede2434cc976a04653b	VEH	7.81E-05	3.36E-05	0.027335886	0.099149317	k__Bacteria; p__Firmicutes; c__Clostridia; o__Clostridiales; f__; g__; s__	0.847336485
b55555c6b6a60a2f523f23533a2b4ddb	M	0.000124595	5.36E-05	0.027730855	0.099149317	k__Bacteria; p__Firmicutes; c__Clostridia; o__Clostridiales; f__; g__; s__	0.941701687
e5fd43aee8c850c433d639ed0531ac29	VEH	0.000219926	9.41E-05	0.027524944	0.099149317	k__Bacteria; p__Tenericutes; c__Mollicutes; o__RF39; f__; g__; s__	1
6f0ec8e4e488fd4085da50803578ad53	M	0.001380458	0.000593854	0.027859036	0.099149317	k__Bacteria; p__Firmicutes; c__Clostridia; o__Clostridiales; f__Lachnospiraceae; g__Coprococcus; s__	0.852668124

Table S3: Oligonucleotides used in this study

Gene	Forward/Reverse	Source	Sequence (5'-3')
AgRP	Forward	[S1]	TGCTACTGCCGCTTCTTCAA
AgRP	Reverse	[S1]	CTTTGCCCAAACAACATCCA
NPY	Forward	[S1]	TAACAAGCGAATGGGGCTGT
NPY	Reverse	[S1]	ATCTGGCCATGTCCTCTGCT
POMC	Forward	[S1]	AGGCCTGACACGTGGAAGAT
POMC	Reverse	[S1]	AGGCACCAGCTCCACACAT
18S *rRNA*	Forward	[S2]	TTCCGATAACGAACGAGACTCT
18S *rRNA*	Reverse	[S2]	TGGCTGAACGCCACTTGTC
16S 515F	Forward	[S3]	GTGCCAGCMGCCGCGGTAA
16S 806R	Reverse	[S3]	GGACTACHVGGGTWTCTAAT
16S 27F	Forward	[S4]	AGAGTTTGATCMTGGCTCAG
16S 1492R	Reverse	[S5]	GGTTACCTTGTTACGACTT

Supplementary References

[S1]. Piper, M. L., Unger, E. K., Myers, M. G. & Xu, A. W. Specific Physiological Roles for Signal Transducer and Activator of Transcription 3 in Leptin Receptor-Expressing Neurons. *Mol. Endocrinol.* **22**, 751–759 (2008).

[S2]. Reichenbach, A. *et al.* Carnitine Acetyltransferase in AgRP Neurons Is Required for the Homeostatic Adaptation to Restricted Feeding in Male Mice. *Endocrinology* **159**, 2473–2483 (2018).

[S3]. Caporaso, J. G. *et al.* Global patterns of 16S rRNA diversity at a depth of millions of sequences per sample. *Proc. Natl. Acad. Sci.* **108**, 4516–4522 (2011).

[S4]. Lane, D. J. 16S/23S rRNA sequencing. in *Nucleic acid techniques in bacterial systematics.* 115–175 (John Wiley and Sons, 1991).

[S5]. Turner, S., Pryer, K. M., Miao, V. P. & Palmer, J. D. Investigating deep phylogenetic relationships among cyanobacteria and plastids by small subunit rRNA sequence analysis. *J. Eukaryot. Microbiol.* **46**, 327–338 (1999).

Chapter 4

CONTEXTUALIZATION AND CONCLUSIONS

The biological processes that govern food intake and the perception of pleasure are extensive and complex. The results contained within this thesis demonstrate that the gut microbiota has a significant impact on the expression of feeding behaviors generated in response to a palatable food, providing a new frontier for exploration into peripheral influences on feeding and perhaps generalized reward.

Our findings are supported by and expand on a recently published study comparing the intake profiles of antibiotic-induced microbiota-depleted mice given simultaneous access to standard chow and a high-fat high-sugar (HFHS) diet.[1] In agreement with our data, the authors claim that antibiotic-treated mice overconsume the HFHS diet compared to vehicle-treated animals. However, our findings provide extensive novelty to the scientific field beyond reporting simple overconsumption behavior in ABX mice. This work demonstrates, for the first time, that the microbiota-depleted hyperphagic phenotype is reversible upon fecal microbiota transplantation and is accompanied by significant changes in feeding bout characteristics. Additionally, the operant conditioning experiments provide evidence that the intrinsic motivation to retrieve a high-sucrose reward differs based on microbiota status, and we perform differential antibiotic treatment and 16S rRNA profiling followed by targeted microbial reconstitution experiments to identify candidate bacterial species that directly mediate the change in host behavior. Furthermore, we tested foods beyond high-sugar stimuli and find a consistently hyperphagic response of ABX mice to multiple palatable foods, including a high-fat diet and Ensure®.

The area of gut-brain communication as it affects the expression of complex host behaviors has proliferated in the past ten years, as high-throughput sequencing, culturing, metabolomic, and gnotobiotic technologies have expanded, enabling pursuit of novel research questions. Indeed, microbiota influences have been reported in animal assays of depression, anxiety, autism, addiction, and reward processing.[2–7] Curiously, many psychiatric and metabolic diseases in humans co-present with consistent shifts in gut microbiota community composition,[8,9] suggesting that perturbations in the microbiota may influence disease etiology or could one day be used in a diagnostic manner.

As increasing evidence mounts for robust microbiota regulation of host systems, the possibility of developing microbiota-based and microbiota-targeted therapeutics has gained interest. Prebiotics, probiotics, fecal transplants, genetically engineered microbial strains designed to deliver therapeutic agents, and molecules designed to remove toxic microbial byproducts have been explored for mood disorders, psychiatric disease, metabolic syndromes, local intestinal inflammation, and for elimination of antibiotic-resistant opportunistic pathogens.[10] While the initial findings in this space appear promising, and federal regulatory agencies have begun to grant approval of microbiota consortiums for treatment of disease, additional basic research is needed to elucidate the fundamental relationships connecting the gut microbiota to the health of the host. This thesis provides foundational evidence of a direct link between the gut microbiota and the behavioral response to palatable foods, the dysregulation of which may contribute to disordered eating, obesity, and additional deleterious effects on human health.

REFERENCES

1. de Wouters d'Oplinter, A., Rastelli, M., Van Hul, M., Delzenne, N.M., Cani, P.D., and Everard, A. (2021). Gut microbes participate in food preference alterations during obesity. Gut Microbes *13*, 1959242. 10.1080/19490976.2021.1959242.

2. Nishino, R., Mikami, K., Takahashi, H., Tomonaga, S., Furuse, M., Hiramoto, T., Aiba, Y., Koga, Y., and Sudo, N. (2013). Commensal microbiota modulate murine behaviors in a strictly contamination-free environment confirmed by culture-based methods. Neurogastroenterology & Motility *25*, 521-e371. 10.1111/nmo.12110.

3. Needham, B.D., Funabashi, M., Adame, M.D., Wang, Z., Boktor, J.C., Haney, J., Wu, W.-L., Rabut, C., Ladinsky, M.S., Hwang, S.-J., et al. (2022). A gut-derived metabolite alters brain activity and anxiety behaviour in mice. Nature *602*, 647–653. 10.1038/s41586-022-04396-8.

4. Sharon, G., Cruz, N.J., Kang, D.-W., Gandal, M.J., Wang, B., Kim, Y.-M., Zink, E.M., Casey, C.P., Taylor, B.C., Lane, C.J., et al. (2019). Human Gut Microbiota from Autism Spectrum Disorder Promote Behavioral Symptoms in Mice. Cell *177*, 1600-1618.e17. 10.1016/j.cell.2019.05.004.

5. Buffington, S.A., Di Prisco, G.V., Auchtung, T.A., Ajami, N.J., Petrosino, J.F., and Costa-Mattioli, M. (2016). Microbial Reconstitution Reverses Maternal Diet-Induced Social and Synaptic Deficits in Offspring. Cell *165*, 1762–1775. 10.1016/j.cell.2016.06.001.

6. Lee, K., Vuong, H.E., Nusbaum, D.J., Hsiao, E.Y., Evans, C.J., and Taylor, A.M.W. (2018). The gut microbiota mediates reward and sensory responses associated with regimen-selective morphine dependence. Neuropsychopharmacol *43*, 2606–2614. 10.1038/s41386-018-0211-9.

7. Kiraly, D.D., Walker, D.M., Calipari, E.S., Labonte, B., Issler, O., Pena, C.J., Ribeiro, E.A., Russo, S.J., and Nestler, E.J. (2016). Alterations of the Host Microbiome Affect Behavioral Responses to Cocaine. Sci Rep *6*, 35455. 10.1038/srep35455.

8. Fang, P., Kazmi, S.A., Jameson, K.G., and Hsiao, E.Y. (2020). The Microbiome as a Modifier of Neurodegenerative Disease Risk. Cell Host & Microbe *28*, 201–222. 10.1016/j.chom.2020.06.008.

9. Ley, R.E., Turnbaugh, P.J., Klein, S., and Gordon, J.I. (2006). Human gut microbes associated with obesity. Nature *444*, 1022–1023. 10.1038/4441022a.

10. Sorbara, M.T., and Pamer, E.G. (2022). Microbiome-based therapeutics. Nat Rev Microbiol *20*, 365–380. 10.1038/s41579-021-00667-9.